uOttawa

L'Université canadienne
Canada's university

FACULTÉ DES ÉTUDES SUPÉRIEURES ET POSTOCTORALES

uOttawa

L'Université canadienne
Canada's university

FACULTY OF GRADUATE AND POSDOCTORAL STUDIES

Valerie Snoulton

AUTEUR DE LA THÈSE / AUTHOR OF THESIS

M.Sc. (Cellular and Molecular Medicine)

GRADE / DEGREE

Department of Cellular and Molecular Medicine

FACULTÉ, ÉCOLE, DÉPARTEMENT / FACULTY, SCHOOL, DEPARTMENT

Testing the Therapeutic Efficacy of Vesicular Stomatitis Virus as a Single Agent or in Combination with the Histone Deacetylase Inhibitor, MS-275, in a Mouse Model of Ovarian Cancer

TITRE DE LA THÈSE / TITLE OF THESIS

Dr. B. Vanderhyden

DIRECTEUR (DIRECTRICE) DE LA THÈSE / THESIS SUPERVISOR

CO-DIRECTEUR (CO-DIRECTRICE) DE LA THÈSE / THESIS CO-SUPERVISOR

EXAMINATEURS (EXAMINATRICES) DE LA THÈSE / THESIS EXAMINERS

Dr. B. Tsang

Dr. R. Parks

Gary W. Slater

Le Doyen de la Faculté des études supérieures et postdoctorales / Dean of the Faculty of Graduate and Postdoctoral Studies

TESTING THE THERAPEUTIC EFFICACY OF VESICULAR STOMATITIS VIRUS AS A SINGLE AGENT OR IN COMBINATION WITH THE HISTONE DEACETYLASE INHIBITOR, MS-275, IN A MOUSE MODEL OF OVARIAN CANCER

By

Valerie Snoulten

This thesis is submitted as a partial fulfillment of the Master of Science program in Cellular and Molecular Medicine

March 2009

Department of Cellular and Molecular Medicine
Faculty of Medicine
Ottawa, Canada

Your file Votre référence
ISBN: 978-0-494-51657-7
Our file Notre référence
ISBN: 978-0-494-51657-7

TABLE OF CONTENTS

ACKNOWLEDGEMENTS

There are many people that I would like to thank for their contribution in the completion of this thesis.

Firstly, I would like to thank my supervisor, Dr. Barbara Vanderhyden, whose guidance and encouragement made my graduate school experience a positive one. Barb provided me with the opportunity to complete a Master's and was kind in providing me with a project that she knew was of keen interest to me. Thank you for allowing me to grow and learn a tremendous amount in such a short period of time. As well thank you for listening and answering the many questions I always seem to have!

Thank you to my advisory committee, Dr. John Bell, Dr. Bruce McKay, and Dr. Robin Parks for your critiques, suggestions, recommendations and support throughout my degree.

I'd like to thank the many members of the Vanderhyden lab who were always there to answer my many questions. Thanks to Liz MacDonald, for your daily entertaining stories and your vast knowledge of PCR. To Kerri Courville, for teaching me everything there is to know about mice. To Ken Garson, for introducing me to the wonderful world of VSV. To my current lab mates, Behnam Azadi, Laura Laviolette, David Pepin, Elizabeth Pitre and Lisa Turchet: thanks for making the lab a fun place to be.

I would also like to thank the many members of the Bell lab who were always there to answer the seemingly endless questions I had. Especially thanks to Kelley Purato, Shane Knowles and Ricardo Marius for providing me with their infinite wisdom of the virus world. As well, a special thanks to Theresa Falls for showing me and eventually completing all of the mouse IV injections needed for my project.

A special thanks to my fellow graduate students and friends, Carin Christou, Val Brule and Jennifer Foucault, who always managed to make me smile. Thank you for all the great talks, great times, support and endless laughter. Thanks to Carin, for the many, many hours of company and entertainment as well as the suggestions and unwaivering support. Thanks to Val Brule for reminding me of the positives in everything.

To my parents, Jo-Ann and Bradley Snoulten: thank you for your steady support and encouragement. I could not have done this without you. As well, thanks to my brother and sister who may not understand my love of science but love me none-the-less. I would also like to thank my future in-laws, the Bouradas, for their support and interest in my project.

Finally, I want to thank my fiancé and best friend, Adam Bourada for his unconditional support and encouragement through this degree. Thank you for listening to my science talk even when you had no idea what I was talking about. Thanks for always being so proud of me. And finally thanks for keeping me laughing.

ABSTRACT

Ovarian cancer is the fifth leading cause of cancer death in Canadian women. Current treatments lack long-term therapeutic benefit, indicating a need for novel approaches. An interesting novel cancer therapeutic is the oncolytic virus, vesicular stomatitis virus (VSV), which has yielded promising results in both *in vitro* and *in vivo* studies. We performed the first tests of VSV in a transgenic mouse model of cancer. Efficacy testing was completed *in vitro* and *in vivo* using cell survival assays and survival studies. Despite promising results *in vitro*, there was a lack of therapeutic benefit *in vivo* of the single agent treatment. To attempt to increase the therapeutic efficacy, we combined VSV with a histone deacetylase inhibitor. *In vitro* combination treatments were effective; however survival was not improved. These results indicate a lack of therapeutic benefit with VSV treatment in this transgenic model of cancer, but optimization of the treatment regimen still needs to be explored.

LIST OF FIGURES

LIST OF ABBREVIATIONS

α	alpha
β	beta
κ	kappa
Δ51M	mutant of VSV that has methionine 51 of the M-protein deleted
αMEM	alpha minimum essential medium
AdCre	adenovirus expressing cre-recombinase
AdEGFP	adenovirus expressing enhanced green florescent protein
ANOVA	analysis of variance
APC	adenomatous polyposis coli gene; classified as a tumour suppressor
AR	androgen receptor
AV1	mutant of vesicular stomatitis virus (wild type); single amino acid substitution within the M protein
AV2	mutant of vesicular stomatitis virus (wild type); two amino acid substitution within the M protein
AV3	another name for Δ51M vesicular stomatitis virus
bp	base pair
CA-125	cancer antigen 125
CAG-TAg	transgenic mice that carry and express large T-antigen
CAG-LS-TAg	transgenic mice that carry but are not expressing large T-antigen.
CK8	cytokeratin 8
CK19	cytokeratin 19
CO_2	carbon dioxide
DES	diethylstilbestrol
DMBA	7,12-dimethyl benz[a]anthracene
DMSO	dimethylsulfoxide
DMEM	Dulbecco's minimum essential medium
DNA	deoxyribonucleic acid
DTT	dithiothreitol
EGF	epidermal growth factor
EGFP	enhanced green florescent protein
EGFR	epidermal growth factor receptor
ELISA	enzyme-linked immunosorbent assay
ER	estrogen receptor
FBS	fetal bovine serum
FSH	follicle stimulating hormone
GFP	green fluorescent protein
GM-CSF	Granulocyte-macrophage colony-stimulating factor

H_2O	water
HAT	histone acetylase
HCl	hydrogen chloride
HDAC	histone deacetylase
HDACi	histone deacetylase inhibitor
H&E	hematoxylin and eosin
HI-FBS	heat inactivated fetal bovine serum
HMGI	high-mobility group I protein
IFN	interferon
IFN-α	interferon alpha
IFN-β	interferon beta
IFNAR	interferon α/β receptor
IFR	interferon regulatory factor
IP	intraperitoneal injection
ISG	interferon stimulated genes
ISRE	interferon stimulated response element
ITSS	insulin transferrin sodium selenite
IV	intravenous injection
IVIS	in vivo imaging system
KCl	potassium chloride
kg	kilogram(s)
l	liter(s)
LH	leutinizing hormone
LOT	left ovarian tumour
LoxP	locus of X over P1
Luc	firefly luciferase
µg	microgram(s)
µl	microliter(s)
µM	micromolar
M	molar
mg	milligram(s)
ml	milliliter(s)
mm	millimeter(s)
mM	millimolar
MAPK	mitogen activated protein kinase
MHC	major histocompatibility complex
MISIIR	Müllerian inhibiting substance type II promotor
MISIIR-TAg(+)	mice positive for the SV40 small and large T-antigen
MISIIR-TAg(-)	mice negative for the SV40 small and large T-antigen
MNU	N-methyl-N-nitrosourea
MOI	multiplicity of infection
MOSE	mouse ovarian surface epithelium

mRNA	messenger ribonucleic acid
MS-275	a histone deacetylase inhibitor
MTD	maximum tolerated dose
MTS	3-(4,5-dimethylthiazol-2-yl)-5-(3-carboxymethoxyphenyl)-2-(4 sulfophenyl)-2H-tetrazolium, salt
nm	nanometer(s)
NDV	Newcastle disease virus
NF-κB	nuclear factor-kappa B
ng	nanogram(s)
OSE	ovarian surface epithelium
OV	oncolytic virus
p53	tumour protein 53
PAGE	polyacrylamide gel electrophoresis
PBS	phosphate buffered saline
PCR	polymerase chain reaction
pfu	plaque forming units
pg	picogram(s)
PKA	protein kinase A
PKC	protein kinase C
PKR	double-stranded RNA activated protein kinase
PMS	phenazine methosulfate
PMSF	pregnant mare serum gonadotropin
Rb	retinoblastoma
RNA	ribonucleic acid
ROT	right ovarian tumour
rpm	rotations per minute
SAHA	a histone deacetylase inhibitor; suberoylanilide hydromaxic acid
SDS	sodium dodecyl sulphate
SEM	standard error of the mean
STAT	signal transducer and activator of transcription
SV40	Simian Virus 40
TAg	large T-antigen
Taq	thermophilic DNA polymerase
TBK-1	Tank-Binding-Kinase 1
TBST	Tris-buffered saline, Tween-20
tk	thymidine kinase
TRAIL	TNF-related apoptosis-inducing ligand
TSA	a histone deacetylase inhibitor; Trichostatin A

U	units
UV VSV	UV attenuated VSV; activates immune system without causing infection
Vero	green monkey kidney epithelial cells
Vi-Cell XR	viability cell counter that uses trypan blue exclusion
VSV	vesicular stomatitis virus
WRN	Werner syndrome helicase
Wt VSV	wild type VSV; New Jersey strain.

Chapter 1: Introduction

1.1 Ovarian Cancer: General Overview

Ovarian cancer affects women of all ages and ethnicity. It is the most fatal gynaecologic malignancy and is the fifth leading cause of cancer death in Canadian women (Canadian Cancer Society). This year alone an estimated 2,500 Canadian women will be diagnosed with ovarian cancer and 1,700 Canadian women will die from the disease (Canadian Cancer Society). If the disease can be diagnosed in the early stages, the five year survival rate is greater than 90% (Moloughney *et al.*, 2000). However, the vast majority of cases, around 75% (Markman 2000), are diagnosed in the advanced stages when the five year survival rate drops dramatically to only 30-40% (Canadian Cancer Society).

1.2 Ovarian Cancer: Classification

Ninety percent of all ovarian cancers appear epithelial in origin and are thought to arise from the ovarian surface epithelium (OSE). The epithelial neoplasms can be further categorized into sub-types: serous, mucinous, endometrioid and clear cell carcinoma. The most common sub-type is serous which resembles the epithelium of the fallopian tube. The other ten percent of ovarian cancers are thought to originate from the other tissues of the ovary. These include sex cord-stromal tumours, granulosa cell tumours, theca tumours, fibromas and germ-cell tumours (Chen *et al.*, 2003).

1.3 Ovarian Cancer Symptoms and Screening

Often referred to as the 'disease that whispers', ovarian cancer tends to have vague symptoms that are often overlooked until diagnosis. According to Ovarian Cancer Canada ovarian cancer symptoms include any or all of the following that persists longer than three weeks: abdominal bloating or discomfort, changes in bowel function, unexplained weight gain and a distended abdomen from fluid build-up, nausea or changes in menstruation patterns.

The physical inaccessibility of the ovaries plays a role in the limited ability to detect early disease. To date a reliable screening method for ovarian cancer does not exist. The tumour associated antigen marker CA-125 has been found to correlate well with disease progression and regression (Shimizu *et al.*, 1985; Shimizu *et al.,* 1986). However, it is not a sufficient marker for screening due to the wide range of benign conditions that can increase serum CA-125 levels (Daoud and Bodor, 1991). Combining CA-125 serum testing with other methods of screening has improved the effectiveness (Cohen and Jennings 1994); despite this, the abundance of false positive and negative results renders the screening methods not sufficiently reliable. Recently, combinations of serum markers are showing promise of having sufficient sensitivity and specificity for early detection although these have not yet been tested in prospective, large scale trials (Visintin *et al.,* 2008; Mor *et al.,* 2005; reviewed in Gagnon and Ye, 2008).

1.4 Treatment of Ovarian Cancer

The current standard treatment for ovarian cancer is cytoreductive surgery followed by an intravenous (IV) chemotherapy treatment consisting of a combination of

taxane and platinum-based agents given 3 times weekly for 6 cycles. Around 80% of patients present with chemosensitive disease (Greenlee *et al.*, 2001). However, almost all patients with advanced disease at presentation relapse, with a median progression-free survival of 18 months (Greenlee *et al.*, 2001). The recurrent disease has a tendency to be chemoresistant and therefore is untreatable by the current standard chemotherapy regimen.

Although it is not yet a standard of care for ovarian cancer, intraperitoneal (IP) delivery of chemotherapy has been thrust into the spotlight by a recent study by the Gynecologic Oncology Group. The study found that IP infusion of the chemotherapeutic agent increased the median duration of progression free survival to 5.5 months longer than the IV therapy group and the median duration of overall survival was 15.9 months longer in the IP therapy group than in the IV therapy group (Armstrong *et al.,* 2006). The National Cancer Institute has reviewed this study together with previous studies testing IP chemotherapy in ovarian cancer patients (Markman *et al.*, 2001) and announced that the preferred method for treatment of advanced stage ovarian cancer is IP delivery of combination chemotherapy.

1.5 Novel Treatments

The dismal survival rate of this disease demands research into novel treatments. A broad range of therapeutic strategies, such as novel cytotoxics and targeted therapies, are currently being evaluated for the treatment of ovarian cancer (Agarwal *et al.*, 2006). Novel therapeutics are currently being designed to reduce chemotherapeutic toxicity, overcome chemotherapy resistance, and target the pathogenesis of cancer. A novel

cytotoxic developed to decrease chemotherapy toxicity, docetaxel (an analogue of paclitaxel), has been shown to be equally effective as paclitaxel and showed significantly less neurotoxicity when combined with carboplatin in a phase II clinical trial (Vasey *et al.,* 2004); to date, it is not yet licensed for ovarian cancer use. In an attempt to overcome chemoresistance, compounds, such as oxaliplatin, decitabine and ET-742, that have been shown to target the DNA mismatch repair and excision repair pathways are being tested for their efficacy in successfully treating this disease. These have been examined in phase I clinical trials which have shown that the compounds are well tolerated (Agarwal *et al.*, 2006). So far any developments in combination with conventional chemotherapies have yet to result in any dramatic improvements in outcome.

The drastic improvement in the last 20 years in the understanding of the pathogenesis of cancer has led to the development of drugs directed toward altering this pathogenesis. Novel therapies are being targeted to growth factor inhibition (antibodies to EGFR), signal transduction interference (MAPK, PKC, PKA), cell cycle inhibition, anti-angiogenic therapy (such as bevacizumab, thalidomide), gene therapy, immunotherapy and oncolytics (reviewed in Agarwal *et al.,* 2006). Evaluation of these therapies is ongoing in both research and clinical settings; promising preliminary data favours the feasibility of using these types of treatments in the future.

1.5.1 Oncolytics: General

The idea of viral mediated oncolysis goes back to the early 1900's when observations showing viral illness or rabies vaccination correlated with regression of tumours in some cancer patients (Dock 1904; Depace 1912). Exploration of replication-

condition viral mutants, also known as oncolytic viruses (OVs), has taken off since the early 1900's in response to advances in biochemistry, molecular biology and genetic engineering. An oncolytic virus is able to selectively enter and replicate in tumour cells, thereby initiating cytopathic effects, such as the rounding up and detachment of cells, cell lysis, swelling of nuclei, fused cells and inclusion bodies, and/or apoptosis (Flint *et al.,* 2004). To date, a variety of viruses that selectively replicate and kill tumour cells have been naturally selected or genetically engineered.

Research into the use of adenovirus as an oncolytic virus has been ongoing for over 15 years. Adenoviruses are part of the adenoviridae family of viruses. They have linear double-stranded DNA genomes and replicate in the nucleus of infected cells. Adenovirus mutants have been studied extensively, and a mutant that exploits tumour defects in p53 called ONYX-015 015 was involved in phase I (Ganly *et al.,* 2000) and phase II (Nemunaitis *et al.,* 2000; Morley *et al.,* 2004, Khuri *et al.,* 2000) clinical trials and is now in phase III clinical trials (Crompton and Kirn, 2007) involving head and neck tumour patients in the United States. As of 2005 China has approved the use of this virus in the treatment of head and neck cancers (Crompton and Kirn, 2007). Many mutants of adenovirus have been created to exploit defects in the Wnt/β-Catenin/T-cell factor pathway (Chen and McCormick 2001), p53 pathway (McCormick 2000), retinoblastoma pathway (Howe *et al.,* 2000) in addition to those that carry specific genes to target tumour cells directly, such as the gene *TRAIL* (TNF-related apoptosis inducing ligand)(Bremer *at al.,* 2008). Adenoviruses that have reached clinical studies based on promising *in vitro* results have shown moderate efficacy however they are limited by the inability of the virus to spread (Bell *et al.,* 2002). These results provide evidence for the

safety of treatment and support continued testing of the anti-tumour potential of viruses. A larger array of viruses is now being tested for potential oncolytic use, such as Newcastle disease virus, vaccinia virus, vesicular stomatitis virus, reovirus, Sindbis virus, Semliki Forest virus and myxoma virus.

Newcastle disease virus (NDV) is a paramyxovirus that shows rapid growth and spread through tumours (Phuangsab *et al.,* 2001). One particular isolate of NDV called PV701, has been examined in two phase I clinical trials. Of the 79 diverse solid tumour advanced cancer patients in the initial trial of the virus, 1 patient has shown a complete response, 1 patient had partial response and 7 other patients had measurable tumour reduction (Pecora *et al.,* 2002). The second phase I trial included 16 patients with incurable solid tumours where 5 of 8 patients, who had not shown disease progression at the time of first response assessment (after 12 viral treatments over 35 days), had prolonged disease stabilization for at least 6 months (Laurie *et al.,* 2006). Both of these phase I trials indicate that NDV has potential as an oncolytic agent and that phase II trials should be initiated.

Vaccinia viruses possess properties such as a rapid life cycle, cytoplasmic replication in infected cells and the ability to affect many cell types, making it suitable for oncolytic study. It has a large double-stranded DNA genome and is part of the poxviridae family of viruses. It shows natural tumour tropism that has been further optimized by deletion of particular genes. The first three phase I/II clinical trials with non-engineered vaccinia virus were completed in the 1970s and 1990s in 44 patients with metastic malignant melanomas. The intra-tumoural infusions showed tumour shrinkage in 25 of the 44 patients, with complete regression seen in 11 out of the 44 patients lasting for

greater then 2 years (Burdick and Hawk 1964; Hunter-Craig *et al.*,1970; Mastrangelo *et al.*, 2000; Roenigk *et al.*, 1974). In addition to the trials with non-modified vaccinia, a thymidine kinase (tk) gene-deleted virus, which targets the virus to rapidly dividing cells, has also been tested: 5 out of 7 patients involved in this study had tumour responses, with 2 having complete regressions (Mastrangelo *et al.*, 1999). Just recently, a vaccinia virus that has a deleted tk gene and an added GM-CSF gene to stimulate the immune system (JX-594) has completed phase I clinical trials for liver cancer (Park *et al.*, 2008, Liu *et al.*, 2008). In two independent but related studies, Park *et al.* (2008) showed that 9 out of the 14 patients treated with this modified vaccinia exhibited tumour responses ranging from partial to stable disease while Lui *et al.*, 2008 showed anti-tumour effects in all 3 patients tested; this encouraging clinical trial data has led to the initiation of phase II clinical trials.

Oncolytic viruses, for use in human cancer therapy, should meet several criteria (Bell *et al.*, 2002). OVs should efficiently replicate and spread within tumours, while being restricted from infecting normal cells. They should also be able to be delivered effectively to sites of metastatic cancers. Other desirable properties include the ability to genetically modify the virus in order to improve its safety and efficacy, as well as having a non-pathogenic profile in humans and domesticated animals.

1.5.1.1 Host Response to Virus

The primary host defences to viral infection are the physical and chemical barriers: the skin, mucous secretions, tears, acid pH and surface cleansing mechanisms. All cells have intrinsic cellular defences that respond to various stresses including:

apoptosis, autophagy, nuclear domain 10-mediated repressions and RNA interference (Flint *et al.,* 2004). Occasionally, these intrinsic cellular defences are unable to contain virions and the viral genomes replicate, resulting in an almost immediate activation of the host immune system; this immune response consists of both an innate and an adaptive response. The innate immune response is composed of cytokines, local sentinel cells (dendritic cells and macrophages), complement and natural killer cells and can be activated within minutes to hours after infection (Flint *et al.,* 2004). The adaptive immune response however, is activated within days to weeks after infection and employs B-cells and T-cells. Most viral invasions are overcome by the innate immune system before viral replication outpaces host defence; however, in instances where this response is insufficient, the adaptive response must then be initiated.

The interferons (IFN), are cytokines synthesized by mammals, birds, reptiles and fish, and are critical signalling proteins of the host anti-viral innate immune response (Flint *et al.,* 2004). Type I interferons include several interferon-alpha subtypes and a single interferon-β. Normal host cells that are infected with virus produce and secrete interferons. Virus replication leading to double-stranded RNA activates the constitutively expressed interferon regulatory factor 3 (IRF-3) and interferon regulatory factor 7 (IRF-7) via the induction of IRF-3 and IRF-7 phosphorylation by the IKK-like kinases TBK-1 and IKKε (Fitzgerald *et al.,* 2003; Sharma *et al.,* 2003) . Phosphorylation of IRF-3 leads to its dimerization and translocation to the nucleus. IRF-3 then assembles with the other transcription factors to the IFN-β promoter resulting in IFN-β transcriptional activation. IFN-β binds to the IFN-α/β receptor (IFNAR) in an autocrine and paracrine manner to initiate a positive feedback loop that results in further production of type I IFNs. IRF-7

has been shown to bind to the promoter of IFN-α resulting in transcriptional activation (Colina *et al.,* 2008). Recently, it has also been shown that IRF-7 is able to bind to the promoter of IFN-β resulting in transcriptional activation (Honda *et al.* 2005). Both IFN-α and IFN-β activate the IFNARs which triggers the activation of the Jak/Stat pathway (**figure 1**). Signalling through this pathway activates the protein production of interferon-stimulated response elements found on more then 300 genes (ISG; interferon stimulated gene). These interferon-induced proteins are functionally diverse and participate in a variety of signal transduction pathways, and are involved in chemokine action and antigen presentation, in addition to being involved in the regulation of transcription, stress response and control of apoptosis (Balachandran *et al.,* 2000; Stojdl *et al.,* 2003; Di Gennaro *et al.,* 2004).

One genetic defect that frequently arises during tumour evolution is diminished interferon responsiveness (Balachandran and Barber, 2000; Stojdl *et al.,* 2003; Shinozaki *et al,.* 2005). Interferon has been shown to play a role in inhibition of cell growth and induction of apoptosis and is therefore a logical target for mutation within a tumour cell (Stark *et al.,* 1998). Additionally, interferon is also a key mediator of a cell's innate anti-viral response, thus mutations that allow a tumour cell to evade interferon-mediated growth control also compromise the cell's innate anti-viral immunity. As such, the identification and use of an interferon-sensitive virus that could be targeted for selected infection and killing in tumour cells would then present a novel approach to selectively treating cancer: it is for this reason that the vesicular stomatitis virus (VSV) has been selected as an oncolytic virus (Stojdl *et al.,* 2000; Lichty *et al.,* 2004).

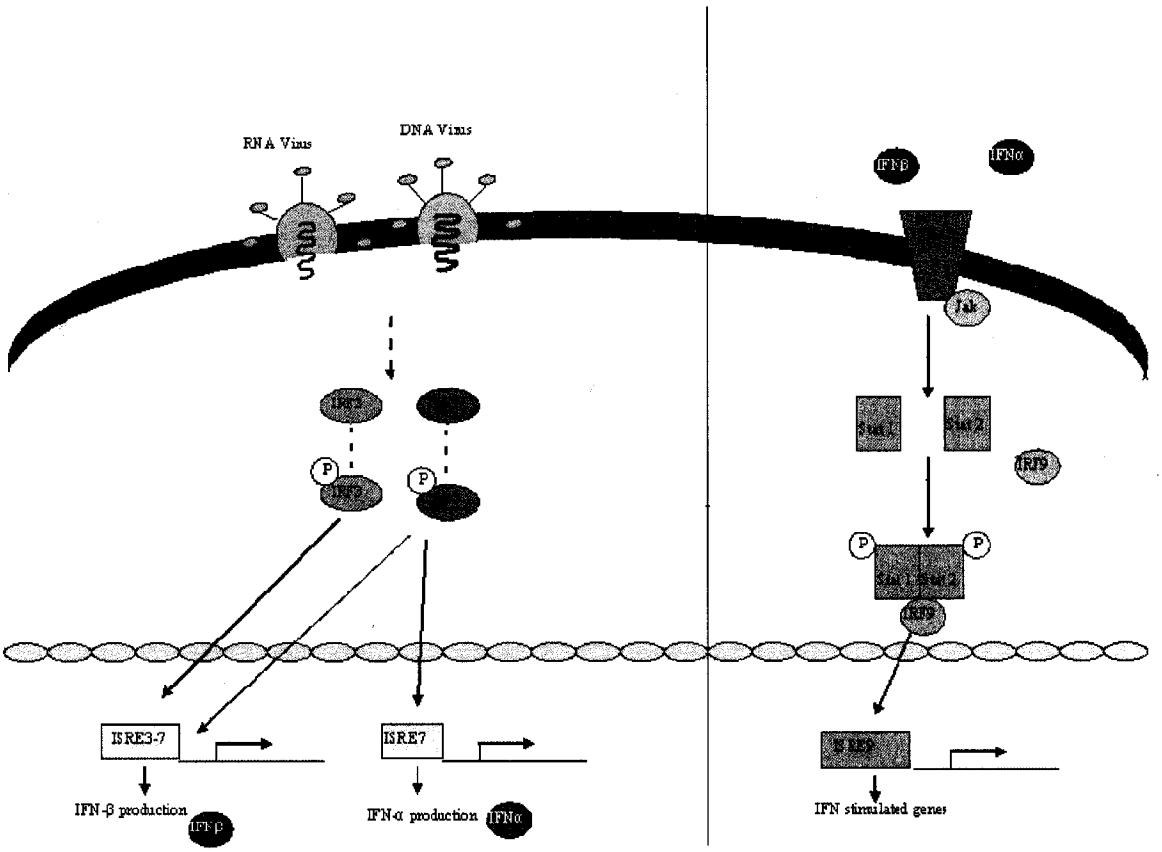

Figure 1: Image depicting the production of the type I interferons.

Virus entry activates the constitutively expressed interferon regulatory factor 3 (IRF-3) and IRF-7 via the induction of IRF-3 and IRF-7 phosphorylation. Phosphorylation (P) of IRF-3 leads to its translocation to the nucleus where it then assembles with the other transcription factors to the IFN-β promoter resulting in IFN-β transcriptional activation. IRF-7 binds to the promoter of IFN-α and IFN-β resulting in transcriptional activation. Both IFN-α and IFN-β activate the interferon α/β receptor (IFNAR) which triggers the activation of the Jak/Stat pathway activateing more then 300 genes. IFR: interferon regulatory factor. ISRE: interferon stimulated response element.

1.5.1.2 Vesicular Stomatitis Virus

Vesicular stomatitis virus (VSV) is a negative-strand RNA virus of the rhabdoviridae family. It is an arthropod-borne virus that primarily affects rodents, cattle, swine and horses but can also infect humans and other species (Flint *et al.,* 2004). Naturally occurring human infections of VSV are rare but have been reported in humans that are in contact with infected livestock or work with the virus (Letchworth *et al.,* 1999). Most infections are asymptomatic in humans and the occurrence of antibodies against VSV in the general human population is extremely low (Letchworth *et al.,* 1999). During infection, VSV synthesizes five subgenomic mRNAs that encode five proteins: the nucleoprotein, the phosphoprotein, the large polymerase protein, the glycoprotein and the matrix protein (Flint *et al.,* 2004; Lichty *et al.,* 2004) (**figure 2**). The glycoprotein allows the virus to bind to the cell surface of the host cell and to fuse the viral and host membranes (Lichty *et al.,* 2004). Together the nucleoprotein, phosphoprotein and the large polymerase protein serve as the RNA-dependent RNA-polymerase complex transcribing the viral genes (Lichty *et al.,* 2004). The matrix protein has been shown to play a role in virus assembly, inhibition of host gene expression and induction of apoptosis (Lichty *et al.,* 2004; Kopecky *et al.,* 2001; Desforges *et al.,* 2001).

Several naturally occurring or recombinant strains of VSV have been developed for therapeutic use (Stojdl *et al.,* 2003). Viruses for oncolytic use are selected and designed for tumour targeting and/or engineered to express marker proteins or suicide genes (Lichty *et al.,* 2004). Stojdl *et al.* (2003) have studied two naturally occurring interferon-inducing strains of VSV, attenuated virus 1 (AV1) and attenuated virus 2 (AV2). Having sequenced the two mutants they found that they differ from the wild type

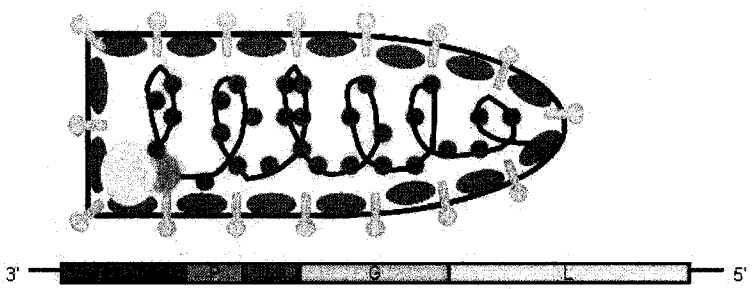

Figure 2: Model depicting the genome of VSV.

VSV has a negative sense, single-stranded RNA genome that consists of five genes. The genes encode the five key viral proteins: the nucleoprotein (N), the phosphoprotein (P), the matrix protein (M), that glycoprotein (G) and the large polymerase protein (L). The five viral proteins are assembled into a bullet shaped virus particle.

Adapted from Lichty *et al.*, 2004.

strain in their M proteins by one and two amino acids for AV1 and AV2, respectively. Stojdl *et al.* (2003) then created a third variant via the deletion of methionine 51 of the M protein (AV3 or Δ51M VSV). Mutations in the matrix protein render the viruses interferon inducing but prevent the M protein from blocking nuclear-cytoplasmic transport and therefore are unable to inhibit host-cell transcription (Lichty *et al.,* 2004). The wild type and mutant strains of VSV are still able to induce the expression of the interferon gene but the mutant strains are unable to block the export and transcription of the interferon mRNA (Stojdl *et al.,* 2003). The induction of interferon and other anti-viral proteins by the mutant viruses induces a 'cytokine cloud', protecting the surrounding normal cells with intact interferon responsiveness from viral infection while tumour cells with defects in interferon responsiveness are vulnerable to infection; this effectively increases the viral therapeutic index (Stojdl *et al.,* 2003) (**figure 3**).

Vast amounts of data regarding the use of VSV as an OV has accumulated over the last 8 years. Early evidence indicated that VSV could selectively replicate and cause cell lysis of human tumour cell lines even in the presence of exogenous interferon at a dose that protects normal cells (Stojdl *et al.,* 2000). Further evidence supported the early data by showing a wide range of human and mouse cancer cells to be susceptible to VSV infection including skin (Fernandez *et al.,* 2002), liver (Lichty *et al.,* 2004), colorectal (Huang *et al.,* 2003), hematologic (Balachandran and Barber, 2000), prostate (Ahmed *et al.,* 2004) and breast (Ebert *et al.,* 2005) whereas normal cells were less susceptible. Studies have shown that within hours, VSV effectively shuts off host mRNA export and rapidly takes over the protein synthesis machinery of the cell (Petersen *at al.,* 2000; von Kobbe *et al.,* 2000; Enninga *et al.,* 2002). The mechanism of VSV oncolysis involves cell

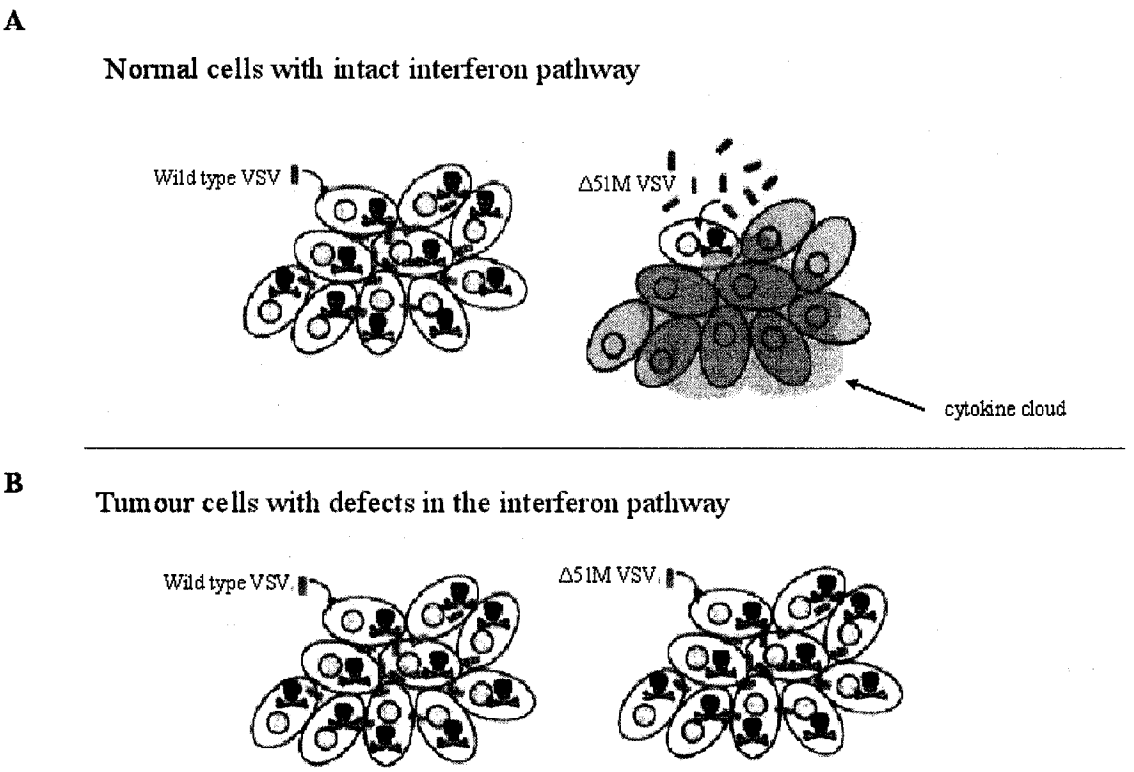

Figure 3: Model depicting how normal and tumour cells respond to wild type and Δ51M VSV.

(A) Normal cells; wild type virus blocks IFN production from infected cells and therefore, uninfected cells are not protected from infection. Δ51M VSV is defective in blocking nuclear-cytoplasmic IFN mRNA export thus allowing IFN production and potently inducing a cytokine cloud from the infected cell protecting other normal cells from infection. (B) Tumour cells; wild type virus and Δ51M are both able to cause significant infection because of defects in the interferon pathway of tumour cells. Adapted from Stojdl *et al.*, 2003.

rounding up and detachment, cell lysis if there is robust replication (Barber 2005), and also the induction of apoptosis (Balachandran *et al.,* 2000b).

The first therapeutic testing of VSV in animals was completed by injecting Balb/C and CD-1 nude mice with the human melanoma cell line SK-MEL-3 (Stojdl *et al.,* 2000). This study was the first of many to show either a repression of tumour growth, a partial regression, complete regression of the tumour and/or an increase in survival when tumour bearing nude mice were treated with VSV; in contrast, untreated nude mice exhibited unabated tumour growth (Balachandran and Barber, 2000; Ahmed *et al.,* 2004). The efficacy of VSV has been further tested in syngeneic models of skin (Fernandez *et al.,* 2002), liver (Ebert *et al.,* 2003), kidney (Obuchi *et al.,* 2003), breast (Ebert *et al.,* 2005) and colon cancer (Stojdl *et al.,* 2003). These studies supported the responses observed in the nude mouse models, rationalizing the therapeutic benefit of VSV in the treatment of many human and mouse cancers.

Although many human and mouse cancer cell lines are responsive to VSV, the degree of the responsiveness varies (Stojdl *et al.,* 2003; Ahmed *et al.,* 2004; Balachandran *et al.,* 2004; Vaha-koskela *et al.,* 2007; Nguyen *et al.,* 2008; Carey *et al.,* 2008; Hadaschik *et al.* 2008). Using two different prostate cancer cell lines, LNCAp and PC3, Ahmed *et al.* (2004) was able to identify a difference in the killing capacity of wild type versus mutant (AV1) VSV. Specifically, both wild type and mutant VSV were observed to have a cytotoxic effect on the LNCAp cell line, whereas the PC3 cell line showed sensitivity to the wild type VSV and a resistance to its mutant counterpart. This same scenario was seen in tumour bearing mice: PC3 bearing mice were resistant to mutant VSV treatment, presenting with unabated tumour growth while LNCAp tumour

bearing mice were susceptible to mutant VSV treatment showing tumour regression. Studies have indicated that the inherent resistance of some tumour cell lines to VSV may in part be due to the variation between cell lines in the magnitude of the defects in their respective interferon pathways (Stojdl *et al.,* 2000, 2003; Balachandran and Barber, 2000; Balachandran *et al.,* 2004; Ahmed *et al.,* 2004).Thus combining VSV with a compound that reversibly compromises the host innate antiviral response may increase their ability to infect cancer cells.

1.5.2 Histone Deacetylase Inhibitors

1.5.2.1 Acetylation and Deacetylation

Chromatin structure is an important factor controlling the expression or repression of certain genes (Hess-Stumpp *et al.,* 2007). In a cell, all the genetic information is packaged as chromatin, which is a highly ordered, dynamic structure in the nucleus of the cell containing DNA, histone and non-histone proteins (Johnstone, 2002). The nucleosomes are the repeating element of chromatin and consist of DNA wrapped around a histone octomer composed of an H3-H4 tetramer and two H2A-H2B dimers. Nucleosomes are folded into higher order structures and are linked and stabilized by histone, H1. Extending out of the nucleosomes are charged amino acids that are referred to as histone "tails". The tails of histones H3 and H4 are targets for various post-translational modifications including acetylation, phosphorylation, methylation and ubiquitination (Hess-Stumpp *et al.,* 2007).

In general, it is considered that increased histone interactions (deacetylation) condense chromatin, resulting in suppression of gene transcription whereas a decrease in

histone interactions (acetylation) will lead to a more open conformation of chromatin allowing gene transcription. The conformation of chromatin is believed to be maintained by the acetylation status of the histones. The acetylation status of histone is reversibly regulated by histone acetyltransferases (HATs) and histone deacetylases (HDACs). HATs are enzymes that acetylate the lysine residues of histones, neutralizing the positive charge associated with the lysine tails of histones. HATs then function with transcriptional activators and are recruited to chromatin by interacting with specific DNA binding proteins (Di Gennaro *et al.,* 2004; Johnstone, 2002) such as p300/CBP and TATA-box binding protein associated factor (Johnstone, 2002).

HDACs, on the other hand, act in opposition to HATs, deacetylating the lysines of histone tails and restoring the positive charge (Johnstone, 2002). Human HDACs are compromised of 18 family members that are divided into four classes: Class I (HDAC 1, 2, 3, 8), Class II (HDAC 4-7, 9, 10), Class III (SIRT 1-7) and Class IV (HDAC 11) (Di Gennaro *et al.,* 2004). Classes I, II and IV share sequence homology and are zinc dependent, whereas Class III do not share homology with the other classes and are NAD+ dependent enzymes (Johnstone, 2002; Di Gennaro *et al.,* 2004). Class I HDACs are expressed ubiquitously in human cell lines and tissues and are almost exclusively found in the nucleus of cells (Di Gennaro *et al.,* 2004). HDAC1 and HDAC2 are part of the multi-protein transcriptional-repression complex known as SIN3-HDAC and the nucleosomes remodeling deacetylase NuRD-Mi2-NRD complex (Johnstone, 2002).

In addition to histones, HATs and HDACs also acetylate/deacetylate non-histone proteins that are found both in the cytoplasm and nucleus, and are involved in such cellular processes as transcription (c-Jun, p53, p73, HMGI, NF-κB), hormone response

(AR, ER), nuclear transport (importin-α7), cytoskeletal structure (α-tubulin) and DNA structure (WRN) and repair (ku-90) (reviewed in Kim *et al.,* 2006). As such, protein acetylation is critical to the overall structure and maintenance of the cell because of its inherent influence on protein stability, protein-protein interactions and DNA binding (Minucci *et al.,* 2006).

Importantly, several studies have indicated that HDAC's are required to activate the transcription of interferon-β (Munshi *et al.,* 1998; Munshi *et al.,* 1999; Nusinzon and Horvath, 2003, 2006) as well as the interferon stimulated genes (ISGs) (Chang *et al.,* 2004; Sakamoto *et al.,* 2004). The combination of a histone deacetylase inhibitor and an OV, could reversibly compromise the innate anti-viral response by suppressing the transcription of interferon and its response genes. Consequently, this would create an environment conducive to viral replication and spread, effectively enhancing the therapeutic potential of both treatments.

1.5.2.2 Histone Deacetylase Inhibitors: General

Histone deacetylase inhibitors (HDACi) are small compounds that can modulate protein transcription via histone or non-histone protein post-translational modifications. HDACi classes now include: short-chain fatty acids (valproic Acid), hydroxamic acids (SAHA, TSA), cyclic tetrapeptides (depsipeptide or FK-228) and benzamides (MS-275). Aberrant acetylation patterns have been found in various leukemias (Johnstone, 2002) and solid tumours (Johnstone 2002; Marks *et al.,* 2001) which served to further *in vitro* and *in vivo* investigations with HDACi inhibitors. HDACi have been shown to induce, although variably, growth arrest, cell differentiation and apoptosis of cancer cell lines *in*

vitro (reviewed in Hess-Stumpp *et al.,* 2007). Growth arrest and cell differentiation are also seen in normal cells, however, cancer cells tend to be more sensitive to the effects of HDACi than normal cells (Johnstone, 2002). Of particular interest, Strait *et al.,* 2002, 2005 completed studies indicating that growth of the ovarian cancer cell line, A2780 was inhibited by the HDACi Trichostatin A (TSA). Interestingly, the cisplatinum-resistant line of A2780 was induced into a G2 checkpoint arrest whereas the cisplatinum-sensitive cell line was induced into a G1 checkpoint arrest. Additionally, Munster *et al.* 2001 have shown that treatment of tumours cells with SAHA increased cells in cell cycle arrest and subsequent withdrawl of this HDACi allowed cells to re-enter the cell cycle indicating that the affects of HDACi are reversible when they are withdrawn. *In vivo* studies have shown that several HDACi can inhibit the growth of tumour cells in tumour bearing animals (reviewed in Marks *et al.,* 2001). Consequently, those HDAC inhibitors that have been shown to induce a therapeutic effect *in vivo* and *in vitro* have provided the rationale for clinical trials. Currently, HDACi's are in phase I and II clinical trials involving different types of solid tumours (Xu *et al.,* 2007; Bolden *et al.,* 2006), including ovarian cancer (Candelaria *et al.,* 2007).

1.5.2.3 MS-275

MS-275 (N-(2 aminophenyl)-4-[N-(pyridin-3-yl-methoxy-carbonyl) aminomethyl] benzamide) is a member of a structural class of HDAC inhibitors known as the benzamides (**figure 4**). The exact interaction of benzamides with the active site of the HDACs remains to be elucidated (Mai *et al.,* 2005). What is known is that MS-275

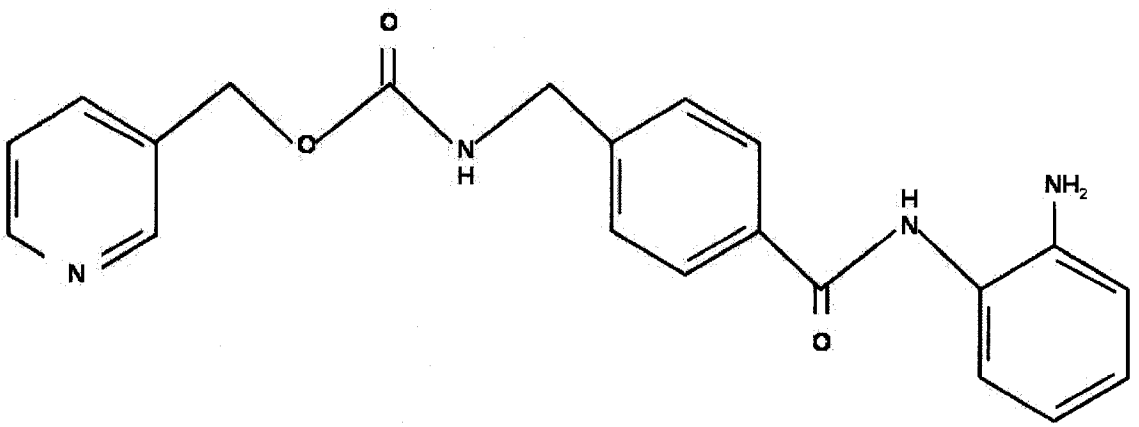

Figure 4: Structure of the histone deacetylase inhibitor MS-275.

The chemical structure of MS-275 which belongs to the class of benzamides is pictured above. Adapted from (Gallinari *et al.*, 2007)

inhibits class I enzymes having a high affinity for HDAC1 and 3 (Hu *et al.,* 2003, Vannini *et al.,* 2004) while also being capable of inhibition of HDAC8 but to a much lesser extent (Inoue *et al.,* 2006). The class I HDACs have been shown to be highly expressed in different types of human cancers (Weichert *et al.,* 2008b, 2008c, 2008d), including ovarian cancer (Weichert *et al.,* 2008a). Additionally, Weichert *et al.,* 2008a, showed that expression of the class I HDACs indicates poor patient prognosis in endometrioid ovarian and endometrial carcinomas.

MS-275 has been demonstrated *in vitro* to have anti-proliferative activity in many human cancer cell lines, including breast (Park *et al.,* 2002, Lee *et al.,* 2001), colon (Saito *et al.,* 1999), lung (Saito *et al.,* 1999), ovary (Saito *et al.,* 1999), prostate (Hess-Stumpp and Hoffman, 2004) and leukemia (Saito *et al.,* 1999). *In vivo* experiments with MS-275 have been positive, with data supporting a halt in tumour growth in tumour-bearing mice models such as breast, ovary, prostate, lung, colon and pancreas (reviewed in Hess-Stumpp *et al.,* 2007). As a result of the relative effectiveness of this HDACi in these and other preliminary studies, MS-275 is currently undergoing phase I and II clinical trials in both a hematologic and a refractory tumor model; to date, these trials have shown that MS-275 is being well-tolerated and continue to support the anti-tumor potential of this HDACi (Gojo *et al.,* 2006, Ryan *et al.,* 2005, Gore *et al.,* 2004, Hauschild *et al.,* 2006). Given the relative effectiveness of HDACi,in combination with the finding that HDACi over-expression has been implicated in ovarian cancers (Weichart *et al.,* 2008a), makes the study of an inhibitor of HDACi more than relevant for the use in ovarian cancer treatment.

The potent activity of MS-275 does in fact warrant investigation into its use as a single agent treatment. However, the interesting effects of HDACi's on dampening the interferon response of cells provides intriguing rationale for the use of them in combination with oncolytic viruses.

1.6 Animal Models of Ovarian Cancer

Animal models of cancer provide the research community with an invaluable tool that recapitulates the progression of human cancer allowing for research into prevention, screening and treatment of disease. The following four types of models of cancer have been used to study ovarian cancer, with each of them having various strengths and weaknesses: chemically/hormonally induced, xenograft, syngeneic and genetic (knockout and transgenic) (reviewed by Garson *et al.,* 2005). In the past, chemically induced models have used chemically impregnated silk sutures that are directly inserted into the ovary. DMBA (7,12-dimethyl benz[a]anthracene) and MNU (N-methyl-N-nitrosourea) have been shown to cause ovarian, as well as breast and uterine tumours (Tunca *et al.,* 1985; Nishida *et al.,* 1998). Hormonal models, based on treatment with testosterone, estradiol and diethylstilbestrol (DES) have shown epithelial changes thought to be of the pre-malignant phenotype (Silva *et al.,* 1997; Silva *et al.,* 1998). Criticism of these models lie in the fact that they do not consistently produce tumours (Stakleff *et al.,* 2003).

Xenograft models, in which human tumour cells are injected into immune-compromised animals, have allowed for the preliminary testing of many therapeutic strategies. Ovarian cancer cell lines such as OVCA-429, A2780s, A2780cp, ES2 and SKOV-3 are commonly used (Shaw *et al.,* 2004). The drawbacks to this model involve

species differences between host and graft and the lack of immune system in the mouse host.

Syngeneic models, however, provide an immune-competent environment for the study of cancer. In this model, cells are taken from the animal and transformed *in vitro*. The transformed cells are then injected back into the immune competent animal of the same strain for experimentation. A commonly used syngeneic mouse model is based on the MOSEC cell line. In this model, ovarian surface epithelial cells were retrieved from the ovaries of C57BL6 mice and underwent spontaneous transformation in culture after repeated passaging. The cells are then injected intraperitoneally or subcutaneously, developing into highly malignant neoplasms (Roby *et al.,* 2000); newer techniques involve surgery to place cells underneath the bursa of the mouse ovary (Greenaway *et al.,* 2008). While these models are routinely used for testing of novel therapeutics, they have the limitation of being simply transplanted cancer cells, and not developing from normal tissues. Human cancers develop spontaneously in the host meaning that the tumour cells that arise acquire mutations without any manipulation by an outside source. The cells used in these syngeneic models are transformed outside of the host which requires manipulations and alterations to the cells that may not necessarily occur naturally. This reduces the ability of researchers to use these models to recapitulate the initiation and early progression of the disease.

Recently, three conditional mouse models of cancer have been reported, based on Cre-*lox*P mediated gene inactivation. All three models target the OSE *in vivo* for the inactivation of "floxed"tumour suppressors or activation of a "flox-stopped" oncogene. Inactivation of the floxed tumour suppressors or activation of the flox-stopped oncogene

was achieved by the injection of a recombinant adenovirus expressing cre recombinase (AdCre) into the intrabursal space encapsulating the ovary. In the first report, researchers utilized homozygous transgenic mice that harbored *lox*P sites flanking a segment of the *p53* gene, the *Rb* gene, or both (Flesken-Nikitin *et al.*, 2003). Aberrations in both these tumour suppressor genes have been reported in epithelial ovarian cancer (Hashiguchi *et al.,* 2001). Mice in which both the *p53* and *Rb* genes had been inactivated developed epithelial ovarian tumours that were mainly classified as either well-differentiated serous neoplasms, or poorly differentiated tumours with positive staining for epithelial markers such as cytokeratin 8 (CK8).

In the second report, Dinulescu *et al.* (2005) administered AdCre intrabursally to conditionally inactivate the *Pten* tumour suppressor gene as well as to activate the expression of a *K-ras* transgene carrying the G12D oncogenic mutation ($K\text{-}ras^{G12D}$). When either gene was inactivated/activated individually, none of the mice developed neoplasms, save for one floxed *Pten* mouse. When the expression of both genes was altered concomitantly, all of the mice developed endometrioid ovarian carcinomas.

In the third report, researchers administered AdCre intrabursally to conditionally inactivate the *APC* and/or the *Pten* tumour suppressor genes (Wu *et al.,* 2007). Tumours developed in all of the ovaries of mice injected with AdCre to inactivate both genes however no tumour development was seen when each gene was inactivated individually. The tumours in the doubly inactivated mice resembled human ovarian endometrioid adenocarcinomas expressing both the epithelial markers CK8 and CK19. The disadvantage of these models lies in the requirement of surgery in order to inject the

AdCre under the ovarian bursa of these mice. In addition to the time and effort, surgery imparts stress unto the animal and requires days of recovery.

Transgenic animals are on the other hand deliberately engineered to carry a gene that will eventually lead to the spontaneous generation of cancer. Specifically, this can be accomplished via microinjecting DNA into fertilized eggs or by retroviral injection into embryonic stem cells. The resulting animals that express the gene of interest can then be bred to create a line of transgene-expressing animals for use in experiments. This model provides "spontaneous" development of a cancer, hence the cancer will be driven by normal promoter activity and function in the animal of interest. Criticism of transgenic models reflects the use of genetic manipulation and the insertion of foreign genes that do not necessarily reflect a human cancer. Several transgenic models have been created to investigate the role of hormones in ovarian cancer, such as luteinizing hormone (LH) (Risma *et al.,* 1995; Keri *et al.,* 2000; Rahman *et al.,* 2001), follicle-stimulating hormone (FSH) (Kumar *et al.,* 1999; Rahman *et al.,* 2001), progesterone (Rahman *et al.,* 2001), inhibin-α (Kananen *et al.,* 1995) and anti-mullerian hormone (Dutertre *et al.,* 2001). Surprisingly, all of the tumours formed in these mice originated from the granulosa cells as opposed to the ovarian surface epithelium. The first transgenic model of epithelial ovarian cancer was reported in 2003 by Connolly *et al.* This model uses the Müllerian inhibiting substance type II (MISIIR) promoter to drive the expression of the Simian Virus 40 early region including the small and large T-antigen (TAg) transgene, a potent oncogene. Bilateral ovarian tumours arose in approximately fifty percent of the female mice between the ages of 6-13 weeks of age. The tumours resemble human serous carcinomas having poorly differentiated areas, as well as grandular structures and tubular

differentiation with expression of the epithelial markers CK8 and CK19 and the absence of α-inhibin a marker often expressed in both granulosa cell tumours and sex-cord stromal tumours (Connolly *et al.,* 2003).

Our lab has developed a mouse model of ovarian cancer, using the plasmid reported by Connolly *et al.* 2003, pMISIIR-TAg, on the FVB/n background. These mice present a slightly different phenotype from the mice developed by Connolly et al. 2003. All of our female mice that are positive for the transgene develop bilateral ovarian tumours with 100% penetrance. The tumours arising in these mice express both CK8 and CK19 as well as α-inhibin. Expression of α-inhibin may indicate regions of the tumour with sex cord stromal phenotype, however this is not necessarily the case as α-inhibin expression has been reported in 13% of poorly differentiated human epithelial ovarian cancers (Cathro and Stoler, 2005).

The use of transgenic models in therapeutic testing of cancer treatments may be more rigorous then any other model due to the "spontaneous" nature of the tumours. The spontaneously arising tumour cells readily recapitulate a human tumour, in that the genetic alterations occur within normal cells in the hosts' bodies, and immune responses and neovascularization are likely to occur in a manner that more closely resembles the process in humans. The MISIIR-TAg mice therefore provide a model of ovarian cancer initiation and progression that can be effectively used for therapeutic testing.

1.7 Project Rationale

Knowing that the five year survival rate for women diagnosed with ovarian cancer is bleak, we wanted to investigate the efficacy of a novel therapeutic. Specifically, we wanted to determine if VSV could be a potential therapy for these women. Also knowing that therapeutic testing of VSV has been completed in xenograft and syngeneic models of cancer with promising results, we wanted to examine its efficacy in a transgenic model of cancer. A transgenic model provides a spontaneous cancer that potentially mimics the growth of a human tumour. Our lab has developed a line of mice from a mouse model of ovarian cancer developed by Connolly *et al.* 2003. The ovarian tumours in these mice develop bilaterally. The transgenic mice have a loss-of-wellness endpoint averaging about 15 weeks of age that provides a wide range of cancer stages. These mice are a tool in which we can examine the therapeutic efficacy of VSV in a spontaneous cancer which will hopefully provide further evidence for clinical trials and application.

1.8 Project Objectives

- To determine if MISIIR-TAg tumour cell lines are susceptible to VSV infection
- To determine the ability of VSV to replicate in the ovarian tumours of the MISIIR-TAg mice
- To compare the therapeutic efficacy of wild type and Δ51M VSV in increasing survival of the MISIIR-TAg mice
- To compare the therapeutic efficacy of intraperitoneal and intravenous administration of VSV
- To determine if MISIIR-TAg tumour cell lines are more susceptible to dual treatment of MS-275 and Δ51M VSV compared to Δ51M VSV alone
- To determine the ability of Δ51M-VSV to replicate in the ovarian tumours of the MISIIR-TAg mice when pre-treated with the HDAC inhibitor MS-275
- To determine the therapeutic efficacy of the co-treatment of MS-275, and Δ51M VSV delivered IP in reducing the tumour burden and increasing survival of the MISIIR-TAg mice

1.9 Hypothesis

Vesicular stomatitis virus (Δ51M) in combination with the HDAC inhibitor, MS-275, is an effective therapy in a mouse model of ovarian cancer.

Chapter 2: Materials and Methods

2.1 Experimental Animals

2.1.1 MISIIR-TAg Mice

MISIIR-TAg mice, which use the Müllerian inhibiting substance type II promoter (MISIIR) to drive the expression of SV40 early region, including both large and small T-antigen (TAg), have previously been described (Connolly *et al.*, 2003). Briefly, the MISIIR promoter was subcloned into a promotorless pGL3 basic luciferase reporter vector, pMISIIR-TOPO TA which was then purified and cloned into the plasmid p2OCRv (pMISIIR-CR). The SV40 genome was digested and subcloned into the plasmid pRIP2-TAg-IS. The resulting plasmids pMISIIR-CR and pRIP2-TAg-IS were then digested and re-ligated to generate the final pMISIIR-TAg plasmid. The resulting purified transgene DNA fragment (MISIIR-TAg) was injected into the pronuclei of day 0.5 embryos of C57BL/6 and C3H mice by microinjection. Injected embryos were then implanted into the oviducts of day 0.5 pseudopregnant female Sweiss Webster mice. Tail clippings from the resulting pups were confirmed for presence of the transgene by PCR amplification of a 773-bp fragment of the large T-antigen using the TAg F4 forward primer (5'-TGCATGGTGTACAACAT-TCC) and the TAg R1 reverse primer (5'-TTGGGACTGTGAATCAATGCC). About 50% of all heterozygous TAg (+) female mice develop ovarian tumours, all developing bilaterally, with an average loss-of-wellness of 105 days (15 weeks). The majority of tumours are CK8 and CK19 positive with no expression of inhibin-α. The tumours are poorly differentiated neoplastic cells that occasionally formed tubules. Ascites is also seen in about 40% of these mice at endpoint.

Our lab has received the plasmid described by Connolly *et al.* (2003), and has created the MISIIR-TAg mice on an FVB/n mouse background. Purified DNA for the transgene was microinjected into the male pronuclei of FVB/N single cell embryos. Embryos were cultured to the two-cell stage and implanted into pseudopregnant recipients. Transgenic founder mice and subsequent generations were identified by PCR analysis of mouse tail or ear punch DNA using methods previously described (Clark-Knowles *et al.*, 2007). MISIIRTAg mice were identified following PCR analysis of genomic DNA using the primers 5'-TGCATGGTGTACAACATTCC-3' and 5' TTGGGACTGTGAATCAATGCC-3' in a standard PCR reaction and a program consisting of 30 cycles of 94°C for 30 seconds, 56°C for 30 seconds and 72°C for 30 seconds. PCR products were analyzed on 1.5% agarose gels for visualization of the 774 base pair product.

The MISIIR-TAg female mice created in our lab develop bilateral ovarian tumours 100% of the time with a loss-of-wellness averaging 105 days (15 weeks). About 40% of the mice develop ascites with no metastasis seen by gross examination. The mice were housed in autoclaved microisolater cages in an air-filtered laminar flow cabinet and were given food and water *ad libitum*. All injections were performed under sterile conditions in a laminar flow hood. All experiments were conducted with the approval of the University of Ottawa Animal Care and Veterinary Service and according to the guidelines for the care and use of animals established by the Canadian Council on Animal Care.

2.1.2 CAG-LS-TAg Mice

Transgenic mice were generated that carry the SV40 T-antigen transgene driven by a ubiquitous CAG promoter. The promoter drives the expression of a lacZ stop sequence that is followed by the TAg gene. The stop sequence is flanked by loxP sites and is excised following exposure to Cre recombinase, allowing the expression of large T-antigen. The pCAG-LS-TAG plasmid was constructed by subcloning the SalI fragment, containing the early region of SV40 (TAg), from plasmid pUBC-TAg into the unique XhoI site of pCALL2-IRES-EGFP (a gift from Dr. Corrine Lobe, University of Toronto, Toronto, ON, Canada). The pCAG-LS-TAg plasmid expresses the β-geo gene (a fusion of β-galactosidase and neomycin phosphotransferase genes) from the ubiquitous CAG promoter. The β-geo gene and three downstream polyA signals (3xpolyA) are flanked by loxP sites. Exposure to cre recombinase results in the deletion of the β-geo/3xpolyA cassette leading to the juxtaposition of the TAg immediately downstream of the CAG promoter to allow its efficient expression.

The pCAG-LS-TAg plasmid was digested with XmnI and the DNA fragment bearing the promoter/gene sequences was separated and purified by agarose gel electrophoresis. Purified DNA for the transgene was microinjected into the male pronuclei of FVB/N single cell embryos. Embryos were cultured to the two-cell stage and implanted into pseudopregnant recipients. Transgenic founder mice and subsequent generations were identified by PCR analysis of mouse tail or ear punch DNA using methods previously described (Clark-Knowles *et al.*, 2007). CAG-LS-TAg mice were identified following PCR analysis of genomic DNA using the primers 5'-

TGCATGGTGTACAACATTCC-3' and 5'-TTGGGACTGTGAATCAATGCC-3' in a standard PCR reaction and a program consisting of 30 cycles of 94°C for 30 seconds, 56°C for 30 seconds and 72°C for 30 seconds. PCR products were analyzed on 1.5% agarose gels for visualization of the 774 base pair product.

2.2 Tissue Culture

2.2.1 Isolation of Primary MOSE

Primary mouse ovarian surface epithelium (MOSE) cells were isolated from ovaries removed from 6-8 week old female FVB/N mice (Charles River Laboratories, Wilmington, MA). Animals were euthanized by carbon dioxide asphyxiation and the ovaries were removed aseptically, with complete removal of the bursal membrane. Ovaries were placed in phosphate buffered saline ((PBS; Hyclone, Logan, UT) 9g/l NaCl, 0.08g/l Na_2PO_4 and 0.14g/l KH_2PO_4) and washed three times, then transferred to 15ml Falcon tubes (Nalge Company, Rochester, NY) containing 0.25% trypsin (Hyclone) in PBS and placed in a 37°C incubator for 40 minutes. Tubes were inverted three times to mechanically remove any surface epithelial cells on the ovary. The supernatant containing the cells was centrifuged at 1000 rotations per minute (rpm) for 10 minutes. The cell pellet was resuspended in fresh MOSE media [α-MEM (alpha- minimum essential media; Hyclone) supplemented with 4% or 10% fetal bovine serum (FBS; HI-FBS, Cansera, Etobicoke, ON), insulin transferrin-sodium selenite (ITSS; 5μg/mL insulin, 5μg/ml transferrin, 5ng/ml sodium selenite, Roche Applied Science, Laval, QC), 2.1 ng/ml epidermal growth factor (EGF; Roche), 1.05μg/ml gentamicin (Invitrogen,

Burlington, ON), and 5.2U/ml penicillin/streptomycin (Invitrogen)] and plated. The same protocol was used to isolate OSE from the CAG-LS-TAg mice.

2.2.2 Isolation of Mice MISIIR-TAg Tumour Cells

Cells were isolated from the right and left ovarian tumours of MISIIR-TAg mice (see below) 6045, 6046, and 6048 to generate cell lines. Each tumour was removed, diced and strained through a microfilter with MOSE media into a 50ml Falcon tube. They were than centrifuged for 4 minutes at 4000 rpm. The cell pellet was then resuspended in fresh MOSE media containing an extra 50µl of gentamicin (0.1µg) and 50µl in 500mL of penicillin/streptomycin (0.26U) and plated. After the fourth passage of the isolated cells, fresh MOSE media supplemented with 10%FBS without the extra gentamicin and penicillin/streptomycin.

2.2.3 Cell Lines

Vero cells, Green monkey kidney cells, were revived from frozen stocks obtained from Dr. John Bell (Ottawa, ON). They were maintained as stated below (2.2.4 Cell Maintenance) in DMEM (Dulbecco's minimum essential medium; Hyclone) +10% FBS.

2.2.4 Cell Maintenance

Cell cultures were maintained in an incubator at 37°C and equilibrated with 5% CO_2. Cells were passaged at confluency, washing with PBS and then incubating at 37°C in 0.05% trypsin. Once cells were detached from the plate, media with FBS was added to inactivate the trypsin and cells were centrifuged at 2 (International Equipment Company

(IEC) clinical centrifuge, Massachusetts; 115VAC, 50/60Hz, 1.2amp) for 4 minutes. The cell pellet was resuspended in fresh media and a fraction was plated.

Cells were aliquoted for long term storage into cryovials (Nalge Company) with 10% dimethylsulfoxide (DMSO; Sigma-Aldrich., Oakville, ON). Cells were frozen at -70°C for temporary storage and than transferred to liquid nitrogen for long-term storage. Cells were thawed in a 37°C water bath, transferred to 15ml Falcon tube (Nalge Company) containing PBS and centrifuged at 2 (IEC clinical centrifuge) for 4 minutes. The pellet was then resuspended in fresh media and plated.

2.2.5 CAG-LS-TAg Adenovirus administration

Recombinant adenoviruses AdCMVEGFP and AdCMVCre are modifications of the adenovirus-5 genome, from which the e1a and e1b regions required for viral replication had been deleted and replaced by enhanced green fluorescent protein (EGFP) or Cre driven by the CMV immediate early regulatory sequence.

CAG-LS-TAg cells were seeded at $2x10^5$ cells/well in a 6 well dish. They were incubated in 1ml of serum-free medium with $4x10^7$ pfu of AdCMVEGFP (AdEGFP) or AdCMVCre (AdCre) (Vector Development Laboratory, Houston, TX). After 2 hours at 37°C, cells were washed twice with PBS and covered with MOSE media containing 5% FBS and maintained as described in 2.2.5.

2.3 Cell Line Characteristic

2.3.1 Cellular Morphology

MOSE and MISIIR-TAg tumour cells were photographed 72 hours post-plating ($4.5x10^4$ cells) at 150x using a Nikon Coolpix 5400 camera mounted onto a Nikon Eclipse TE2000-U microscope.

2.3.2 Growth Assay

MOSE cells and MISIIR-TAg tumour cell lines were plated at 45,000 cells per well in a 6 well dish. Cell counts were completed using trypan blue exclusion (Vi-Cell XR, Beckman Coulter) at 0, 24, 48, 72 and 96 hours post-plating. Cells were washed with PBS and trypsonized for 5 minutes, and then MOSE media was added to each well. The supernatant from each well was centrifuged at 2 (IEC clinical centrifuge) for 4 minutes and the cell pellet was resuspended and used in the total cell count. Viable cell counts were graphed using Graphpad Prism 3.0.

2.3.3 Western Blot Analysis probing for Simian Virus 40 T-Antigen

Protein samples were collected by adding 4xSDS (sodium dodecyl sulphate) + Fracks to cell culture dishes on ice after two washes with PBS. The cells were then collected and placed in an eppendorf. This was heated for 5 minutes at 100°C, put on ice for 5 minutes and then sonicated for 30 seconds. The eppendorf with cells was then centrifuged at maximum for 20 minutes at 4°C. The supernatant was collected and frozen at -20°C. Protein content was measure using a commercially available protein assay (Bio-Rad Protein Assay Kit, Bio-Rad Laboratories, Mississauga, ON). Samples were separated

on a 4-12% polyacrylamide gel (Invitrogen) and transferred to a nitrocellulose membrane (Hybond C Extra, Amersham, Oakville, ON). Blocking was carried out with 5% skim milk in Tris-buffered phosphate with Tween-20 (1xTBST).The primary antibody (Santa Cruz Biotechnology Inc., Santa Cruz, CA,), SV40-TAg 1:1000, was diluted in 5% skim milk in 1xTBST and incubated with the blot overnight at 4°C. The secondary antibody, goat anti-mouse (Santa Cruz Biotechnology Inc.) 1:4000, was diluted in 5% skim milk in 1xTBST and incubated for 1 hour at room temperature. Visualization of protein bands was performed using Amersham ECL Plus detection reagents (GE Healthcare, Piscataway, NJ) and image acquisition system (SRX-101A, Konica, Minola). The membrane was then washed for 5 minutes in 1xTBST and Restore Western Blot Stripping Buffer (Thermo Scientific, Rockford, Illinois) was applied for 20 minutes. Three washes of 1xTBST for five minutes were applied. The loading control β-actin antibody (Cedarlane Laboratories Ltd., Burlington Ont) was used at a dilution of for 1:500 for 1 hour at room temperature. A goat-anti mouse secondary (Santa Cruz Biotechnology Inc.) was used at 1:4000 and incubated for 1 hour before visualization of protein bands by Amersham ECL Plus detection reagents (GE Healthcare)and image acquisition systems (SRX-101A, Konica, Minola).

2.4 Experimental Procedures:

2.4.1 Viral Growth

Aliquots of the recombinant AV3 or Δ51M strain of VSV with an attenuating deletion of methionine 51 of the matrix protein and with or without a transgene encoding GFP (green florescent protein) or luciferase (described further Stojdl *et al.*, 2003) and wild type VSV with or without a transgene encoding GFP or luciferase, were obtained from the laboratory of Dr. John Bell at the Ottawa Health Research Institute. The viruses were all propagated on Vero cells; Vero cells were grown to 90% confluency and then infected with the virus at an MOI of 0.1 for 18-24 hours. Virions were purified from cell culture supernatants by passage through a 0.2 mm Steritop filter (Millipore, Billerica, MA) and centrifugation at 30, 000 x g before resuspension in PBS for all studies. Samples were frozen at -70˚C until use. UV attenuated VSV was obtained from Dr. John Bell from the Ottawa Health Research Institute.

Plaque assays were carried out on Vero cells to determine viral titer. Vero cells were grown to 90-100% confluency in 6-well dishes. Each well was then infected with serial dilutions of the virus for 45 minutes. An overlay of 1:1 of 2xDMEM (Gibco BRL, Burlington, ON) supplemented with 20% FBS and 1% agarose in distilled H_20 was applied to each well. After 20 minutes at room temperature, the plates were incubated at 37˚C overnight. Plaques were then counted.

2.4.2 Interferon Dose-Response Assay

In each experiment, MOSE cells were seeded into 24-well plates at $5x10^5$ viable cells/well in MOSE media. Cells were pre-treated with MOSE media or MOSE media

supplemented with 5U/ml, 50U/ml or 500 U/ml of universal interferons (PBL Biomedical Laboratories, Piscataway, NJ) for 18h. Cells were then challenged with Δ51M or wild type VSV at an MOI 0.01. The virus was aspirated off the cells after 1 hour and replaced with MOSE media. Cell viability counts were taken 48 hours post-infection using trypan blue exclusion (Vi-Cell XR, Beckman-Coulter).

2.4.3 Viral Sensitivity Assays

For each experiment, MOSE, 6045 R, 6045 L, 6048 R and 6048 L cells were seeded in 96-well plates at 30,000 cells/well (300,000 cells/ml) in growth media (MOSE media) and pre-treated with or without universal interferon (PBL Biomedical laboratories) at 500U/ml for 18 hours. The cells were then challenged with varying MOI's (0, 0.0001, 0.001, 0.01, 0.1, 1, 10, 100) with either Δ51M or wild type VSV. Cell viability was determined 48 hours post-infection using an MTS assay.

MTS (3-(4,5-dimethylthiazol-2-yl)-5-(3-carboxymethoxyphenyl)-2-(4-sulfophenyl)-2H-tetrazolium) assay (Promega Corporation, Madison, WI) were completed using the following concentrations: MTS (2mg/ml): PMS (phenazine methosulfate; 0.92mg/ml) 1ml: 0.05ml. The MTS:PMS was then further diluted in MOSE media 1:5 respectfully. Each well of a 96 well plate is given 100μl of [MTS:PMS] in media and incubated in a humidified atmosphere containing 5% CO_2 at 37°C until the absorbance readings (Dynex Technologies MRX, Revelation v3.04) were between 0.6-1.5.

2.4.4 *In Vivo Viral Maximum Tolerated Dose*

Three 6-8 week old MISIIR-TAg(+) mice were treated with $5x10^8$pfu of wild type VSV by either IP or IV injection. The resulting death of all of the animals within 48 hours required the testing of a lower dose of wild type VSV; 3 mice at $1x10^8$pfu delivered either IP or IV. Simultaneously, three mice received the same doses of Δ51M VSV by either IP or IV injection.

2.4.5 *Ex-vivo Fluorescent Imaging*

MISIIR-TAg(+) and MISIIR-TAg(-) mice at 6 weeks of age were treated once with either PBS (100μl), Δ51M VSV or wild type VSV at $1x10^8$pfu/injection by either IP or IV injection. Mice were sacrificed by CO_2 asphyxiation 72 hours post-viral injection and bilateral ovaries or ovarian tumors were examined using a Leica MZFLIII dissecting microscope with a standard GFP filter set. Images were captured with a Nikon Coolpix 100 camera.

2.4.6 *Quantification of VSV infection in tumours*

Tumours were excised from euthanized mice at specified time points and homogenized in PBS. The extent of VSV infection was measured by plaque assay (described above).

2.4.7 *In Vivo Imaging System (IVIS) determination of VSV replication*

MISIIR-TAg mice at 10-13 weeks of age that were either transgene positive (TAg+) and transgene negative (TAg-), were treated with wild type VSV delivered IP.

The mice were injected with d-luciferin 4, 24, 48, 72 hours later (Molecular Imaging Products Company, Ann Arbor, MI; 200 ml IP at 10 mg/ml in PBS) for Firefly luciferase imaging. Mice were anesthesized with 3% isofluorane (Baxter Corp., Deerfield, IL) and imaged with IVIS 200 Series Imaging System (Xenogen Corporation, Hopkinton, MA). Data acquisition and analysis were performed using Living Image v2.5 software. For each experiment, images were captured under identical exposure, aperture and pixel binning settings, and bioluminescence was plotted on identical color scales.

2.4.8 VSV Single Treatment Survival Study

MISIIR-TAg(+) mice at 6-8 weeks of age were treated with 6 doses of UV attenuated VSV ($1x10^8$pfu/100µl), Δ51M VSV ($1x10^8$pfu/100µl), wild type VSV ($1x10^8$pfu/100µl) or PBS (100µl) by either IP or IV injection over a two week period. Mice were then euthanized at endpoint by CO_2 asphyxiation. The criteria used to determine survival endpoint were defined as any or all of the following: complete anorexia lasting longer than 24 hours, dehydration lasting longer than 24 hours despite fluid therapy, presence of respiratory distress, presence of palpable abdominal mass that impairs mobility or wellness, progression of the illness (hunching, scruffy fur) and abdominal distension.

Mice that reached survival endpoint were sacrificed and a necropsy was performed recording date of death, weight, tumour weights, amount of ascites if present, overt metastasis, phenotype of the tumour and abnormalities of any kind. The liver, spleen, lungs and the right and left ovarian tumours were removed, fixed in formalin and paraffin-embedded.

2.5 Dual Treatment Experimental Procedures

2.5.1 Histone Deacetylase inhibitor

DMSO was used to dissolve MS-275 (Axxora LLC, SanDiego, CA). For all *in vitro* studies, MS-275 was dissolved in DMSO and was diluted in PBS to a concentration of 2mM. The highest percent of DMSO applied to cells was 0.1%. For the *in vivo* studies, MS-275 was dissolved in DMSO to create a 0.012mg/μl solution. Based on the weight of the animal, more DMSO was added up to 25μl and then 25μl of PBS was added for a 50μl injection of 1:1 DMSO to PBS.

2.5.2 Combination Treatment Sensitivity Assay

For each experiment, MOSE, 6045 R and L, 6048 R and L cells were seeded in 96 well plates at 30,000 cells /well in growth media. After 18 hours, cells were treated with or without varying MOIs (0, 1.0, 0.1, 0.01) of Δ51M VSV and incubated at 37°C for 1 hour. Virus was removed and the cells were treated with media supplemented with or without MS-275 at varying doses (0.5, 1, 1.5, 2 or 4μM). The media control contained 0.1% DMSO or media alone. Forty-eight hours post-infection cell viability was measured using MTS assays. Absorbance was measured at 490nm in a micro-plate reader and displayed in the program Revelation (v3.04).

2.5.3 Combination Treatment Fluorescent Imaging

For each experiment, MOSE, 6045 R & L, 6048 R & L cells were seeded in 6 well plates at 500,000 cells /well in growth media. After 18 hours, cells were treated with or without Δ51M VSV (MOI 0.01) and incubated at 37°C for 1 hour. Virus was removed

and the cells were treated with media supplemented with or without MS-275 at (4μM). Images were taken 24 hours post infection with a Leica MZFLIII dissecting microscope with a standard GFP filter set. Images were captured with a Nikon Coolpix 100 camera.

2.5.4 Interferon ELISA

MOSE, 6045 R and L, 6048 R and L cells were seeded in 24 well plates at 500,000 cells /well in growth media. After 18 hours, the cells were either infected with Δ51M VSV (MOI of 0.1 or 1) or treated with PBS. An hour later, the virus or PBS was aspirated and the wells were washed once with PBS. Wells were then treated with MOSE media, MOSE media+0.1% DMSO or MS-275 (4μM) in MOSE media. Supernatants were collected from each well at 24 hours (MOI 1.0) and 48 hours (MOI 0.1) post-viral infection and frozen at -20°C until use.

CAG-LS-TAg cells or CAG-TAg cells were seeded in 24 well plates at 100, 000 cells/well. After 18 hours, the cells were either infected with Δ51M VSV (MOI of 10) or treated with PBS. An hour later, the virus or PBS was aspirated and the wells were washed once with PBS. Wells were then treated with MOSE media, MOSE media+0.1% DMSO or MS-275 (4μM) in MOSE media. Supernatants were collected from each well at 24 hours (MOI 10) post-viral infection and frozen at -20°C until assay.

A standard curve (0-500pg/ml) was constructed by serial dilutions of the Mouse Interferon Alpha solution that was part of the kit (PBL Biomedical Laboratories). Precisely 100μl of the interferon standard curve samples and the samples obtained from the above experiments were placed in individual wells. The plate was covered and incubated for 1 hour at room temperature. After the incubation, the contents were

emptied and washed once with a final wash solution then 100µl of antibody solution was added to each well. The plate was covered and incubated at room temperature for 24 hours.

After the incubation, the liquid contents were emptied and the wells were washed three times with the final wash solution. HRP conjugate solution (100µl) was added to each well. The plate was then covered and incubated for 1 hour at room temperature. After the incubation, the liquid contents were emptied and the wells were washed four times with the final wash solution. TMB substrate solution (100µl) was added to each well. The plate was covered and incubated for 15 minutes at room temperature. After the incubation, 100µl of Stop solution was added to each well. A microplate reader (Dynex Tachnologies MRX, Revelation v3.04) was used to determine the absorbance at 450nm within 5 minutes of the addition of the stop solution.

By graphing the standard curve, the interferon titer in the samples was determined. Five plates were used to assay all the samples. Each treatment is reported as the average of 3 individual experiments run in duplicate.

2.5.5 Western Blot Analysis probing for Acetylation Time-Course

MISIIR-TAg(+) mice were treated with MS-275 at a dose of 12mg/kg or 24mg/kg IP. Mice were sacrificed at 0, 4, 6, 12, 24, 48 hours post-injection. Bilateral tumours were removed and flash frozen. Acid-extraction of histones was then performed (described in 2.5.6). Protein content was measured using a commercially available protein assay (Bio-Rad Protein Assay Kit, Bio-Rad Laboratories). Samples were separated on a 4-12% polyacrylamide gel and transferred to a nitrocellulose membrane (Hybond C Extra).

Blocking was carried out with 3% skim milk in 1xTBST.The primary antibody, Pan-Acetyl-H4 (Millipore, Billerica, MA) 1:2000, was diluted in 3% skim milk in 1xTBST and incubated with the blots for 3 hours at room temperature. The secondary antibody, goat anti-mouse (Santa Cruz Biotechnology Inc.) 1:5000, was diluted in 3% skim milk in 1xTBST and incubated for 1.5 hours. Visualization of protein bands was performed using Pierce ECL (Thermo Fisher Scientific Inc., Rockford, IL) and image acquisition system (SRX-101A, Konica, Minola). The membrane was washed in 1xTBST and Restore Western Blot Stripping Buffer was applied for 30 minutes. Three washes of 1xTBST were used before the loading control histone-4 antibody (Abcam Inc., Cambridge, MA) was added at a dilution of for 1:1000 for 13 hours at 4°C. A goat-anti mouse secondary (Santa Cruz Biotechnology Inc.) was used at 1:5000 and incubated for 1 hour before visualization of protein bands by Pierce ECL (Thermo Fisher Scientific Inc.) and image acquisition system (SRX-101A, Konica, Minola).

2.5.6 Acid-Extraction of Histones

The left and right tumours of MISIIR-TAg mice treated with treated with MS-275 at a dose of 12mg/kg or 24mg/kg IP were homogenized in 1ml of PBS and then a 22 1/2 gauge needle and syringe if necessary. Homogenates were than centrifuged at 200 x g for 10 minutes. The supernatant was discarded and the cell pellet was resuspended in 5-10 volumes of lysis buffer (10mM HEPES; pH 7.9, 1.5mM $MgCl_2$, 10mM KCl, 0.5mM DTT, 1.5mM PMSF, 0.2M HCl). This was incubated on ice for 30 minutes and centrifuged at 11, 000 x g for 10 minutes at 4°C. The supernatant was collected and dialyzed against 0.1M acetic acid, twice for 1.5 hours and dialyzed three times against

H_2O for 1hour, 3 hours and overnight. The supernatant was collected, flash frozen and stored at -70°C until use.

2.5.6 In Vivo Imaging System Determination of Viral Dosing

Eight 10-11 week old MISIIR-TAg(-) or MISIIR-TAg (+) mice were treated with one dose of either 1:1 DMSO:PBS (100µl) and PBS (100µl) [vehicle], 1:1 DMSO:PBS (100µl) and Δ51M ($1x10^7$pfu/100µl), MS-275(12mg/kg) and PBS (100µl), MS-275 (12mg/kg) and Δ51M ($1x10^7$pfu /100µl) or MS-275 (12mg/kg) and Δ51M ($5x10^7$pfu/100µl). Twenty-four hours later the mice were injected with d-luciferin (Molecular Imaging Products Company) (200 ml intraperitoneally at 10 mg/ml in PBS) for Firefly luciferase imaging. Mice were anesthesized under 3% isofluorane (Baxter Corp.) and imaged with the IVIS 200 Series Imaging System (Xenogen Corporation). Ovaries and ovarian tumours were then excised and imaged using the same machine. Data acquisition and analysis were performed using Living Image v2.5 software. For each experiment, images were captured under identical exposure, aperture and pixel binning settings, and bioluminescence was plotted on identical color scales.

2.5.7 Combination Treatment Survival and Tumour Burden Studies

MISIIR-TAg(+) mice, 9-10 weks old, were treated with 3 doses of either 1:1 DMSO:PBS (100µl) and PBS (100µl) [vehicle], 1:1 DMSO:PBS (100µl) and Δ51M ($1x10^7$pfu/100µl), MS-275 (12mg/kg) and PBS (100µl), MS-275 (12mg/kg) and Δ51M ($1x10^7$pfu /100µl) over a one week period. Three mice from each treatment group were euthanized by CO_2 asphyxiation one week after completion of treatment to measure and

compare tumour burden. Eight mice per treatment group were left to compare differences in the length of survival. These mice were euthanized when they had reached a survival endpoint, as described in section 2.4.8.

Mice sacrificed for the tumour burden study had each ovarian tumour (with the ovarian fat pad and bursal membrane) removed individually. Each ovary was then cleaned under the microscope removing the fat pad and bursal membrane and the weight of each tumour was measured and recorded. Each tumour was then fixed in formalin, paraffin embedded and serial sectioned (5μm) for hematoxylin and eosin staining. Images were then taken with the ScanScope CS (Aperio)

Mice that reached survival endpoint were sacrificed and a necropsy was performed recording date of death, weight, tumour weights, amount of ascites if present, overt metastasis, phenotype of the tumour and abnormalities of any kind. The liver, spleen, lungs and the right and left ovarian tumours were removed, fixed in formalin and paraffin-embedded.

2.6 Statistical Analyses

Growth curve and interferon dose response cell counts were done in three independent experiments with at least two samples per group in each replicate, and are expressed as mean count ± standard error of the mean (SEM). For the growth curve, the comparison between cell lines at each time-point was completed using a two-way analysis of variance (ANOVA) test with significance differences inferred when $p<0.05$. Comparisons between groups in the interferon dose-response assay were completed using a one-way ANOVA.

MTS assays were performed in triplicate in three independent experiments for each cell line and treatment. Statistical comparisons were made by ANOVA; a two–way ANOVA when comparing between cell lines and a one-way ANOVA when comparing treatment effects on a single cell line. Bonferroni's post-test was used to determine significance between specific groups when whole group differences were detected by ANOVA.

Tumour burden and tumour titering statistical analyses were completed using a one-way ANOVA. Survival data was plotted using Kaplan-Meier plots and were compared using a Log-Rank test. For all analyses, significance was inferred at $p<0.05$. Analyses were performed using Graphpad Prism statistical software (Graphpad Software, San Diego, CA).

Chapter 3: Results: Use of VSV as a single agent treatment for Ovarian Cancer

3.1 MISIIR-TAg cell line morphology, proliferation and SV40-TAg expression

Cell lines were established from primary cultures of MOSE cells, and from the right and left tumours of three MISIIR-TAg mice: 6045 R, 6045 L, 6046 R, 6046 L, 6048 R and 6048 L. Photomicrographs of primary cultures of MOSE and the MISIIR-TAg tumour cell lines were taken to compare cellular morphology. **Figure 5** shows that all of the cell lines have a cobblestone appearance. Images taken show that cells from either 6045 R or 6045 L appear smaller than MOSE cells whereas cells from 6048 R and L are of similar size to the MOSE cells. Growth curves were then completed to compare the growth rates of each cell line. **Figure 6** shows that over a 96 hour time period the MOSE and MISIIR-TAg tumour cell lines have similar growth rates, although there was a tendency for two of the tumour cell lines to grow more rapidly than the others.

To further characterize the cell lines and compare the levels of SV40 T antigen expression, cell lysates from the MOSE and MISIIR-TAg tumour cell lines were probed for SV40 TAg by western blot analysis. The results show that all of the isolated cell lines from the MISIIR-TAg mouse tumours (6045, 6046, 6048) express the protein whereas the negative control, normal MOSE, do not (**figure 7**). However, the amount of SV40-TAg expressed by each cell line was variable. The cell lines from 6046 R and L had similar amounts of SV40-TAg protein whereas, interestingly, the cell lines from the right tumours from 6045 and 6048 had lower amounts of TAg protein than the left tumours. Also interesting was the observation that the tumour cell lines that expressed the lower amounts of TAg protein were the ones that tended to grow more rapidly.

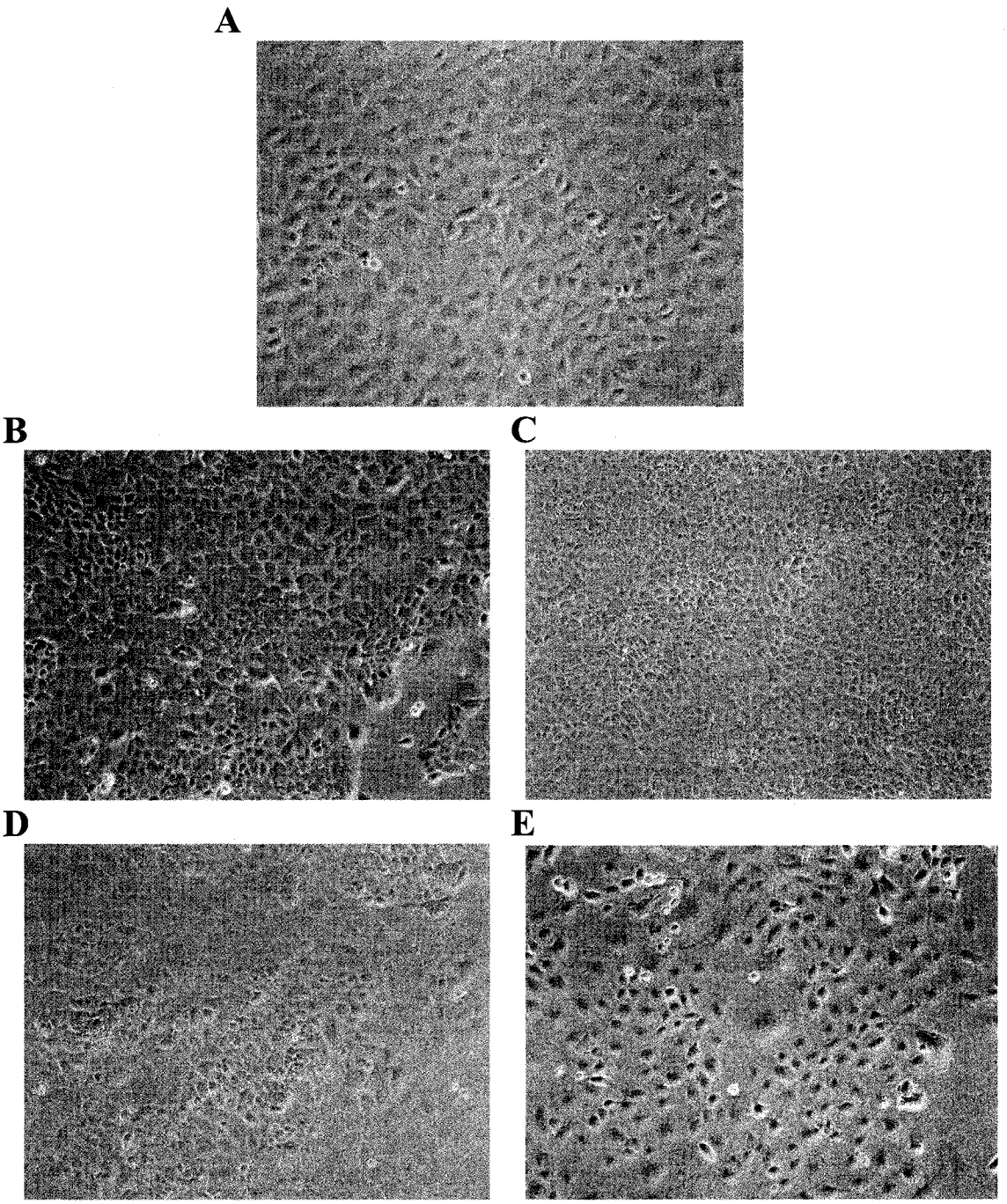

Figure 5: Photomicrographic images of MOSE and MISIIR-TAg cell lines.

Cells were seeded at a density of $4.5x10^4$ and cultured for 72 hours: cell lines were derived from (A) mouse ovarian surface epithelial cells (B) mouse 6045 right tumour (C) mouse 6045 left tumour (D) mouse 6048 right tumour (E) mouse 6048 left tumour. Live cells were photographed at 150x magnification

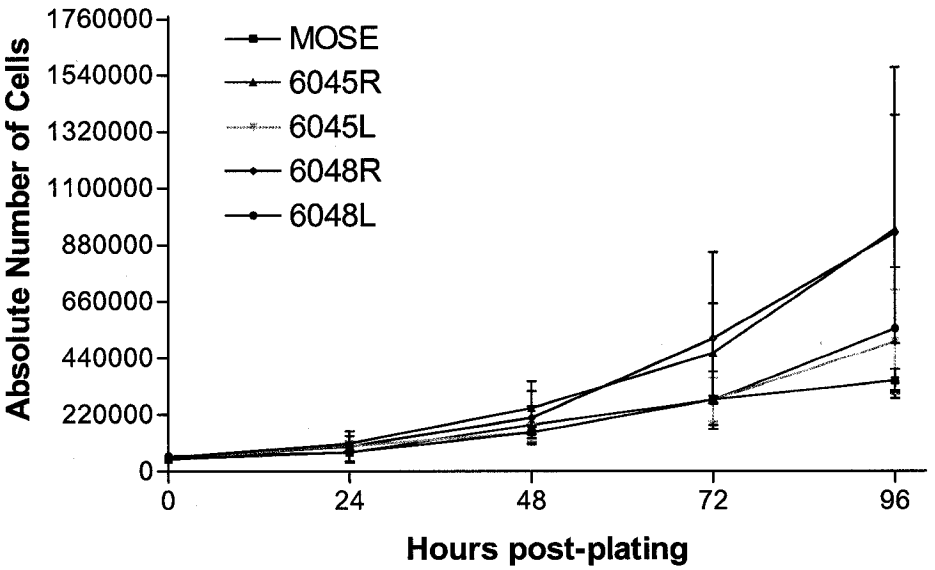

Figure 6: Growth curves show no significant difference between MOSE and MISIIR-TAg tumour cell lines.

Cells were seeded at a density of $4.5x10^4$ for up to 96 hours. Cell counts were determined at 0, 24, 48, 72 and 96 hours post-plating. Each data point represents 3 experiments ± SEM.

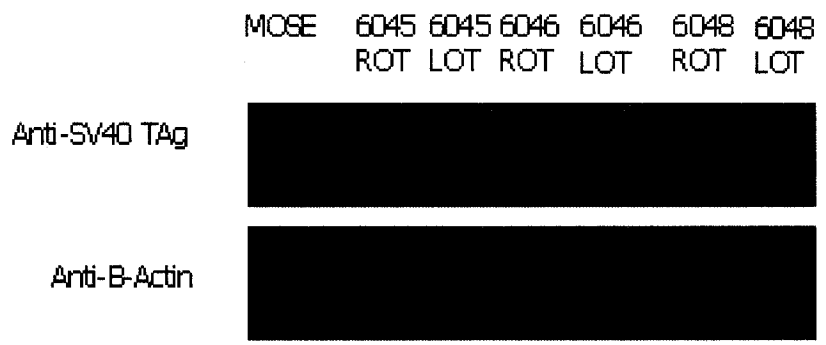

Figure 7: MISIIR-TAg tumour cell lines differentially express SV40 Large T-antigen.

Determination of the expression of SV40 large T-antigen in the MOSE and MISIIR-TAg tumour cells was done using SDS-PAGE and immunoblotting. Forty μg of protein was separated on an SDS gel and immunoblotted for SV40 large T-antigen. Detection of β-actin was used as a loading control.

3.2 Characterization of the response of MOSE and MISIIR-TAg cell lines to VSV infection

At a high MOIs wild type VSV is able to cause cell death in most normal and tumour cells (Stojdl *et al.* 2000). Addition of exogenous interferon has been shown to protect normal cells with intact interferon pathways from wild type VSV infection but not tumour cells that have defects in their interferon pathways (Stojdl *et al.*, 2000). Therefore initial experiments were performed to determine an appropriate dose of interferon that could protect MOSE from VSV infection. For these experiments, a dose-response assay of interferon was performed on MOSE cells treated with wild type and Δ51M VSV. **Figure 8a** shows that Δ51M VSV at an MOI of 0.01 is able to significantly decrease the number of viable cells compared to the non-infected MOSE cells; however, pre-treatment of the cells with 5, 50 or 500 U/ml of exogenous interferon had no effect on cell viability compared to cells infected with virus alone. Pre-treatment with interferon at all doses failed to protect MOSE cells against Δ51M VSV infection at an MOI of 0.01. **Figure 8b** indicates that wild type VSV at an MOI of 0.01 is able to cause a statistically significant decrease in the number of viable cells compared to non-infected MOSE cells, the number of viable cells was reduced by almost 50%. No significant differences were seen between the cells treated without interferon and virus compared to cells treated with interferon and virus. However, there is a trend that indicates that increasing doses of interferon are able to protect the MOSE cells from the cytotoxic effects of wild type VSV. Due to this trend, a dose of 500U/mL of interferon was chosen to complete the viral sensitivity assays.

A

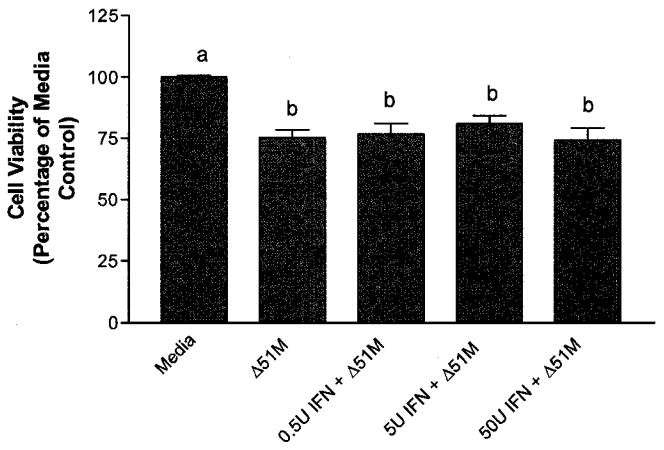

B

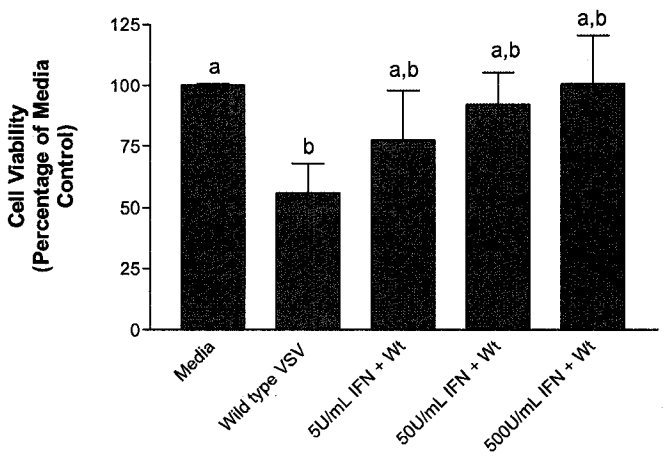

Figure 8: Exogenous interferon pre-treatment of MOSE cells is able to protect them from wild type VSV but not from Δ51M VSV cytotoxicity.

MOSE cells ($6.5x10^5$) were pre-treated for 18 hours with either 5, 50 or 500U/ml of universal interferon and then infected with (A) Δ51M or (B) wild type VSV at an MOI of 0.01. Cell viability counts were completed 48 hours post-infection using trypan blue exclusion (ViCell Counter) and were calculated as mean percentages of the control cells ± SEM where each data point represents three independent experiments. Bars with different letters indicate a statistical significance ($p<0.05$).

The susceptibility of MOSE cells and the MISIIR-TAg tumour cell lines to VSV was determined by performing a sensitivity assay. Four MISIIR-TAg tumour cell lines, 6045 R and L and 6048 R and L and the MOSE cell line were either pre-treated with interferon or media as a control, and then infected with increasing MOIs of either Δ51M (**figure 9a**) or wild type VSV (**figure 9b**). Both viral sensitivity assays indicate that the MOSE and MISIIR-TAg tumour cell lines are responsive to interferon, as shown by the ability of exogenous interferon to protect the cell lines from VSV infection at high MOIs. As indicated by figure 9a, the tumour cell lines show different sensitivities to Δ51M VSV. Two of the four MISIIR-TAg tumour cell lines, 6045 R and 6048 R, show a loss of cell viability at an MOI of 1.0 compared to the MOSE cell line (without interferon). However, the other two tumour cell lines, 6045 L and 6048 L, do not show a significant loss of cell viability compared to the MOSE cells at any MOI (without interferon) acting in a similar manner to the normal cells. In contrast, wild type VSV (figure 9b) is able to cause a significant decrease in cell viability in all of the MISIIR-TAg tumour cell lines at an MOI of 0.1 whereas an MOI of 1.0 (one logarithm difference) was required to cause a significant decrease in the viability of MOSE cells, without pre-treatment with interferon.

3.3 Determining the maximal tolerated dose of VSV in the MISIIR-TAg(+) mice

The maximum tolerated dose of VSV that could be given to the MISIIR-TAg(+) mice needed to be determined in order to complete VSV therapeutic efficacy studies *in vivo*. The maximal tolerated dose of VSV that could be given to the MISIIR-TAg(+) mice was determined by the identifying the highest dose of wild type virus that the animals were able to survive. Three MISIIR-TAg(+) mice were treated with wild type VSV at

A

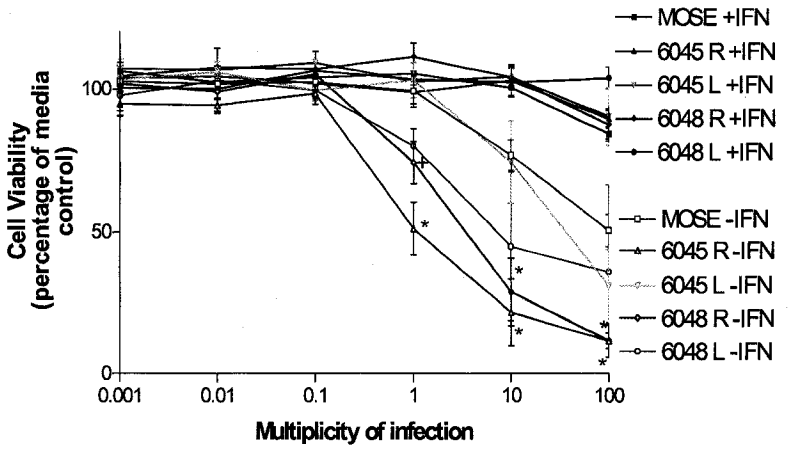

B

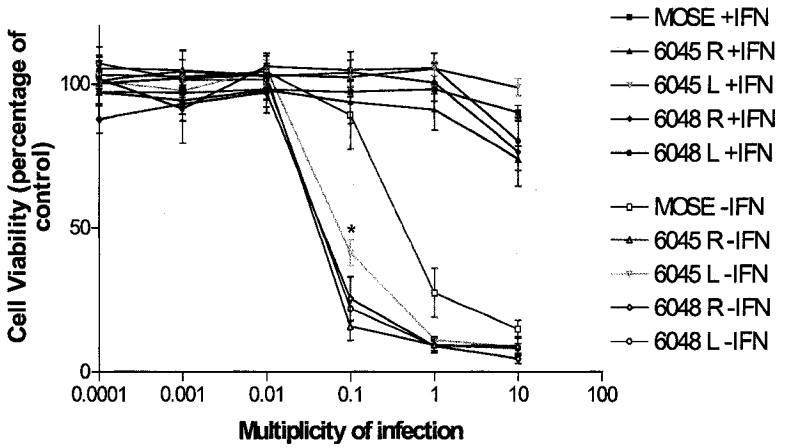

Figure 9: Δ51M VSV oncolysis is variable in the MISIIR-TAg tumour cell lines. MTS cell viability assays were performed 48 hours after MOSE and MISIIR-TAg tumour cell lines ($3x10^4$) were pre-treated with or without interferon (500U/ml) for 18 hours and then infected with (A) Δ51M VSV or (B) wild type VSV at MOI's of 0.001, 0.01, 0.1, 1, 10, 100. Each point represents the mean of data from three independent experiments ± SEM. The symbol (+) indicates statistical significance ($p<0.05$) and the asterisk (*) indicates statistical significance ($p<0.001$) both compared to the MOSE cells.

$5x10^8$pfu/injection given by IP and IV injection, based on the use of this dose in previous animal studies (Stojdl *et al.,* 2003; Wu *et al.,* 2008); however none of these mice survived longer than 48 hours, so a lower dose was then tested. Three MISIIR-TAg(+) mice were treated with $1x10^8$pfu/injection of wild type virus given by IP and IV injection. All of these mice survived longer than 1 week, and therefore this dose was used in subsequent experiments.

3.4 Susceptibility of MISIIR-TAg tumours to infection by VSV

The goal of the initial *in vivo* experiments was to determine the ability of VSV to infect the MISIIR-TAg tumours For this purpose, GFP- or luciferase-tagged virus was tested in both transgenic MISIIR-TAg(+) female mice with tumours and non-transgenic MISIIR-TAg(-) siblings with normal ovaries and virus infection was evaluated using three methods: GFP imaging of isolated tumours, titering of virus in isolated tumours and in vivo imaging of tumours. MISIIR-TAg(+) and MISIIR-TAg(-) mice were given either an IP or IV injection of either Δ51M or wild type VSV expressing GFP and then sacrificed 48 or 72 hours post-injection and tumours were removed for GFP imaging. Images shown in **figure 10** illustrate that a limited amount of VSV is able to enter and replicate in the tumours, as indicated by GFP positive areas. The lack of GFP expression following Δ51M VSV-GFP injection IP or IV reveals that Δ51M VSV fails to replicate within the tumour. As well, tumours of mice injected with wild type VSV-GFP IV fail to express GFP. Images of tumours injected with wild type VSV-GFP IP show that viral entry and replication is occurring as indicated by GFP expression, however the viral load

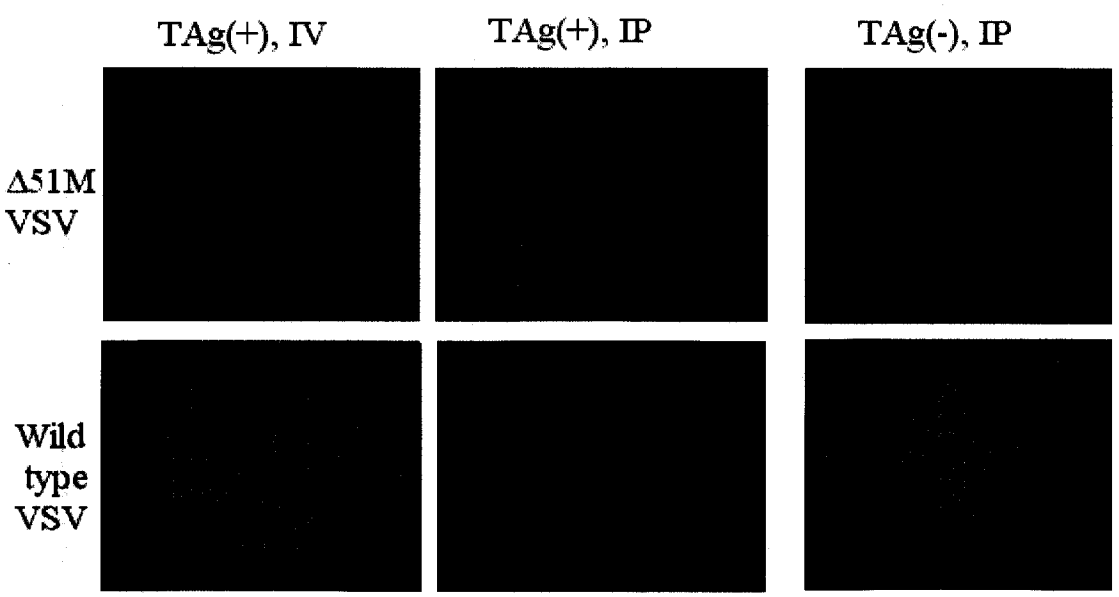

Figure 10: Wild type VSV given IP shows evidence of viral entry and replication in the tumours of MISIIR-TAg(+) mice.

MISIIR-TAg(+) and MISIIR-TAg(-) mice were given an IP or IV injection of either Δ51M or wild type VSV expressing GFP and then sacrificed 72 hours post-injection when tumours were removed for GFP imaging.

was found to be insignificant, as demonstrated by subsequent viral titering of the tumours.

Validation of the imaging results was done by titering the tumours. Tumours were resuspended in PBS and homogenized and supernatants were used to infect Vero cells. Plaques were counted the following day to determine the amount of virus in the tumour. All of the tumour homogenates contained less than 100 pfu/ml, confirming that VSV alone is unable to replicate in the MISIIR-TAg tumours to any significant degree, including in those tumours that expressed GFP (i.e. mice treated with wild type VSV given IP).

Further validation of these results was performed using an *In Vivo* Imaging System (IVIS). MISIIR-TAg(+) mice were treated with wild type VSV expressing Firefly luciferase IP and imaged 4, 24, 48 and 72 hours after virus injection. **Figure 11** shows that there is some viral replication in the spleen and liver at 4 hours as indicated by luciferase expression, however the replication is completely gone by 24, 48 and 72 hours post-injection, further validating the previous results.

In order to determine whether the bursa (a membranous layer that surrounds murine ovaries) played a role in preventing the entry of VSV into the tumours when given IP, ex-vivo imaging of tumours with or without the bursa was performed. MISIIR-TAg(+) mice were treated with wild type VSV tagged with GFP by IP injection and then euthanized 48 post-injection. Tumours were excised and imaged first with the bursa intact and then with the bursa removed. Imaging (**figure 12**) revealed that the bursa did not prevent viral infection.

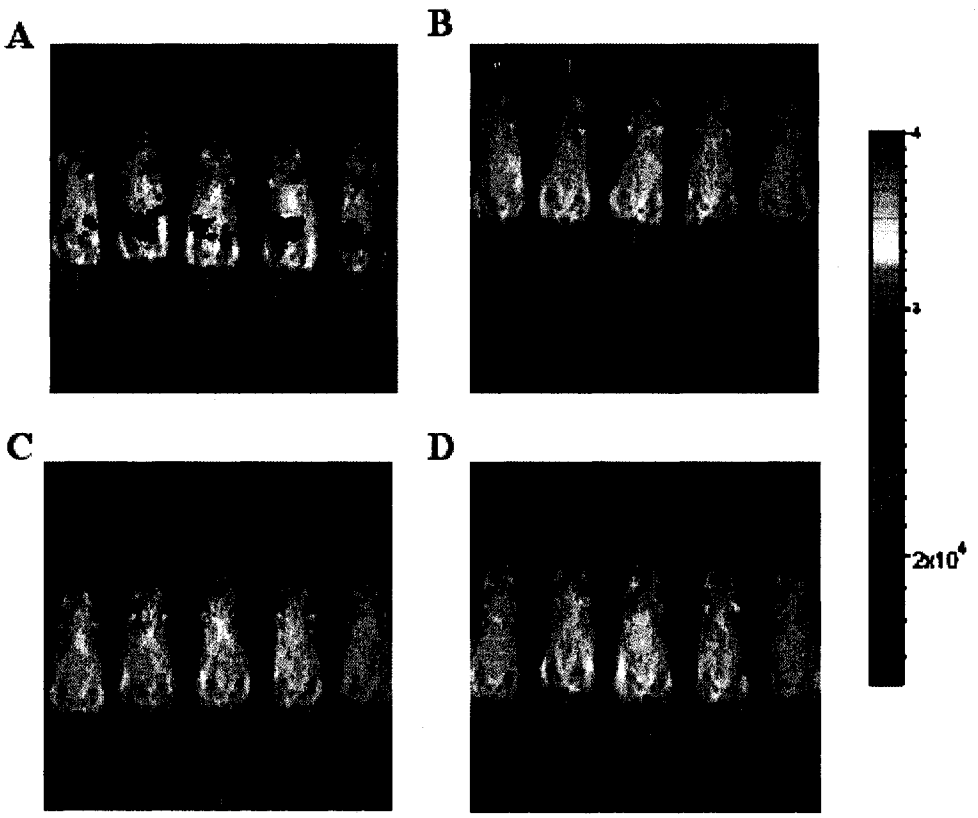

Figure 11: Wild type VSV given IP is not able to sustain replication in the tumours of MISIIR-TAg(+) mice.

Six week old MISIIR-TAg(-) and MISIIR-TAg(+) mice were given either wild type VSV IP ($1x10^8$pfu/100µl), and then imaged using an IVIS system 4, 24, 48 and 72 hours after viral injection. In all images the first 3 mice are TAg(+) and the last two mice are TAg(-). (A) 4 hours after viral injection (B) 24 hours post viral injection (C) 48 hours post viral injection (D) 72 hours post viral injection.

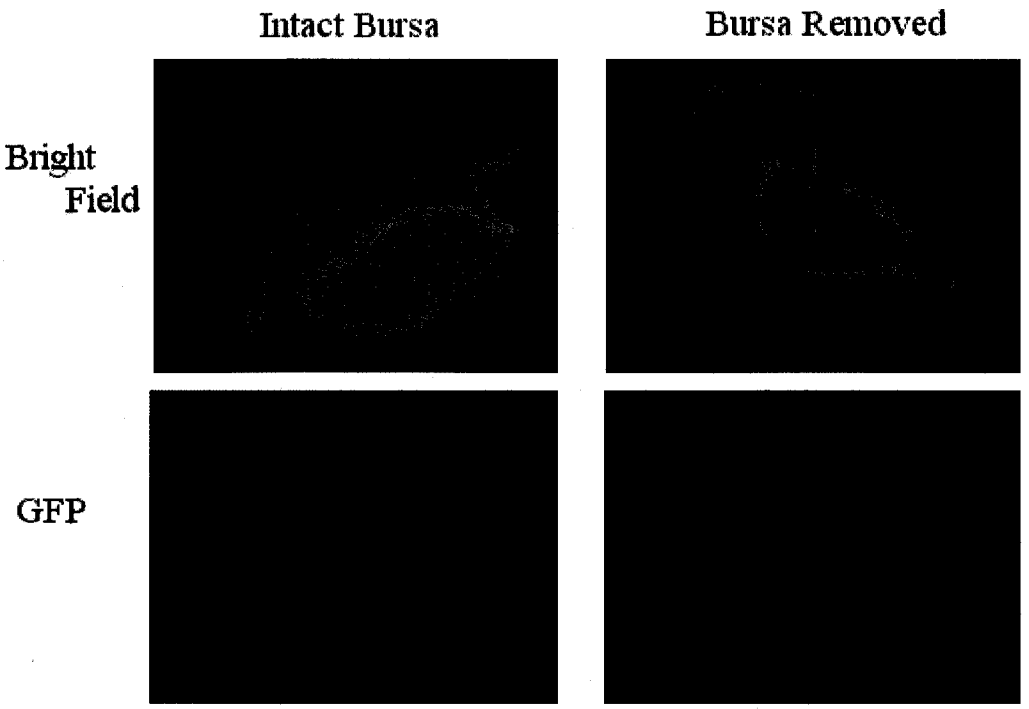

Figure 12: The bursal membrane of the ovary does not prevent VSV infection. MISIIR-TAg(+) mice were treated with wild type VSV tagged with GFP by IP injection and then euthanized 48 hours post-injection. Tumours were then excised and imaged with the bursa intact. The bursa was then removed and the tumour was imaged again.

3.5 Effect of VSV on the survival of MISIIR-TAg(+) mice

In order to examine the therapeutic efficacy of wild type and Δ51M VSV in the MISIIR-TAg(+) mice a survival study was completed. MISIIR-TAg(+) mice between 6 and 8 weeks of age were treated 6 times over a two week period with either PBS, UV attenuated VSV, wild type VSV or Δ51M VSV by either IP or IV injection. The mice were then left until they reached a loss-of-wellness endpoint when a necropsy was completed.

The presentation of the mice when they reached their loss of wellness endpoint was similar in all treatments groups. Endpoint of survival was reached when mice developed large, palpable masses and abdominal distension, and showed a lack of mobility and an increased respiration rate. Necropsy revealed that all mice in the study had developed bilateral ovarian tumours and at least one mouse from each treatment group had developed bloody ascites (**figure 13**). **Figure 14** illustrates the general appearance of the tumours upon necropsy. The median time to loss-of-wellness in the control mice was as follows: PBS injected IP was 107 days (n=3) and IV was 123 days (n=3) or UV inactivated VSV injected IP (n=4) was 111.5 days and IV was 119.5 days (n=6). The median time to loss-of-wellness of mice treated with Δ51M VSV IP was 110 days (n=5) or IV was 115 days (n=5) and mice treated with wild type VSV IP was 106 days (n=5) and IV was 112 days (n=5). Comparison of the survival times of the treatment groups revealed no significant differences (**figure 15**).

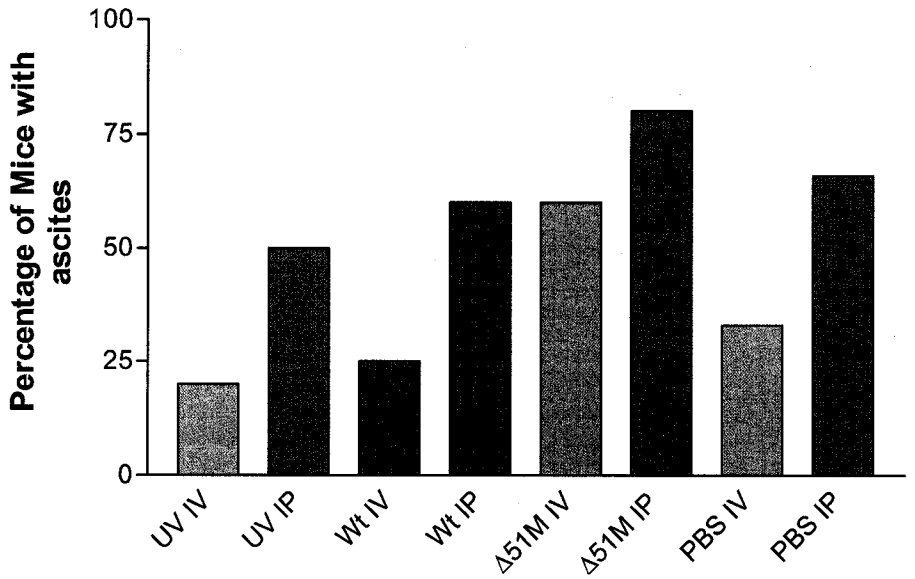

Figure 13: MISIIR-TAg(+) mice develop ascites at survival end point with all of the single treatments given IP or IV.

Six to eight week old MISIIR-TAg(+) mice were treated with either UV attenuated VSV (UV), wild type VSV (Wt), Δ51M VSV (Δ51M) or PBS by either IP or IV injection six times over a two week period. They were then monitored until endpoint was reached. At endpoint of survival, mice were euthanized and the presence or absence of ascites was recorded.

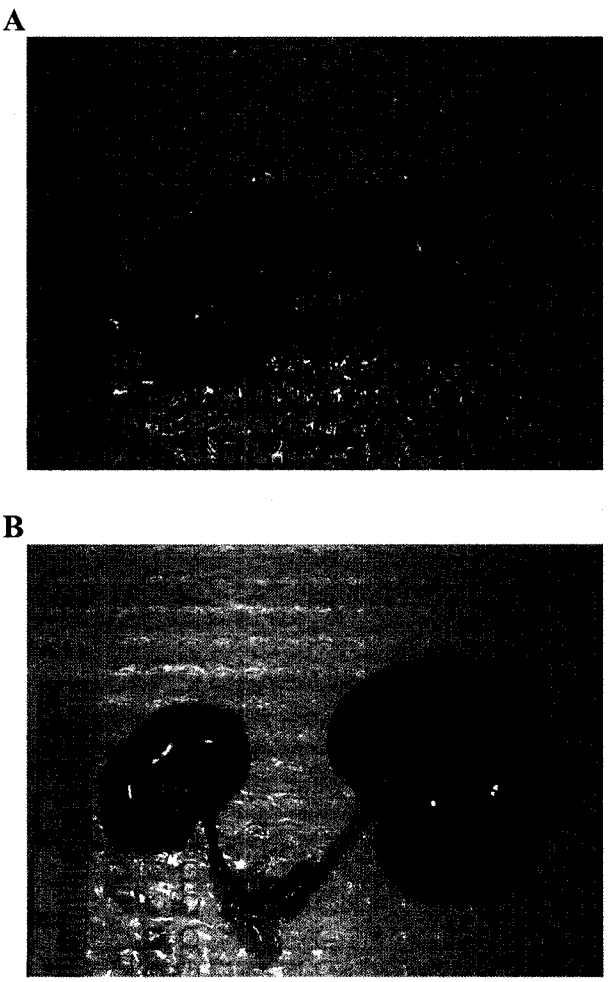

Figure 14: Typical appearance of MISIIR-TAg(+) mouse ovarian tumours at endpoint.

(**A**) ex-vivo ovarian tumours from a MISIIR-TAg(+) mouse treated with UV attenuated VSV intraperitoneally (**B**) ex-vivo ovarian tumours from a MISIIR-TAg(+) mouse treated with wild type VSV intravenously.

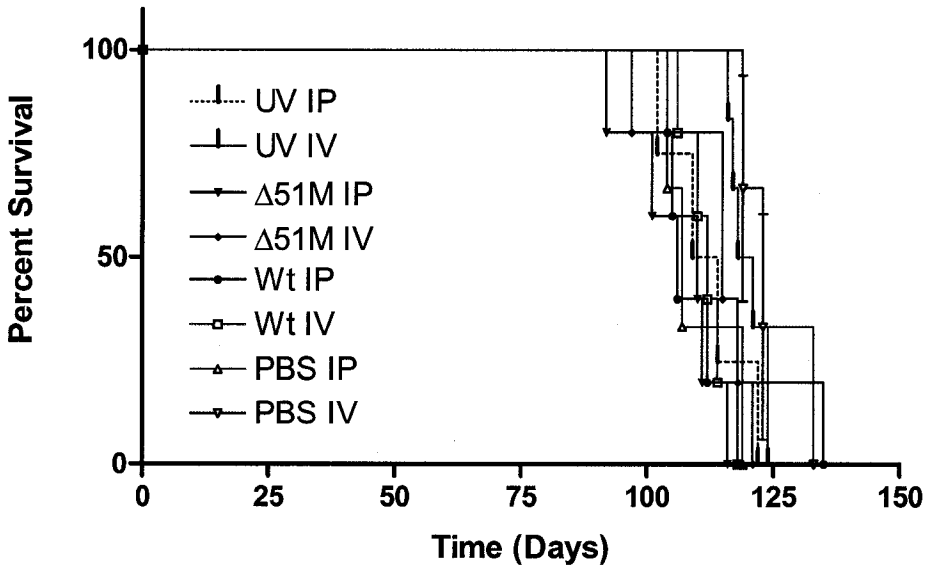

Figure 15: Therapeutic efficacy is not seen in the MISIIR-TAg(+) mice treated with Δ51M or wild type VSV given IP or IV.

Six week old MISIIR-TAg(+) mice were treated with either Δ51M VSV, wild type VSV (Wt), UV attenuated VSV (UV) or PBS by either IP or IV administration. Mice were monitored until endpoint was reached and survival is plotted on a Kaplan-Meier curve. The median times to loss-of-wellness in the control mice were as follows: PBS injected IP was 107 days (n=3) and IV was 123 days (n=3) or UV inactivated VSV injected IP (n=4) was 111.5 days and IV was 119.5 days (n=6). The median time to loss-of-wellness of mice treated with Δ51M VSV IP was 110 days (n=5) or IV was 115 days (n=5). Wild type VSV IP treated mice reached a loss-of-wellness at a median of 106 days (n=5) while wild type VSV IV treated mice the median was 112 days (n=5) Log-rank test was performed and confirmed no significant difference among the groups.

Tumour burden (**figure 16a**) and tumour weights (**figure 16b**) were recorded and compared at endpoint, revealing no statistical differences among treatment groups. Tumour appearance at endpoint was similar between treatment groups. All tumours were well vascularized and encapsulated by the ovarian bursa.

A

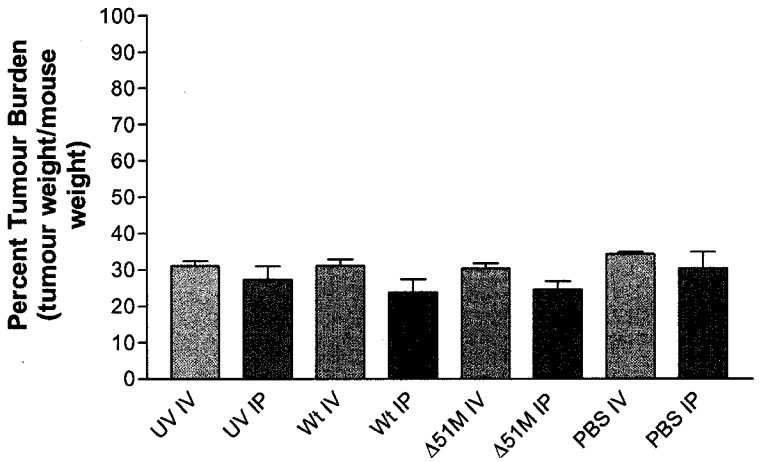

B

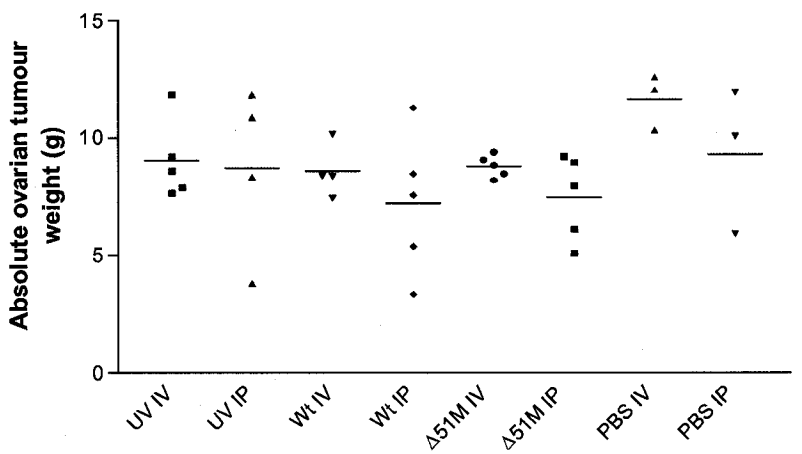

Figure 16: Endpoint tumour burden is similar between all single agent treatment groups.

Six week old MISIIR-TAg(+) mice were treated with either Δ51M VSV, wild type VSV (Wt), UV attenuated VSV (UV) or PBS by either IP or IV administration. Mice were monitored until endpoint was reached. At the time of necropsy MISIIR-TAg mice body weights and tumour weights were measured: (**A**) tumour burden as a percentage of body weight. Each bar represents the average percent tumour burden for each group ± SEM (**B**) absolute tumour weight in grams. Each point represents the combined weight of the left and right tumours of a mouse.

Chapter 4: Results: The combination of Δ 51M VSV and the Histone Deacetylase Inhibitor, MS-275, as a treatment for Ovarian Cancer

The use of VSV as a single agent treatment for therapeutic efficacy in our mouse model of ovarian cancer revealed no significant benefit (Chapter 3). However, options to try to increase the therapeutic efficacy of VSV existed. Our results in Chapter 3, indicated that the tumour cell lines isolated from the MISIIR-TAg(+) mice tumours produce and respond to interferon. This indicated that this ability could play a role in the MISIIR-TAg(+) mice tumour resistance to VSV infection *in vivo*. Therefore, dampening or inhibiting the tumour cells from producing interferon may increase the therapeutic efficacy of VSV treatment *in vitro* and *in vivo*. HDACi have been shown to decrease the interferon production and response of tumour cells *in vitro* (Nunsinzon and Horvath 2003, 2006; Chang *et al.,* 2004; Nguyen *et al.,* 2008; Balakristran *et al.,* 2008) and therefore has the potential to do so *in vivo*. We therefore began investigating the use of the HDACi, MS-275, in combination with Δ51M VSV for the therapeutic treatment of MISIIR-TAg(+) ovarian tumours *in vitro* and *in vivo*.

4.1 Determining the susceptibility of MOSE and MISIIR-TAg tumour cell lines to treatment with MS-275 and Δ51M VSV

Determining the susceptibility of MOSE and MISIIR-TAg tumour cell lines to combination treatment required examing Δ51M VSV alone and MS-275 alone and then in combination for each cell line. An MTS assay was used to determine the cell viability 48 hours post-treatment with each treatment alone or a combination. **Figure 17** shows

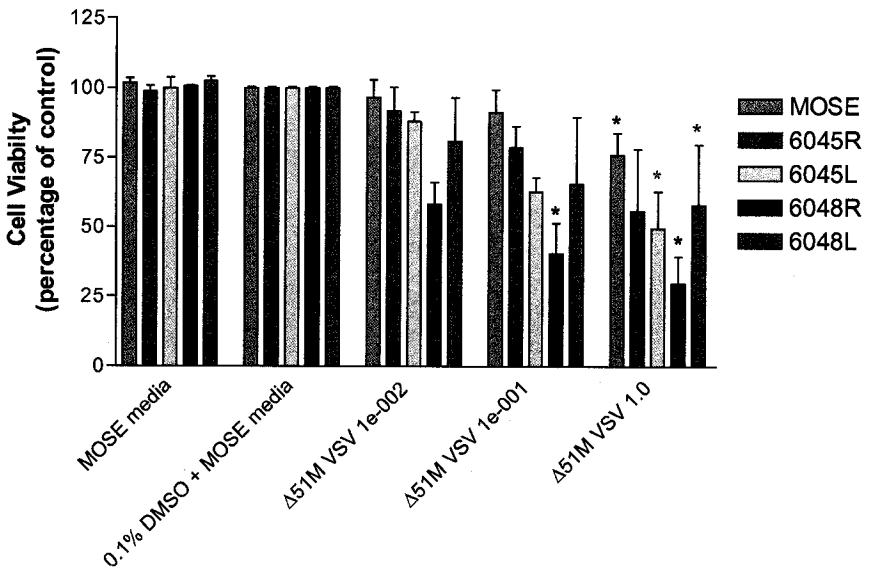

Figure 17: Δ51M VSV oncolysis occurs at an MOI of 1.0 in MOSE and MISIIR-TAg tumour cell lines.

MTS assays were performed 48 hours after MOSE and MISIIR-TAg cells ($3x10^4$) were treated with MOI's (0.01, 0.1, 1.0) of Δ51M VSV. Each bar represents triplicate readings from 3 independent experiments ± SEM, standardized to the value for the control treatment (0.1% DMSO) for that same cell line. An asterisk (*) indicates a statistical significance $p<0.05$ compared to the same cell line at the previous multiplicity of infection.

that Δ51M VSV treatment of each cell line at an MOI of 1.0 causes a significant loss of cell viability in all cell lines compared to the previous MOI of 0.1, as was seen in the previous MTS assays (figure 9a). The histone deacetylase inhibitor, MS-275, caused a tumour cell line specific decrease in cell at the concentrations tested. **Figure 18** shows that all of the MISIIR-TAg tumour cell lines treated with MS-275 have decreased cell viability at a concentration of 4μM, whereas the MOSE cells do not show a significant loss of viability at any of the MS-275 concentrations tested. These results indicate that the MISIIR-TAg tumour cells are more susceptible to MS-275 treatment than normal MOSE cells.

Combining the virus and MS-275 treatments resulted in a tumour cell specific loss of cell viability. **Figures 19** and **20** show that three of the four MISIIR-TAg tumour cell lines (6045 R, 6045 L, 6048 R) have a significant loss of viability after combination treatment, compared to either Δ51M VSV (MOI 0.01 or MOI 0.1) or MS-275 (4μM) treatment alone, whereas MOSE cells do not show a significant decrease with combination treatment when compared to Δ51M VSV or MS-275 treatment alone. These results show that the combination of VSV and MS-275 treatments can cause up to 75% cell death in mouse ovarian cancer cell lines.

Images taken of MOSE and MISIIR-TAg tumour cell lines 24 hours after treatment with the Δ51M VSV GFP show that there are more GFP-positive areas in the combination-treated cells than in cells treated with Δ51M VSV alone, suggesting that more replication of the virus is occurring in the combination treated MISIIR-TAg tumour cells (**figure 21**). To quantify this, cell supernatants were collected 48 hours after Δ51M VSV infection from all treatment groups. Supernatants were then titered for

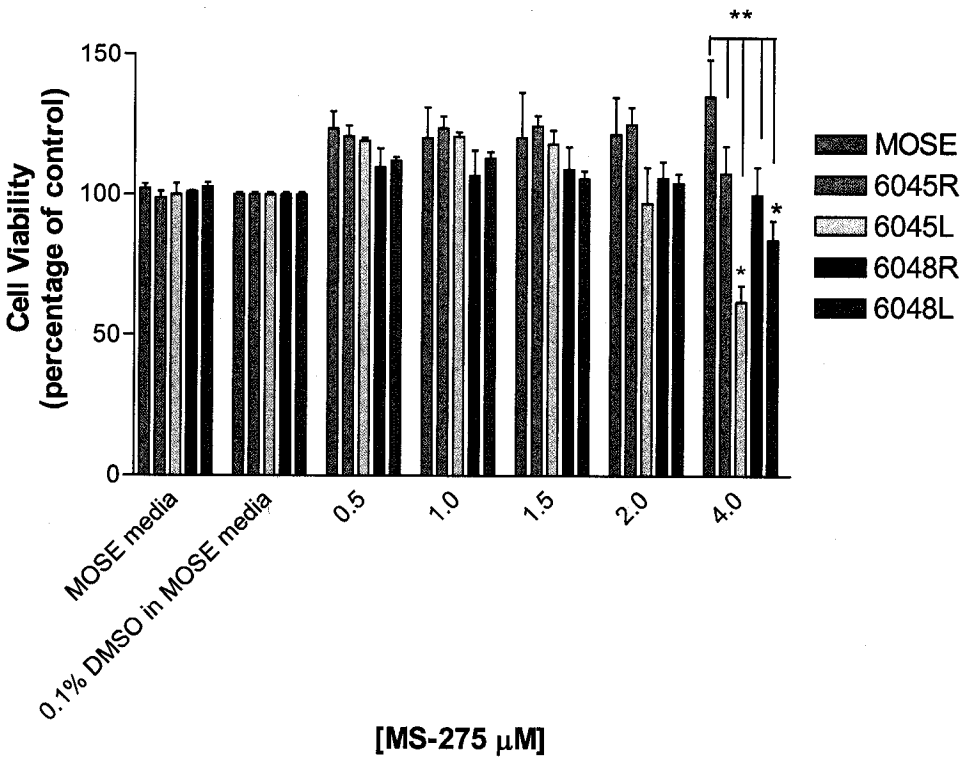

Figure 18: MS-275 at 4μM decreased the cell viability of all MISIIR-TAg tumour cell lines but not MOSE cells.

MTS assays were performed 48 hours after MOSE and MISIIR-TAg tumour cell lines ($3x10^4$) were treated with concentrations of MS-275 (0.5, 1, 1.5, 2, 4 μM). One asterisk (*) indicates statistical significance of $p< 0.001$ compared to the same cell line at the previous concentration of MS-275 and two asterisks (**) indicates statistical significance of $p<0.05$ compared to MOSE cells at 4μM.

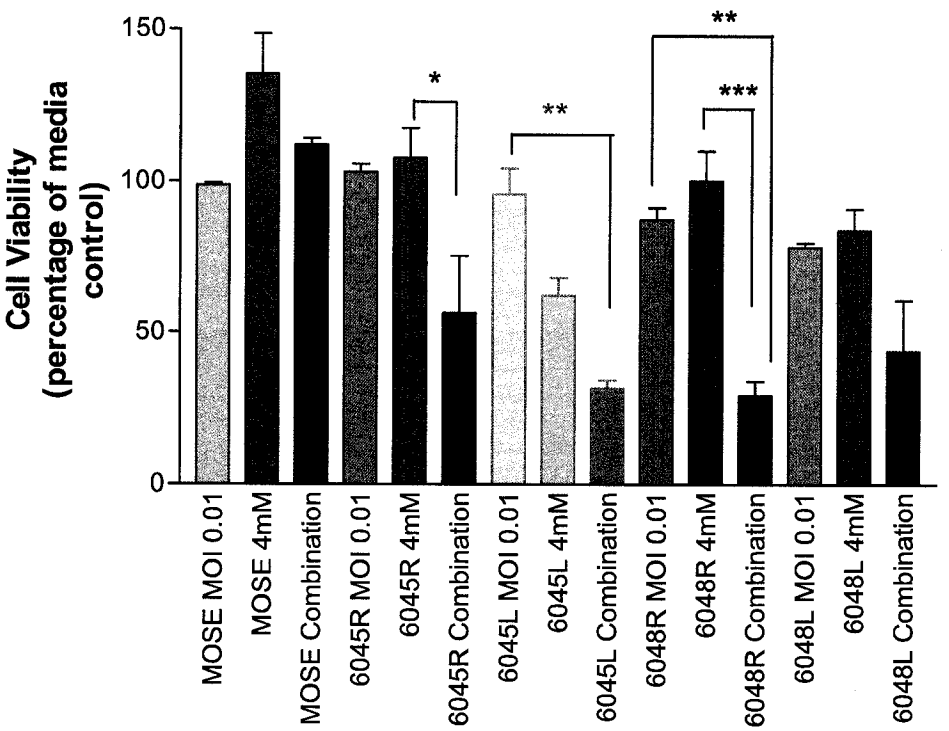

Figure 19: The combination treatment of MS-275 (4μm) and Δ51M VSV (MOI 0.01) significantly decreased the cell viability of the MISIIR-TAg cell lines compared to MS-275 or Δ51M VSV alone.

MTS assays were performed 48 hours after MOSE and MISIIR-TAg tumour cell lines ($3x10^4$) were treated with either Δ51M VSV (MOI 0.01), MS-275 (4uM) or both. Each bar represents triplicate readings from three independent experiments ± SEM, standardized to the same cell line without treatment. One asterisk (*) indicates statistical significance at $p<0.05$, two asterisks (**) indicates a statistical significance at $p<0.01$ and three asterisks (***) indicates a statistical significance at $p<0.001$.

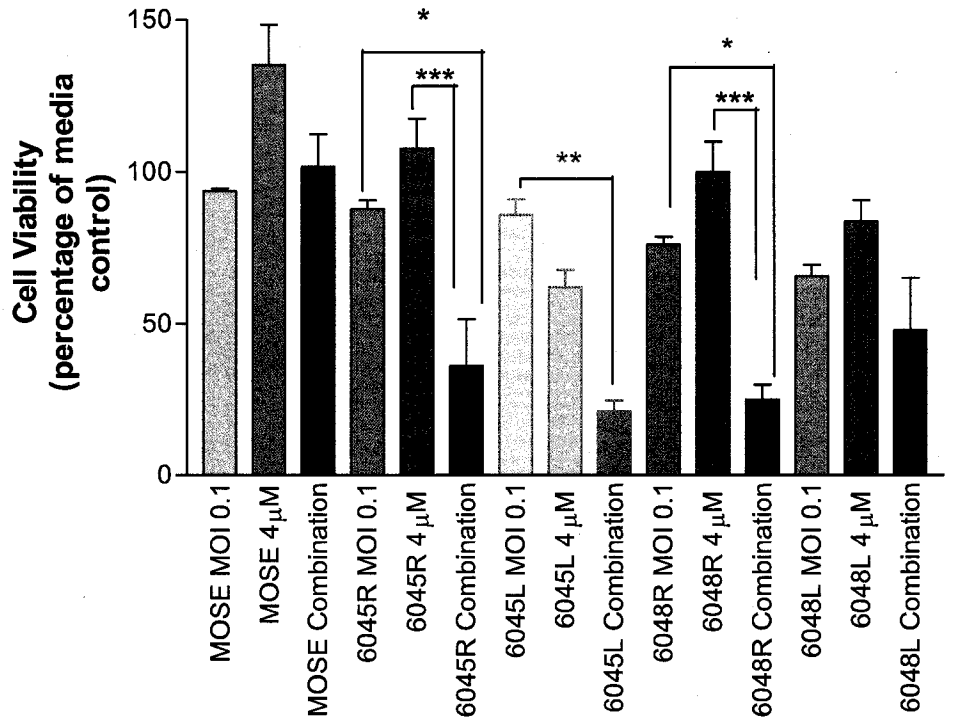

Figure 20: The combination treatment of MS-275 (4μm) and Δ51M VSV (MOI 0.1) significantly decreased the cell viability of the MISIIR-TAg cell lines compared to MS-275 or Δ51M VSV alone.

MTS assay results 48 hours after MOSE and MISIIR-TAg tumour cell lines ($3x10^4$) were treated with either Δ51M VSV (MOI 0.1), MS-275 (4uM) or both. Each bar represents triplicate readings of three independent experiments ± SEM. One asterisk (*) indicates statistical significance of $p<0.05$, two asterisks (**) indicates a statistical significance of $p<0.01$ and three asterisks (***) indicates a statistical significance of $p<0.001$.


Δ51M VSV alone
Combination
MOSE
6045 R
6045 L
6048 R
6048 L

Figure 21: Combination treatment of MS-275 and Δ51M VSV increases viral entry and replication in MISIIR-TAg tumour cell lines.

MOSE and MISIIR-TAg tumour cell lines were treated with MOSE media, MS-275 (4μM), Δ51M VSV (MOI 0.01) or the combination of MS-275 (4μM) and Δ51M VSV (MOI 0.01). Images were taken 24 hours post VSV infection. Images of MOSE media and MS-275 treated cells are not shown.

VSV. **Figure 22** shows that there are no significant differences in the amount of Δ51M VSV present when cells were infected with Δ51M VSV alone or in combination with MS-275. However, there is a trend that suggests that there is an increase in viral particles in the combination-treated cells compared to cells treated with Δ51M VSV alone.

4.2 Determining the interferon response of MISIIR-TAg cells to Δ51M VSV infection with and without MS-275

Given that over 80% of tested human cancer cell lines have defects in their interferon response, and that MISIIR-TAg tumour cells are interferon-responsive, it was necessary to determine if, unlike most human cancer cells, the MISIIR-TAg tumour cells could produce interferon in response to viral infection. This is important for understanding the poor ability of Δ51M VSV to infect MISIIR-TAg tumour cells and could explain the inability of virus treatment to impact on MISIIR-TAg mouse survival. The ability of MISIIR-TAg tumour cell lines to produce interferon in response to viral infection was therefore determined. MOSE cells and MISIIR-TAg cell lines were treated with MOSE media, MOSE media +0.1%DMSO, MS-275, Δ51M VSV or combination treatment of Δ51M VSV and MS-275. Cell supernatants were then collected 24 (MOI 1) or 48 (MOI 0.1) hours post-treatment and assessed for interferon-α content by ELISA. The results indicate that MOSE and all the MISIIR-TAg tumour cell lines produce similar amounts of interferon-α in response to Δ51M VSV infection (**figure 23**). Importantly, no significant differences were seen in the amount of interferon-α produced when cells were treated with Δ51M VSV alone or in combination with MS-275.

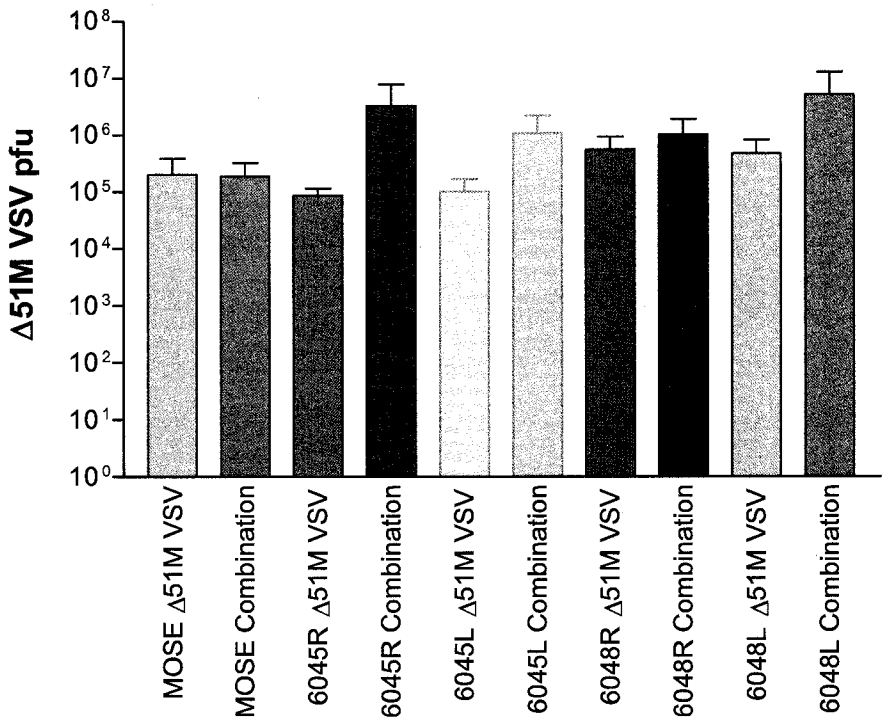

Figure 22: MOSE and MISIIR-TAg tumour cell lines do not produce significantly increased amounts of Δ51M VSV when comparing MS-275 and Δ51M VSV treatment to Δ51M VSV alone.

Cell supernatants were collected 48 hours after MOSE and MISIIR-TAg cells were cultured without treatment, in MOSE media +0.1%DMSO (solvent control for MS-275), or in MOSE media + MS-275 (4μM), Δ51M VSV (MOI 0.1). The cell supernatants were then titered using plaque assay. Each bar represents duplicate samples from three independent experiments ± SEM. Media controls and MS-275 alone when titered had no plaques (data not shown).

A

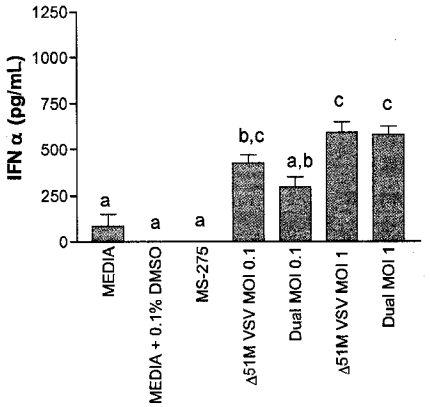
IFN α (pg/mL)
1250
1000
750
500
250
0
a
a
a
b,c
a,b
c
c
MEDIA
MEDIA + 0.1% DMSO
MS-275
Δ51M VSV MOI 0.1
Dual MOI 0.1
Δ51M VSV MOI 1
Dual MOI 1

B

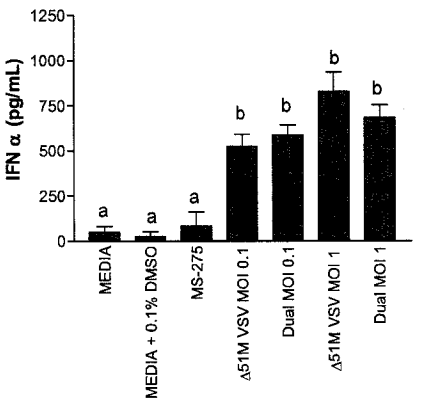
IFN α (pg/mL)
1250
1000
750
500
250
0
a
a
a
b
b
b
b
MEDIA
MEDIA + 0.1% DMSO
MS-275
Δ51M VSV MOI 0.1
Dual MOI 0.1
Δ51M VSV MOI 1
Dual MOI 1

C

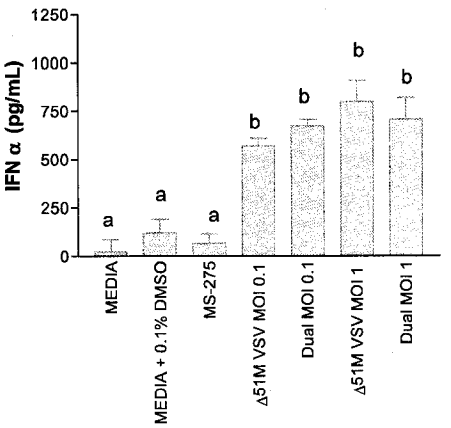
IFN α (pg/mL)
1250
1000
750
500
250
0
a
a
a
b
b
b
b
MEDIA
MEDIA + 0.1% DMSO
MS-275
Δ51M VSV MOI 0.1
Dual MOI 0.1
Δ51M VSV MOI 1
Dual MOI 1

D

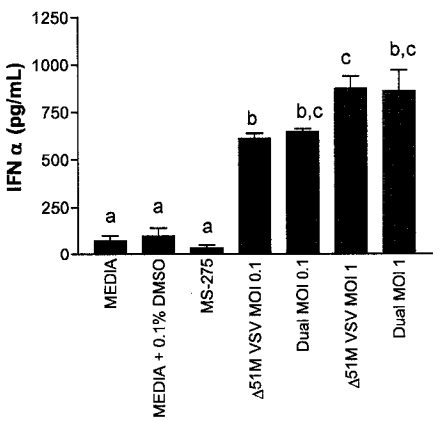
IFN α (pg/mL)
1250
1000
750
500
250
0
a
a
a
b
b,c
c
b,c
MEDIA
MEDIA + 0.1% DMSO
MS-275
Δ51M VSV MOI 0.1
Dual MOI 0.1
Δ51M VSV MOI 1
Dual MOI 1

E

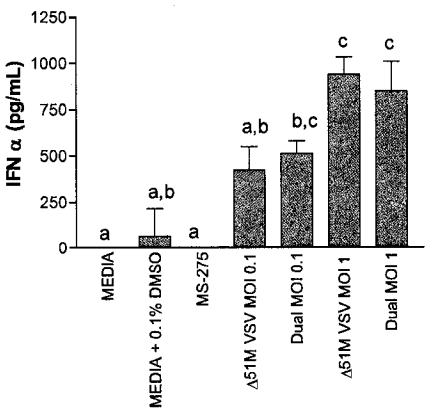
IFN α (pg/mL)
1250
1000
750
500
250
0
a
a,b
a
a,b
b,c
c
c
MEDIA
MEDIA + 0.1% DMSO
MS-275
Δ51M VSV MOI 0.1
Dual MOI 0.1
Δ51M VSV MOI 1
Dual MOI 1

Figure 23: MOSE and MISIIR-TAg tumour cell lines produce interferon-α in response to Δ51M VSV infection.

Cell supernatants from MOSE and MISIIR-TAg tumour cell lines were collected 24 hours (MOI 1) or 48 hours (MOI 0.1) post-treatment with either no treatment, MOSE media +0.1%DMSO (solvent control for MS-275), MOSE media + MS-275 (4μM), Δ51M VSV (MOI 0.1) or both. The supernatants were then assessed in an interferon-α ELISA. Each bar represents mean values ± SEM from three independent experiments performed in duplicate. (**A**) MOSE cells; bars with different letters denote statistically significant differences at $p<0.01$. (**B**) 6045 R MISIIR-TAg tumour cells; bars with different letters denote statistically significant differences at $p<0.001$. (**C**) 6045 L MISIIR-TAg tumour cells; bars with different letters denote statistically significant differences at $p<0.01$. (**D**) 6048 R MISIIR-TAg tumour cells; bars with different letters denote statistically significant differences at $p<0.05$. (**E**) 6048 L MISIIR-TAg tumour cells; bars with different letters denote statistically significant differences at $p<0.05$.

4.3 Determining the effect of TAg on the interferon response

MISIIR-TAg mice are tumourigenic due to the constitutive expression of SV40 T-antigen, and the experimental results shown in Figure 3 confirmed that the cell lines derived from these tumours continue to express TAg protein, albeit at different levels. The observation that the MISIIR-TAg tumour cell lines that express lower amounts of TAg are more susceptible to VSV infection (Figure 7, 9a), suggests that high levels of TAg expression may decrease the susceptibility of the cells to VSV infection. We therefore hypothesized that TAg expression may be increasing the interferon production of the tumour cells.

In order to address the role of TAg in interferon production more directly, MOSE cells from CAG-LS-TAg mice were used to determine the levels of interferon-α expression in the presence or absence of TAg expression. CAG-LS-TAg mice carry a transgene in which a ubiquitous promoter, CAG, drives expression of a lacZ stop (LS) sequence followed by the TAg gene. The stop sequence is flanked by loxP sites and is excised following exposure to Cre recombinase, allowing the expression of large T-antigen. Thus, in order to induce T-antigen expression, MOSE cells were removed from the ovaries of CAG-LS-TAg mice, and a subset of the cells were infected with an adenovirus expressing Cre recombinase (AdCre; control cells were incubated with AdEGFP). Cell lysates were then probed for SV40 large T-antigen to confirm induced expression of the transgene. **Figure 24** demonstrates that CAG-LS-TAg MOSE cells that were not exposed to AdCre do not express SV40-TAg (lane 2) whereas the MOSE cells that were infected with AdCre (CAG-TAg) did express SV40-TAg (lane 3). After transgene expression was verified, CAG-LS-TAg and CAG-TAg cells were treated with

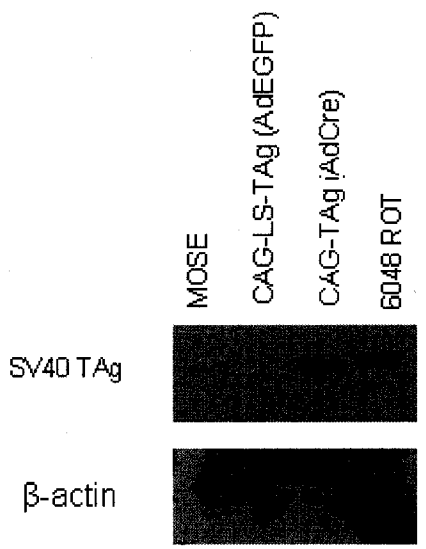

Figure 24: CAG-LS-TAg MOSE cells infected with adenovirus expressing Cre-recombinase (AdCre) express SV40 large T-antigen.

Ovarian surface epithelial cells that were retrieved from CAG-LS-TAg transgenic mice were infected in vitro with AdCre or AdEGFP. Determination of the expression of SV40 large T-antigen in the uninfected (CAG-LS-TAg) or infected (CAG-TAg) cells was done using SDS-PAGE and immunoblotting. Forty μg of protein was separated on an SDS gel and immunoblotted for SV40 large T-antigen. β-actin was used as a loading control. MOSE cells were used as a negative control and the MISIIR-TAg tumour cell line, 6048 right ovarian tumour (ROT) was used as a positive control.

MOSE media, MOSE media +0.1%DMSO, MS-275, Δ51M VSV or the combination treatment of Δ51M VSV and MS-275. Cell supernatants were then collected 24 hours post-treatment and assayed for levels of interferon-α by ELISA. The results show that both TAg-expressing and non-expressing MOSE cells produced interferon-α in response to Δ51M VSV infection at similar levels (**figure 25**). Combination treatment with both Δ51M VSV and MS-275 did not result in significantly altered levels of interferon-α, in either cell type (figure 25).

4.4 Determining the dose of combination treatment to use in the MISIIR-TAg(+) mice

The results thus far have shown that the combination treatment of VSV and MS-275 has efficacy in cell killing when tested with mouse and human ovarian cancer cell lines. Before beginning the testing of the combination treatment on tumour burden and survival experiments *in vivo*, the optimal dosing regimen had to be determined. This required three steps: first, determining the appropriate dose of MS-275; second, determining the combination treatment doses (including the appropriate doses of virus and MS-275); and finally, determining the number and frequency of treatments. To determine the optimal dose and frequency for MS-275, MISIIR-TAg mice were treated with one injection of either 12mg/kg or 24mg/kg IP of MS-275 and then sacrificed at 0, 4, 8, 12, 24, and 48 hours post-injection, at which point the tumours were excised in order to determine the time course of histone acetylation. Acid-extraction of histones was carried out on the tumour lysates and western blot analysis for histone 4 acetylation was performed. The time course of histone 4 acetylation in the tumours of MISIIR-TAg mice

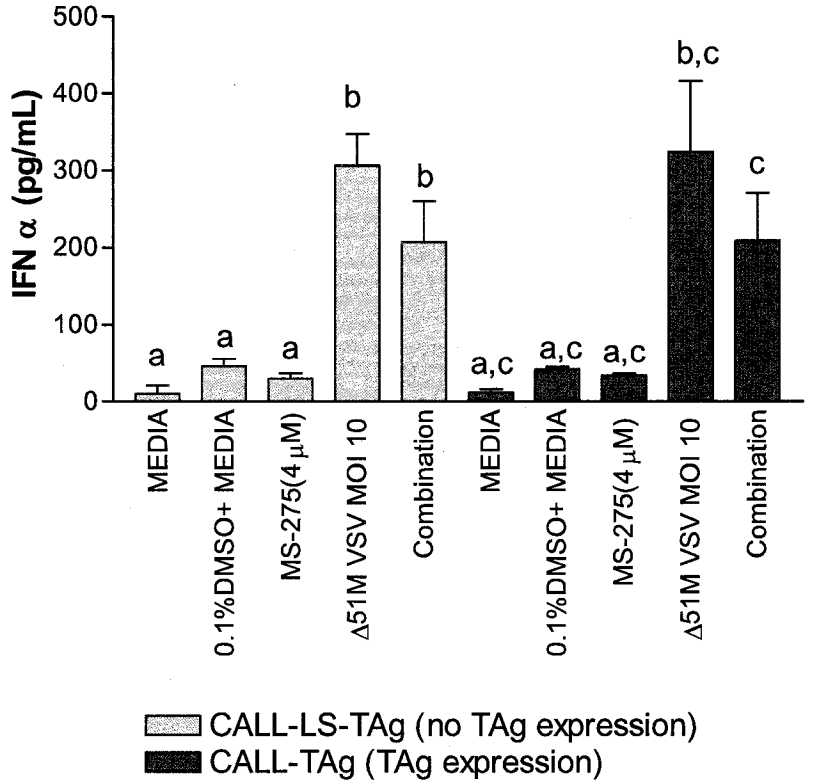

Figure 25: Both CAG-LS-TAg and CAG-TAg MOSE cells produce interferon-α in response to Δ51M VSV infection.

Cell supernatants from CAG-LS-TAg and CAG-TAg MOSE cells were collected after 24 hours of culture with no treatment, in MOSE media +0.1%DMSO (solvent control for MS-275), or in MOSE media + MS-275 (4μM), Δ51M VSV (MOI 10) or both (combination). The supernatants were tested in an interferon-α ELISA. Each bar represents mean values ± SEM of three independent experiments performed in duplicate. Bars with different letters indicate significant differences at $p<0.05$.

treated with either dose of MS-275 indicates that maximal hyperacetylation occurs by 4 hours post-injection (**figure 26**). The hyperacetylation continues until at least 48 hours post-injection in the tumours of the mice treated with 24mg/kg IP of MS-275. The tumours of mice treated with 12mg/kg IP of MS-275 showed continued hyperacetylation up to 24 hours with a decrease in acetylation at 48 hours. However, even the lower level of acetylation on H4 in the tumours of mice at 48 hours post-injection remains higher than that of control tumours (vehicle). These results indicate that a dose of 12 mg/kg MS-275 every 48 hours is sufficient to maintain hyperacetylation within the tumours of the MISIIR-TAg mice.

IVIS imaging was used to determine the appropriate dose of virus to deliver per injection in combination with the optimal MS-275 dose. Ten week old transgenic MISIIR-TAg(+) and non-transgenic MISIIR-TAg(-) mice were given either Δ51M VSV ($1x10^7$pfu/100μl, IP), MS-275 (12mg/kg, IP) or the combined treatment of Δ51M VSV at either $5x10^7$pfu/100μl or $1x10^7$pfu/100μl and MS-275 (12mg/kg) and then imaged 24 hours later. **Figure 27** (the left upper and lower panels) indicates that the tumours of mice receiving the combination treatment at both viral doses are able to sustain viral replication. However, mice that do not express the TAg transgene that were treated at the high viral dose also seem to display viral replication in the vicinity of the ovaries (mouse #2), which is not evident when the ovaries are removed from the animal and imaged in isolation (lower panel). The bottom-right panel indicates that the TAg expressing mouse that received only virus (mouse#5) has some viral replication in the tumour, while the upper right panel shows that TAg expressing and non-expressing mice treated with MS-275 alone do not show viral replication at 24 hours post-treatment. Importantly, the mice

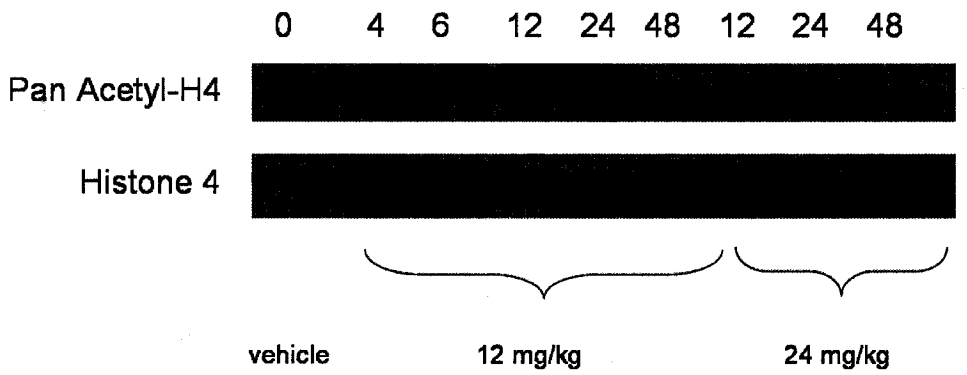

Figure 26: Histone 4 is hyperacetylated in ex-vivo tumour lysates from MISIIR-TAg(+) mice that were treated with MS-275.

MISIIR-TAg mice were treated with one injection of either 12mg/kg or 24mg/kg intraperitoneally of MS-275 and then sacrificed at 0, 4, 8, 12, 24, and 48 hours post-injection, at which point tumours were excised in order to determine the time course of acetylation. Acid-extraction of histones was carried out on the tumour lysates and western blot analysis for histone 4 acetylation was performed using SDS-PAGE and immunoblot. Forty μg of protein was separated on an SDS gel and immunoblotted for histone 4 acetylation. Histone 4 protein expression was used as a loading control.

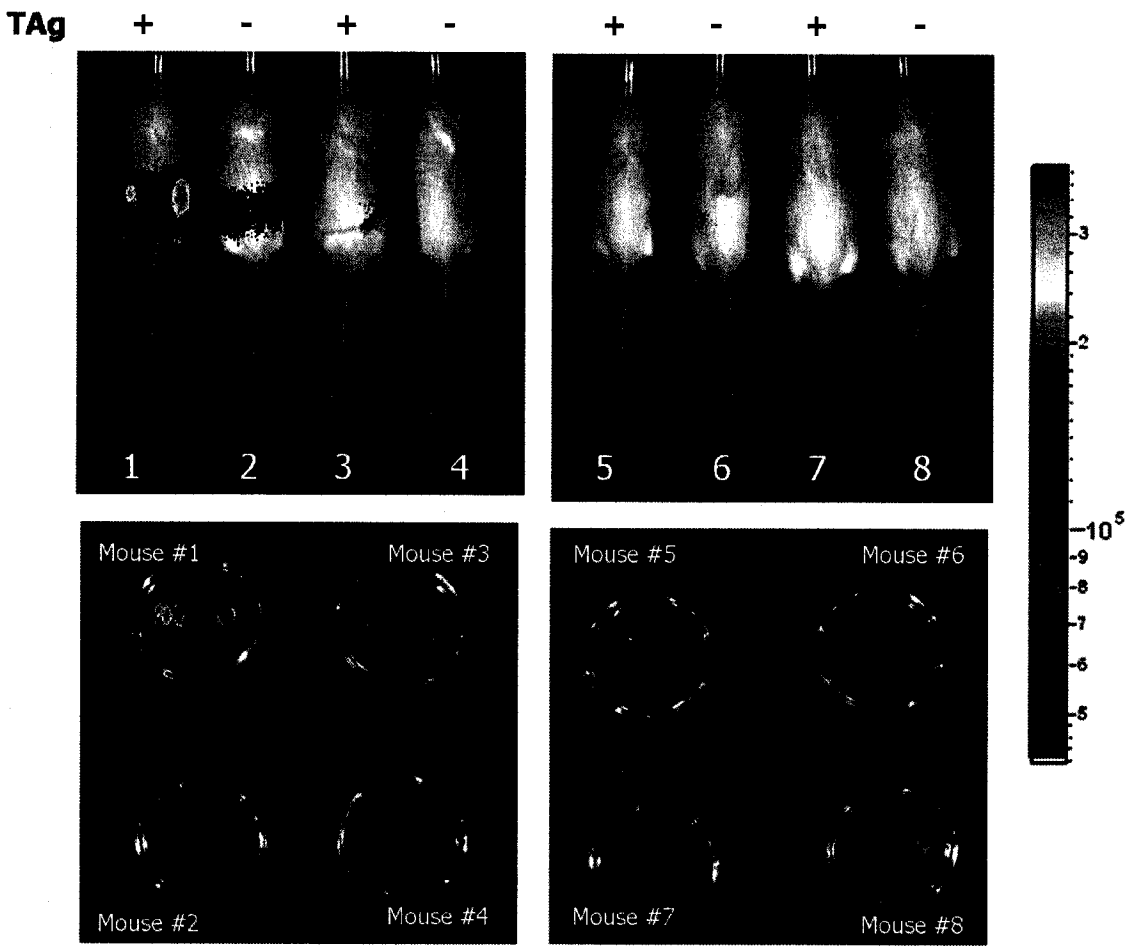

Figure 27: Treatment of MISIIR-TAg(+) mice with both MS-275 and Δ51M VSV allows for sustained Δ51M VSV replication in the ovarian tumours.

Ten week old MISIIR-TAg(-) and MISIIR-TAg(+) mice were given either Δ51M VSV ($1x10^7$pfu/100μl, IP; mice 5 and 6), MS-275 (12mg/kg, IP; mice 7 and 8) or the combined treatment of Δ51M VSV at either $5x10^7$pfu/100μl (mice 1 and 2) or $1x10^7$pfu/100μl (mice 3 and 4) and MS-275 (12mg/kg). Whole mice (top images) and ex-vivo tumours of the same mice (bottom images) were imaged using an IVIS system 24 hours after viral injection.

that received the dual treatment at the higher dose, mouse#1 and mouse #2, were morbidly sick displaying respiratory distress, hunching and lack of mobility all endpoint criteria.

The tumours from the mice that were imaged above were then taken and analyzed for viral content by plaque assay (**figure 28**). Titering tumours (TAg+) and ovaries (TAg-) from mice receiving the combination treatment at the higher viral dose of $5x10^7$pfu/100µl indicates that there is viral replication in both the tumours (TAg+) and in the ovaries (TAg-), with a 3-log difference in titer between normal ovaries and tumours. Titering of the tumours (TAg+) and ovaries (TAg-) from the MISIIR-TAg mice treated with the combination treatment with a lower viral dose of $1x10^7$pfu/100µl indicates that there is viral replication in the tumours (TAg+) but not in the ovaries (TAg-) of these mice. There is also some viral replication in the tumours (TAg+) of mice treated with only the virus. Notably, this has been the only instance that tissue titering has shown a significant viral load in the tumours of mice treated with virus alone. As expected, no virus was found in the tumours (TAg+) and ovaries (TAg-) of mice receiving MS-275 alone.

From these IVIS imaging and tumour titering experiments, it was determined that the lower dose of Δ51M VSV ($1x10^7$pfu/100µl) in combination with MS-275 (12mg/kg) would be used for the *in vivo* survival studies. It was also determined that 3 doses of both treatments a week would be sufficient for maintaining maximal acetylation in the tumours and delivering a therapeutic amount of VSV to the tumours.

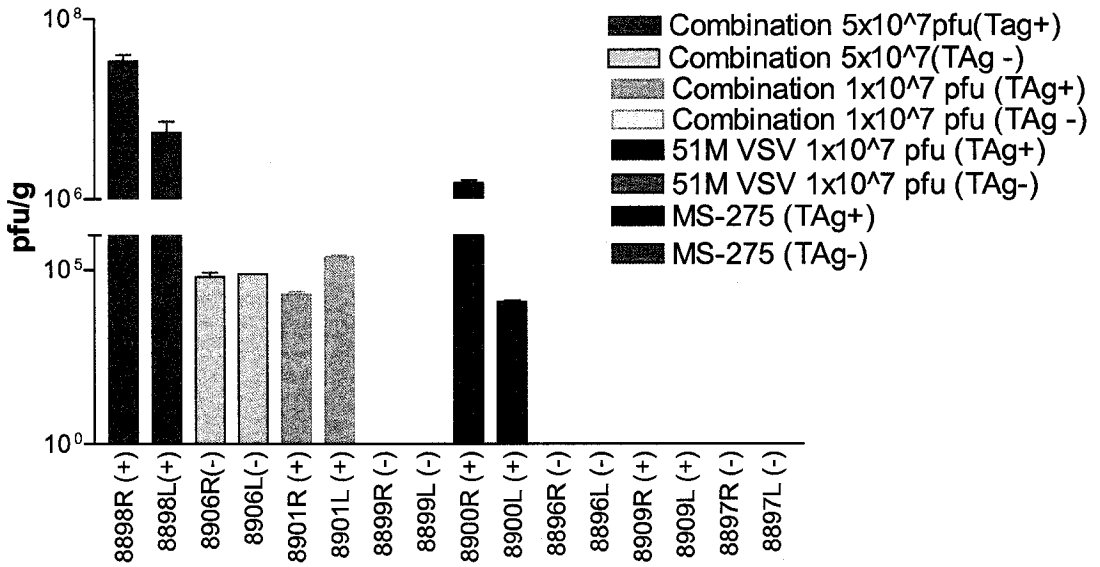

Figure 28: Δ51M VSV infectious particles are found in the MISIIR-TAg(+) mice treated with both MS-275 and Δ51M VSV.

Ex-vivo right and left tumours (+) or ovaries (-) from transgenic and non-transgenic MISIIR-TAg mice, respectively, that were treated with either Δ51M VSV (1x10^7pfu IP), MS-275 (12mg/kg) or combination treatment (12 mg/kg MS-275 IP and either 5x10^7pfu or 1x10^7 pfu Δ51M VSV IP) were plaque assayed in order to determine Δ51M VSV levels in the tumours. The bars represent the average of two plaque assays per tumour.

4.5 Effects of Δ51M VSV and MS-275 on the tumour burden and survival of MISIIR-TAg(+) mice

The dose of combination treatment determined in *4.4* was then used to examine the therapeutic efficacy of the treatment by completing a survival study. MISIIR-TAg mice at 10 weeks of age were treated 3 times over the course of one week with one of four treatments: vehicle, vehicle and Δ51M VSV IP, MS-275 alone, and MS-275 in combination with Δ51M VSV IP. Three mice from each group were sacrificed one week after the last treatment, the tumours were excised and weighed, and tumour burden was compared between groups. **Figure 29a** and **29b** reveal that no significant differences in tumour burden were seen between treatment groups; however there is a notable trend indicating that mice treated with the combination treatment have a reduced tumour burden one week post-treatment compared to vehicle treated mice (29a: p=0.06; 29b: p=0.078). H&E sections of the tumours from each treatment group revealed no obvious differences in tumour morphology 1 week post-treatment (**figure 30**). All tumours were encapsulated and highly vascularized.

The remaining 8 mice per group were monitored until they reached a survival endpoint, which included large, palpable masses, abdominal distention, a lack of mobility and an increased respiration rate. The presentation of the MISIIR-TAg mice when they reached their loss of wellness endpoint was similar in all treatment groups. Necropsy revealed that all mice had developed bilateral ovarian tumours. The median time to loss-of-wellness in the control mice was 124.5 days. The median time to loss-of-wellness of mice treated with Δ51M VSV IP was 109 days (n=8), MS-275 IP was 128.5 days (n=8)

A

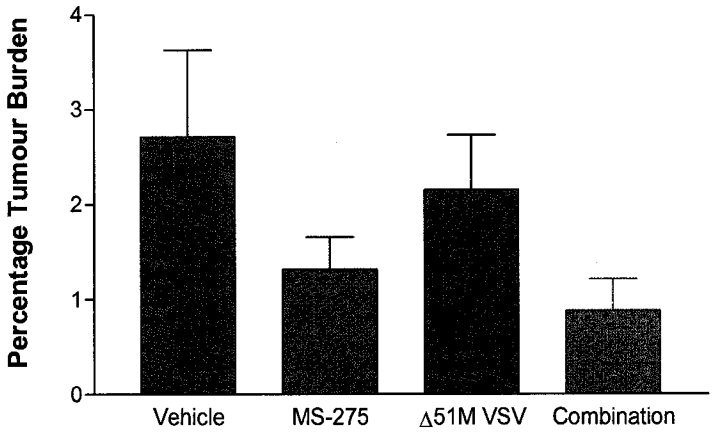

B

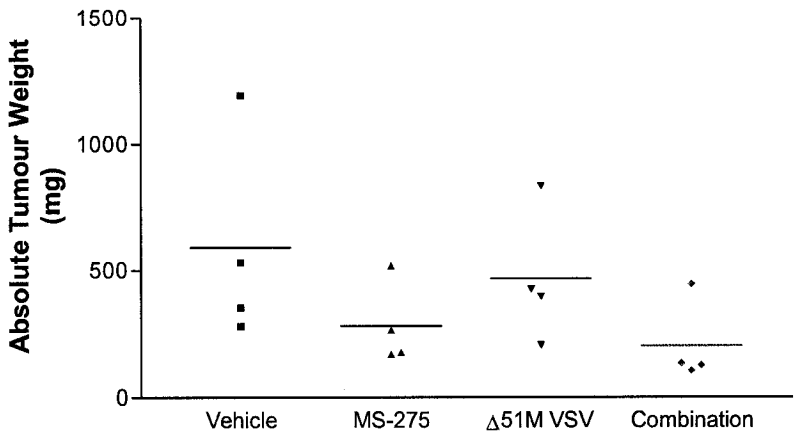

Figure 29: Treatment of MISIIR-TAg(+) mice with Δ51M VSV alone, MS-275 alone or both in combination does not decrease the tumour burden of mice 1 week after treatment.

Ten week old MISIIR-TAg mice were treated with vehicle, MS-275, Δ51M VSV or the combination of the two, three times over the course of one week and then were sacrificed. Ovarian tumours weights were then measured and recorded for comparison; (**A**) tumour burden as a percentage of body weight. Each bar represents the average percent tumour burden for each group ± SEM (**B**) absolute tumour weight. Each point represents the combined weight of the left and right tumours of a mouse.

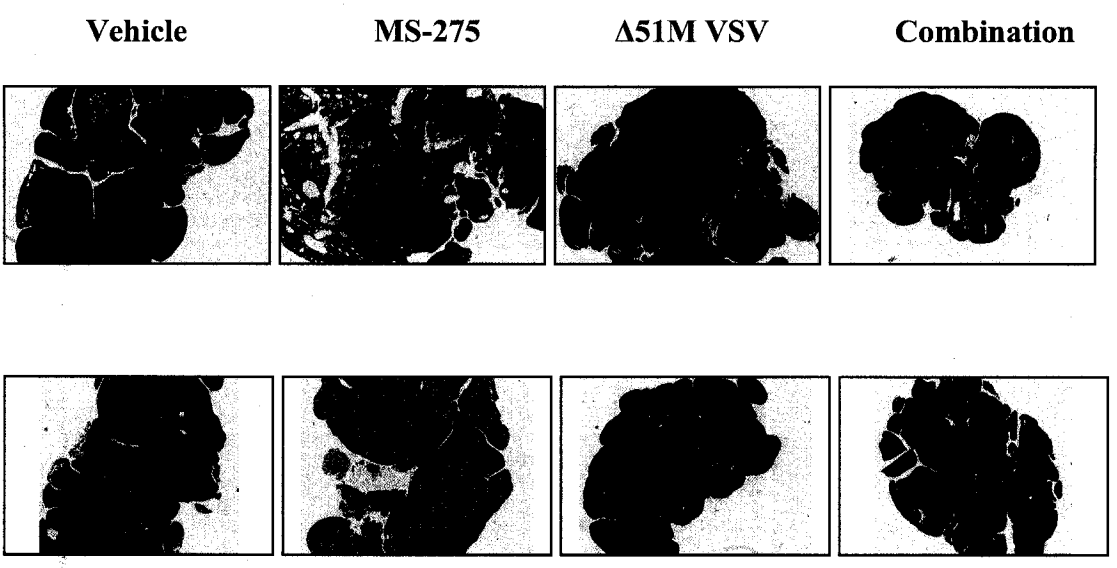

Figure 30: H&E images of the ex-vivo tumours of the MISIIR-TAg(+) mice after 1 week of single or combination treatment reveal no obvious morphological differences between treatment groups.

Top row: right ovarian tumours. Bottom row: Left ovarian tumours.

and the combination treatment was 129.5 days (n=8). Comparison of the survival times of the treatment groups revealed no significant differences between the control group and the treatment groups (**figure 31**). However, both the MS-275 alone and the combination treatment significantly prolonged survival compared with Δ51M VSV alone.

Tumour burden (**figure 32a**) and tumour weights (**figure 32b**) were recorded and compared at endpoint, both revealing no significant difference between control mice and single or combination treated mice. Importantly, both revealed a trend indicating that combination treated mice have a decreased tumour burden at endpoint compared to control mice.

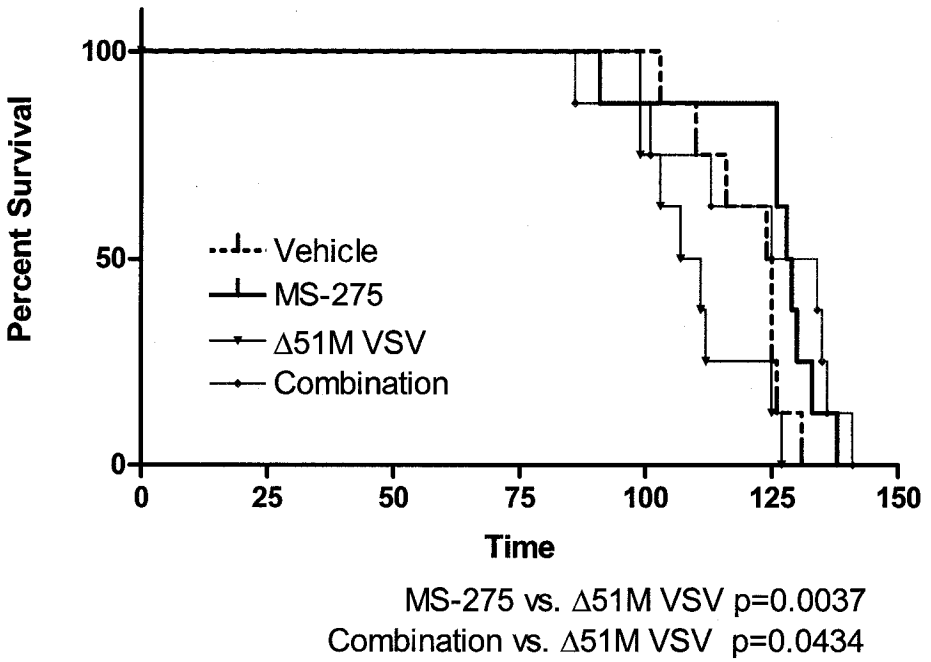

Figure 31: The combined treatment of MS-275 and Δ51M VSV has no therapeutic efficacy in MISIIR-TAg mice with ovarian tumours.

Ten week old MISIIR-TAg tumour bearing mice were treated with either phosphate buffered saline (PBS), Δ51M VSV ($1x10^7$; IP), MS-275 (12mg/kg; IP) or the combination of Δ51M VSV ($1x10^7$; IP) and MS-275 (12mg/kg; IP), 3 times over the course of one week. Mice were then monitored until endpoint was reached. The median time to loss-of-wellness in the control mice was 124.5 days. The median time to loss-of-wellness of mice treated with Δ51M VSV was 109 days (n=8), MS-275 was 128.5 days (n=8) and the combination treatment was 129.5 days (n=8). Log-rank test was performed.

A

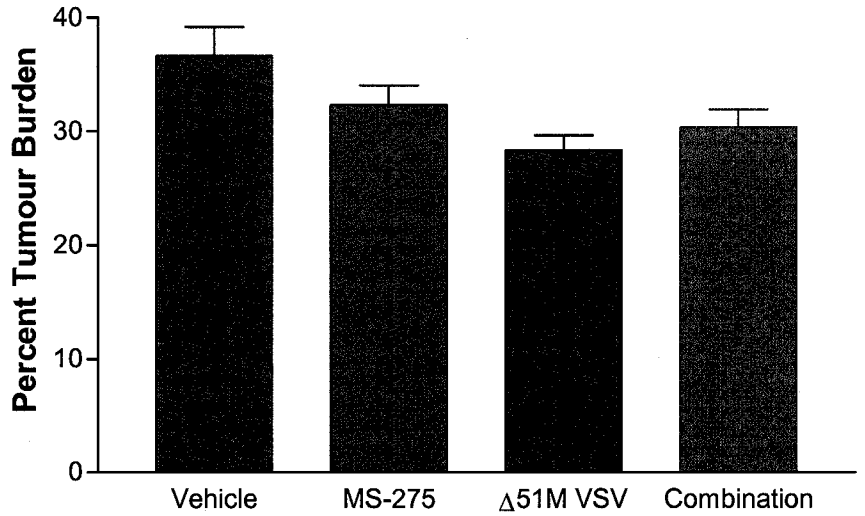

B

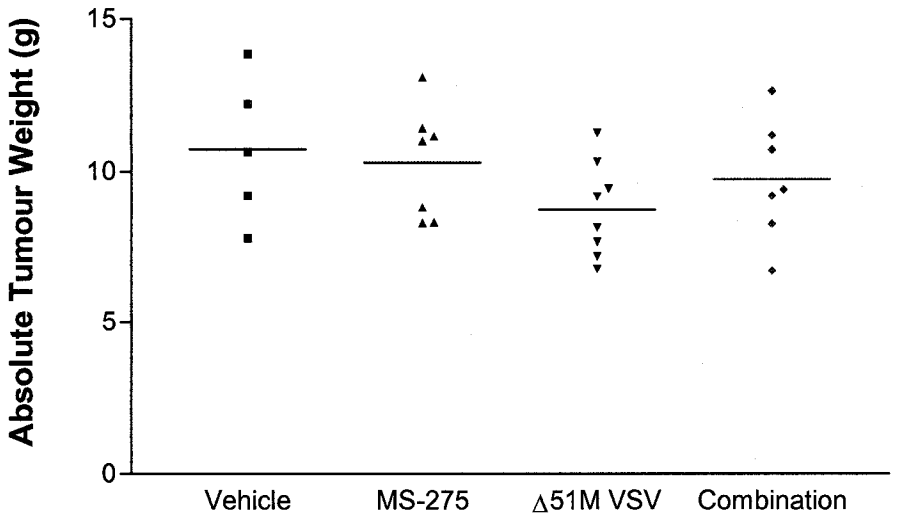

Figure 32: Tumour burden at survival endpoint of the MISIIR-TAg(+) mice was not statistically significant between single and combination treatment groups.

At the time of necropsy (endpoint), the body weights and tumour weights of the MISIIR-TAg(+) mice were measured. (A) percent tumour burden. Each bar represents the average percent tumour burden for each group ± SEM (B) absolute tumour weight in grams. Each point represents the combined weight of the left and right tumours of a mouse.

Chapter 5: Discussion

Ovarian cancer affects 1 in 70 women in the Western world and is the fifth leading cause of cancer death in Canadian women. The current treatments for ovarian cancer lack long-term therapeutic benefit as is evident by the dismal 5-year survival rate of only 30-40%. There can be no doubt that novel treatments are required to aid and perhaps even replace those therapies that are currently in use. An interesting novel cancer therapeutic is the oncolytic virus, VSV. VSV as a single agent has been tested extensively *in vitro* as well as *in vivo,* and has so far provided promising results. However, there are a number of tumour cell lines that are refractive to VSV infection which is thought to be due to a lack in interferon pathway defects. Thus, exploration into combination treatments with VSV and reversible inhibitors of the innate anti-viral response is currently underway. Importantly, this project is the first to examine the therapeutic efficacy of VSV in a transgenic mouse model. This study began by investigating VSV as a single agent and has ended with data to support the use of combination treatment with an HDAC inhibitor to enhance the therapeutic benefit of VSV in a mouse model of ovarian cancer.

In vitro a variety of responses have been observed from the MISIIR-TAg tumour cell lines in response to both wild type VSV and Δ51M VSV single-agent treatment. In particular, all of the MISIIR-TAg tumour cell lines tested were found to be susceptible to the cytotoxic properties of wild type VSV at an MOI of 0.1 whereas at an MOI of 1.0 only half of the MISIIR-TAg tumour cell lines were susceptible to the cytotoxicity of Δ51M VSV. The differences in response to both viruses can be explained by the altered matrix protein of the Δ51M mutant. Stojdl *et al.* (2003) created this mutant in order to

increase the therapeutic safety index of the wild type virus by deleting methionine 51 of the matrix protein, rendering the virus unable to block the export of transcripts from the nucleus. Hence, this deletion enables a cell without defects in the interferon pathway (i.e. normal cells) to elicit an interferon response to viral entry by allowing export of mRNAs for the IFNs and ISGs from the nucleus (Stojdl *et al.,* 2003), protecting the cell from viral infection. The potent cytotoxic effects of wild type VSV may be due to the ability of the virus to halt the interferon response of the MISIIR-TAg tumour cells lines by blocking the export interferon mRNA's from the nucleus whereas the varied ability of Δ51M VSV to induce cytotoxicity in the MISIIR-TAg tumour cell lines may be due to the virus's inability to block the interferon response of the cells allowing the cells to protect themselves from infection.

The varying responses to Δ51M VSV between the mouse tumour cell lines is interesting, particularly because the differences are sometimes seen in paired cell lines derived from the right and left tumours of the same mouse. In two paired cell lines, the right tumours from both mice were susceptible to the cytotoxic effects of Δ51M VSV, whereas the left tumours from both mice were resistant to Δ51M VSV infection and they responded in a similar manner to the control MOSE cells. Differences in growth tendencies and cell morphology were not significantly different when examined; however, there was a distinct difference in the expression level of SV40 T-antigen between the cell lines. Specifically, both cell lines from right tumours exhibited low SV40 T-antigen expression whereas both cell lines from left tumours showed high expression. Since the cells with low TAg expression had the greater susceptibility to VSV infection, we hypothesized that the level of TAg expression may contribute to the

mechanisms regulating the susceptibility to this virus. This hypothesis is supported by previous studies describing transfected T-antigen cells, 293T and Hela, as having higher levels of interferon expression (Moens *et al.,* 1997; Sameulsson *et al.,* 2005). Therefore, we chose to examine Δ51M VSV-mediated induction of interferon production in the MISIIR-TAg tumour cell lines. The results indicated that MISIIR-TAg tumour cell lines respond to exogenous interferon in addition to producing interferon in response to Δ51M VSV infection. However, there does not appear to be a difference in interferon production in response to this infection when comparing normal MOSE and the MISIIR-TAg tumour cell lines. This finding suggests either that SV40-TAg does not play a role in susceptibility to VSV infection, or that TAg expression could be potentially altering the susceptibility of the mouse tumour cell lines via another pathway.

The proteins produced during SV40-TAg infection have been shown to have pleiotropic effects on a wide variety of cellular processes, such as the regulation of host cell gene expression (Moens *et al.,* 1997). For example, MHC class I genes, cyclin A mRNA and DNA polymerase α mRNA are induced whereas activity of interleukin-6, interleukin-8 and α-actinin are repressed by SV40 transformation or TAg transfection in various cell types (Moens *et al.,* 1997). There is the possibility that the effects of SV40 T-antigen on various cellular processes could inhibit the ability of the MISIIR-TAg tumour cells to produce large amounts of virus. Altstein *et al.* (1969) showed Vero cells infected with SV40 to be capable of supporting the multiplication of other RNA and DNA containing viruses. Yet infection with SV40 followed by either vaccinia virus or Simian adenovirus 15 after 2, 24, or 48 hours showed decreased amounts of hemaglutinin titers of the secondary virus, indicating decreased multiplication of the second virus.

Interestingly, our data indicates that the amount of Δ51M VSV produced from infected MISIIR-TAg tumour cells is no different than the amount produced from the normal MOSE cells. The amount produced from the MOSE and MISIIR-TAg tumour cells tested is in the same logarithmic range as normal primary human cell cultures (Stojdl *et al.,* 2000b). Conversely, every human cancer cell line tested produced virus at a magnitude of 1-4 logarithms higher than the normal primary human cell cultures. These two findings taken in combination suggest that MISIIR-TAg tumour cells do not share the same characteristics as the typical human cancer cell line since they are incapable of acting as 'viral production factories' and they retain the ability to respond and produce interferon in response to virus infection.

A limited number of tumours are refractory to VSV infection (Stojdl *et al.,* 2003; Vaha-Koskela *et al.,* 2007; Ahmed *et al.,* 2004; Nguyen *et al.,* 2008; Carey *et al.,* 2008; Hadaschik *et al.,* 2008), a finding that has been attributed to the fact that 20% of tumours tested do not have defects in their interferon pathways (Stojdl *et al.,* 2003). However, the possibility exists for tumours to be refractory to this virus by producing interferons, particularly since the *in vitro* data has shown that MISIIR-TAg tumour cells respond to and produce interferons. The initial imaging of ex-vivo tumours of the MISIIR-TAg(+) mice treated with VSV indicated that wild type VSV given IP was the only treatment tested that was able to enter and replicate in the tumours. However, subsequent examination using plaque titering and IVIS imaging indicated that even wild type VSV via IP injection was unable to cause a significant infection of the MISIIR-TAg tumours of mice. Thus the refractive nature of this tumour model may in part be due to the proven ability of the MISIIR-TAg tumour cell lines to respond and produce interferons.

Previous *in vivo* studies with VSV as a single agent in xenograft and syngeneic models of cancer have been successful in showing the regression, halting of growth and increased survival of the treated tumour-bearing mice. While these models are routinely used for testing of novel therapeutics, they have the limitation of being simply transplanted cancer cells, and not developing from normal tissues. Transgenic models of cancer could pose a greater challenge for therapeutic testing because tumour development, including neovasculaturization and immune response take place within the context of normal tissues. For these reasons, the transgenic models of cancer may be more difficult to treat, and have greater clinical relevance. We therefore designed a survival study in the MISIIR-TAg(+) mice in which we compared four different treatments including the administration of PBS, UV attenuated VSV, Δ51M VSV and wild type VSV by IP and IV administration, respectively. The results showed that no statistically significant differences were seen among any of the treatments in the overall survival outcome of the MISIIR-TAg mice. These results indicate that, although the mouse ovarian cancer cell lines undergo cell death in response to virus exposure *in vitro*, the use of VSV, wild type or Δ51M, as a single agent treatment of epithelial ovarian cancer *in vivo*, specifically in this mouse model, had no therapeutic benefit.

The *in vitro* results infer that there are two possible reasons for the lack of therapeutic efficacy of VSV treatment in the MISIIR-TAg(+) mice: first, the *in vitro* results show MISIIR-TAg tumour cells retain the ability to respond to and produce interferon, indicating that the tumour cells of MISIIR-TAg(+) mice can still mount a defence against VSV infection. Previous studies have clearly shown that the ability of tumour cells to respond to and produce interferon decreases their susceptibility to VSV

infection (Stojdl *et al.,* 2000; Ahmed *et al.,* 2004). Thus, this lack of defect in the interferon pathway should inhibit VSV infection. Secondly, the *in vitro* results suggest that SV40 T-antigen expression may play a role in the susceptibility of the MISIIR-TAg tumour cells lines to VSV infection. Previously reported studies have indicated that some tumours are refractory to VSV infection (Stojdl *et al.,* 2003; Vaha-Koskela *et al.,* 2007; Ahmed *et al.,* 2004; Nguyen *et al.,* 2008; Carey *et al.,* 2008; Hadaschik *et al.,* 2008). While host anti-viral response provides one explanation of this phenomena, other host factors including translational and growth regulatory mechanisms may also play a role in VSV susceptibility (Balachandran *et al.,* 2004; Balachandran and Garber, 2000; Baltzis *et al.,* 2004; Durbin *et al.,* 2002). Investigation into the exact mechanism responsible for the differences in replicative capabilities of viruses in cells requires further investigation. The use of microarray analysis to compare the paired MISIIR-TAg tumour cell lines that have different responses to Δ51M VSV would be one approach to understand the pathways that are different between cell lines.

Lastly another reason for the lack of therapeutic benefit of the VSV in the mouse model of ovarian cancer could be the dose of VSV given. For the simplicity of comparison, the MTD of wild type VSV in the MISIIR-TAg(+) mice was used to set the dose of all the treatments in the single dose experiments. Studies have shown that strains of mice differ in their maximum tolerated dose of VSV which also varies by variant of VSV and route of exposure (Stojdl *et al.,* 2003; Ahmed *et al.,* 2004). Stojdl *et al.* (2003) showed that CD-1 mice could tolerate a magnitude of two logarithms of pfu greater of a VSV mutant similar to Δ51M VSV than wild type virus. They also showed that CD1 mice could tolerate up to a maximum of two logarithms of pfu greater of wild type VSV

when given IV rather than by intranasal administration. The experiments to determine the MTD of wild type VSV indicated that the MISIIR-TAg(+) mice tolerated Δ51M VSV at the highest dose of wild type VSV tested, however this dose of wild type VSV was not tolerated in the mice so could not be used for experimental purposes. The MTD of Δ51M VSV was not tested in the MISIIR-TAg(+) mice, however it was presumably higher than the dose that was used in the in vivo study, which most likely had an impact on the outcome of these experiments. The current theory in viral therapy is to dose with the highest viral titer tolerated, in order to provide the greatest probability of virus entry and infection of the tumours. A reasonable experiment to perform to investigate this possibility further would be to increase the dose of Δ51M VSV to the MTD and re-examine the ability of the virus to enter and replicate the MISIIR-TAg tumours, as well as determine if there is a survival benefit.

The lack of a positive response to VSV as a single agent therapeutic in the MISIIR-TAg(+) mice required a novel approach to be used in order to increase the therapeutic benefit of VSV in these mice. The previous results indicated that interferon might be playing a role in the VSV refractive characteristics of the tumours and therefore another therapeutic agent that could interfere with interferon response in a reversible manner was investigated. Several studies have indicated that HDACs are required to activate the transcription of interferon-β (Nusinzon *et al.,* 2003, 2006; Munshi *et al.,*1998; Munshi *et al.,*1999) as well as the ISGs (Chang *et al.,* 2004 ;Sakamoto *et al.,* 2004). In accordance with these findings, the combination of a HDAC inhibitor (HDACi) and VSV could reversibly compromise the innate anti-viral response by suppressing the transcription of interferon and its response genes, creating an

environment conducive to viral replication and spread, and effectively enhancing the therapeutic potential of both treatments.

MS-275 is a small compound that is classified as an HDACi. *In vitro* it has been shown to cause growth arrest, differentiation, and in some cases apoptosis of cancer cells (reviewed Hess-Stumpp *et al.,* 2007); *in vivo* it has been shown to halt tumour growth in tumour bearing mice (reviewed Hess-Stumpp *et al.,* 2007). As a direct consequence of the positive outcomes elicited in the mouse cancer cell lines when using MS-275 as a singular therapeutic agent, we decided to examine the use of this inhibitor in combination with VSV. *In vitro* investigation of the combination treatment of MS-275 and Δ51M VSV showed an increase in the amount of cell killing in the MISIIR-TAg tumour cell lines when compared to either Δ51M VSV alone or MS-275 alone, a finding that has been supported by other recent studies (Otsuki *et al.,* 2008; Nguyen *et al.,* 2008; Balakrishnan *et al.,* 2008). Two studies, one conducted by Otsuki *et al.* (2008) and the other by Nguyen *et al.* (2008), both indicate that viral yield is increased and that innate anti-viral gene expression decreases, specifically interferon and the interferon stimulated genes, after combination treatment. Interestingly, our results from similar experiments in MISIIR-TAg tumour cell lines do not support the findings of these two studies. In fact, our results indicate that there is more viral replication in the MISIIR-TAg cells however the viral yield from the MISIIR-TAg cells does not change when co-treated with MS-275 and VSV. This suggests that perhaps viral assembly and/or budding may be altered in the MISIIR-TAg cells. Investigation into the interferon-α production in the MISIIR-TAg tumour cell lines show that there is no change in the expression level when comparing combination treatment therapy to its single treatment counterpart. An important

difference between the latter two studies and the work reported here is that the combination treated cells were pre-treated with HDACi before viral treatments, whereas the cells were treated simultaneously in our study. Otsuki *et al.* (2008) explored pre-treatment and co-treatment in their study showing that pre-treatment but not co-treatment of the HDACi enhanced the propagation of the oncolytic virus. Certainly, re-examining the combination treatment using a pre-treatment regimen of MS-275 in the MISIIR-TAg tumour cells may increase the efficacy however we were still able to see an increase in the cell killing by VSV with co-treatment. The mechanism through which this enhanced cell killing is achieved has yet to be determined.

The encouraging results *in vitro* provided the rationale to examine the efficacy of combination treatment *in vivo*, and both a tumour burden study as well as a survival study were performed in the MISIIR-TAg(+) mice. Mice were treated with 3 doses of either Δ51M VSV, MS-275 or the combination of MS-275 and Δ51M VSV over a one week period. The tumour burden analysis, completed one week after the third treatment, indicated that there existed no statistically significant difference between the groups when comparing total tumour burden or the tumour burden as a percentage of body weight. However, there was a trend indicating that tumour burden was decreased in the treatments compared to the control. The survival study showed that survival was not changed with any of the treatments compared to the control. However, there was a difference in the survival of mice treated with Δ51M VSV alone compared to both the MS-275 alone and the combination treated mice. The tumour burden at endpoint indicated no difference between any of the treatment groups. These results were surprising given our preliminary results *in vitro* as well as the recent studies indicating

potent therapeutic efficacy of treatment in tumour-bearing mice (Otsuki *et al.,* 2008; Nguyen *et al.,* 2008; Balakrishnan *et al.,* 2008), and may strengthen the hypothesis that transgenic models of cancer present a more challenging and clinically relevant disease for the testing of novel therapeutics.

Although our results *in vivo* did not produce any significant differences between treatment groups and controls, there are multiple ways that the efficacy of combination therapy could be potentially enhanced. For example, the dosing of MS-275 could be altered. This study examined only two treatment doses given by one route of administration. A study completed by Camphaussen *et al.* (2004) demonstrated tumour growth inhibition in mice with the use of two daily doses of 6mg/kg MS-275 given intraperitoneally. Another study by Saito *et al.* 1999 examined the use of MS-275 given orally once daily and resulted in growth inhibition of tumours in nude mice. These two studies and others suggest that examining other dosing regimes for MS-275 may enhance the therapeutic efficacy.

Next, the use of a different HDACi may enhance the activity of VSV in this model. Multiple HDACi exist that have been shown to have therapeutic benefit *in vitro* and *in vivo* (reviewed Johnstone 2002). MS-275 is a known inhibitor of the class I HDAC's (Hu *et al.,* 2003; Vannini *et al.,* 2004), however there are other HDACi that are more globally effective such as trichostatin A (TSA) or suberoylanilide hydromaxic acid (SAHA) (Hess-Stumpp *et al.,* 2007) which may increase the therapeutic efficacy. Although human ovarian cancers have been shown to overexpress class I HDACs, the expression profile of HDACs in the MISIIR-TAg tumours has not yet been performed, and such analysis would prove useful in selecting the appropriate HDACi to test in vivo.

Additionally, the route of virus administration could also be re-examined. Our studies tested IP administration whereas other studies have examined IV administration of VSV such as the studies conducted by Stojdl *et al.,* 2003, Ebert *et al.,* 2005, Shinozaki *et al.,* 2005, and Wu *et al.,* 2008. All of these studies have shown that Δ51M VSV is well tolerated when injected IV which supports the need to test various routes of VSV administration in treating our mouse model.

Another approach to evaluating the therapeutic potential for oncolytic viruses in this model would be the use of a different OV. Many different strains of virus are now being tested as OVs, such as Newcastle disease virus, vaccinia virus, reovirus, Sindbus virus, Semliki Forest virus and myxoma. All of these viruses have different characteristics that can be used to target different types of cancers. The use of vaccinia virus in this particular model would be of great interest, because vaccinia has been shown to preferentially localize to the ovaries in mice (Puhlmann *et al.,* 2000; McCart *et al.,* 2001), and thus may be the best virus to use to target ovarian cancer. Hung *et al.* (2006) tested the ability of vaccinia virus to infect human and murine ovarian cancers in mice. In their study they observed human and murine ovarian tumour-bearing mice treated with vaccinia virus survived at least 60 days post-treatment, whereas the untreated tumour-bearing mice survived only 40 days. The ovarian tropism of the virus is not only promising, but provides grounds for further testing as a potential novel therapy for the treatment of ovarian cancers.

Another strategy in the attempt to increase the efficacy of this treatment model is to alter the duration of treatment. Our experiments were completed after 3 rounds of treatment over 1 week, however it may be that the animals would have been able to

respond well to treatment for longer which may have lead to greater efficacy in response to the treatment. A study conducted by Saito *et al.* (1999) is a perfect example of how duration of treatment can affect the outcome by treating the mice with leukemia, lung, pancreatic, ovarian and colorectal xenograft tumours orally with MS-275 daily for four weeks they showed growth inhibition of tumours in nude mice. The results of this study are closely mirrored by a study conducted by Nguyen *et al.* 2008 where they treated syngeneic breast and colorectal tumour bearing mice twice daily with IP administration of MS-275 for 10 consecutive days, resulting in a decreased tumour size. Although neither of these studies examined different durations of treatment, the ability to treat mice for longer with MS-275 is demonstrated suggesting that it is imperative to re-examine the duration of treatment administration.

Lastly, the age of the MISIIR-TAg(+) mice when treatment begins could also be addressed. Ovarian tumour growth in the MISIIR-TAg mouse model developed by our lab has been characterized (Garson, Courville and Vanderhyden, unpublished results). MISIIR-TAg(+) mice were euthanized at specific time points to determine tumour weight. This revealed that tumours grow in a linear fashion until around 11-12 weeks of age at which point tumours begin to grow at an exponential rate. In our experiments, we decided to treat the tumours before the time for exponential growth, however this is a large time period, and therefore the efficacy of the treatment may be altered by the timing of the treatment. Re-examination of the different time points during the initiation and progression of tumour development may prove therapeutic efficacy of VSV in this model.

In conclusion, the MISIIR-TAg mouse model of ovarian cancer has proven to be a robust model for the therapeutic testing of VSV in the treatment of cancer. The model represents a small proportion of human cancers that would be interferon responsive and therefore provides opportunities to test strategies to enhance the therapeutic efficacy in those patients exhibiting interferon responsive tumours. The results of this study do not suggest promising therapeutic benefit for the use of VSV as a single agent or in combination with MS-275 for ovarian cancer. Yet, there are multiple alterations that could be made to the investigate these strategies further, such as changes in the dosing regime, choice of HDACi and/or OV, mode of virus administration, and the duration of the treatment itself, that could result in improved efficacy. Evidently, there are many questions that remain to be answered; however, the continued accumulation of evidence provided by this and other studies concerning the use of VSV as an oncolytic may one day lead to clinical trials and hopefully, clinical applications for cancer patients.

References

Agarwal, R., M. Linch and S. B. Kaye. Novel therapeutic agents in ovarian cancer. *European Journal of Surgical Oncology :The Journal of the European Society of Surgical Oncology and the British Association of Surgical Oncology* 2006. 32; 8: 875-886.

Ahmed, M., S. D. Cramer and D. S. Lyles. Sensitivity of prostate tumors to wild type and M protein mutant vesicular stomatitis viruses. *Virology* 2004. 330; 1: 34-49.

Altstein, A. D., N. N. Dodonova, G. A. Nadtochey and A. F. Bykovski. Interaction between SV 40 and other viruses in tissue culture: interference and double infection. *Archiv fur die Gesamte Virusforschung* 1969. 28; 1: 7-18.

Armstrong, D. K., B. Bundy, L. Wenzel, H. Q. Huang, R. Baergen, S. Lele, L. J. Copeland, J. L. Walker, R. A. Burger and Gynecologic Oncology Group. Intraperitoneal cisplatin and paclitaxel in ovarian cancer. *The New England Journal of Medicine* 2006. 354; 1: 34-43.

Balachandran, S. and G. N. Barber. Defective translational control facilitates vesicular stomatitis virus oncolysis. *Cancer Cell* 2004. 5; 1: 51-65.

Balachandran, S. and G. N. Barber. Vesicular stomatitis virus (VSV) therapy of tumors. *IUBMB Life* 2000. 50; 2: 135-138.

Balachandran, S., M. Porosnicu and G. N. Barber. Oncolytic activity of vesicular stomatitis virus is effective against tumors exhibiting aberrant p53, Ras, or myc function and involves the induction of apoptosis. *Journal of Virology* 2001. 75; 7: 3474-3479.

Balachandran, S., P. C. Roberts, L. E. Brown, H. Truong, A. K. Pattnaik, D. R. Archer and G. N. Barber. Essential role for the dsRNA-dependent protein kinase PKR in innate immunity to viral infection. *Immunity* 2000. 13; 1: 129-141.

Balakrishnan, L. and B. Milavetz. HDAC inhibitors stimulate viral transcription by multiple mechanisms. *Virology Journal* 2008. 5; 43.

Baltzis, D., L. K. Qu, S. Papadopoulou, J. D. Blais, J. C. Bell, N. Sonenberg and A. E. Koromilas. Resistance to vesicular stomatitis virus infection requires a functional cross talk between the eukaryotic translation initiation factor 2alpha kinases PERK and PKR. *Journal of Virology* 2004. 78; 23: 12747-12761.

Barber, G. N. VSV-tumor selective replication and protein translation. *Oncogene* 2005. 24; 52: 7710-7719.

Belien, A., S. De Schepper, W. Floren, B. Janssens, A. Marien, P. King, J. Van Dun, L. Andries, J. Voeten, L. Bijnens, M. Janicot and J. Arts. Real-time gene expression analysis in human xenografts for evaluation of histone deacetylase inhibitors. *Molecular Cancer Therapeutics* 2006. 5; 9: 2317-2323.

Bell, J. C., K. A. Garson, B. D. Lichty and D. F. Stojdl. Oncolytic viruses: programmable tumour hunters. *Current Gene Therapy* 2002. 2; 2: 243-254.

Bolden, J. E., M. J. Peart and R. W. Johnstone. Anticancer activities of histone deacetylase inhibitors. *Nature Reviews.Drug Discovery* 2006. 5; 9: 769-784.

Bremer, E., G. M. van Dam, M. de Bruyn, M. van Riezen, M. Dijkstra, G. Kamps, W. Helfrich and H. Haisma. Potent Systemic Anticancer Activity of Adenovirally Expressed EGFR-Selective TRAIL Fusion Protein. *Molecular Therap :The Journal of the American Society of Gene Therapy* 2008.

Burdick, K. H. and W. A. Hawk. Vitiligo in a Case of Vaccinia Virus-Treated Melanoma. *Cancer* 1964. 17; 708-712.

Camphausen, K., T. Scott, M. Sproull and P. J. Tofilon. Enhancement of xenograft tumor radiosensitivity by the histone deacetylase inhibitor MS-275 and correlation with histone hyperacetylation. *Clinical Cancer Researc : an official journal of the American Association for Cancer Research* 2004. 10; 18 Pt 1: 6066-6071.

Canadian Cancer Society/National Cancer Institute of Canada (2008). Canadian Cancer Statistics 2008. Toronto, Canada. www.cancer.ca

Candelaria, M., D. Gallardo-Rincon, C. Arce, L. Cetina, J. L. Aguilar-Ponce, O. Arrieta, A. Gonzalez-Fierro, A. Chavez-Blanco, E. de la Cruz-Hernandez, M. F. Camargo, C. Trejo-Becerril, E. Perez-Cardenas, C. Perez-Plasencia, L. Taja-Chayeb, T. Wegman-Ostrosky, A. Revilla-Vazquez and A. Duenas-Gonzalez. A phase II study of epigenetic therapy with hydralazine and magnesium valproate to overcome chemotherapy resistance in refractory solid tumors. *Annals of Oncology : Official Journal of the European Society for Medical Oncology / ESMO* 2007. 18; 9: 1529-1538.

Carey, B. L., M. Ahmed, S. Puckett and D. S. Lyles. Early steps of the virus replication cycle are inhibited in prostate cancer cells resistant to oncolytic vesicular stomatitis virus. *Journal of Virology* 2008.

Cathro, H. P. and M. H. Stoler. The utility of calretinin, inhibin, and WT1 immunohistochemical staining in the differential diagnosis of ovarian tumors. *Human Pathology* 2005. 36; 2: 195-201.

Chang, H. M., M. Paulson, M. Holko, C. M. Rice, B. R. Williams, I. Marie and D. E. Levy. Induction of interferon-stimulated gene expression and antiviral responses require protein deacetylase activity. *Proceedings of the National Academy of Sciences of the United States of America* 2004. 101; 26: 9578-9583.

Chen, R. H. and F. McCormick. Selective targeting to the hyperactive beta-catenin/T-cell factor pathway in colon cancer cells. *Cancer Research* 2001. 61; 11: 4445-4449.

Chen, V. W., B. Ruiz, J. L. Killeen, T. R. Cote, X. C. Wu and C. N. Correa. Pathology and classification of ovarian tumors. *Cancer* 2003. 97; 10 Suppl: 2631-2642.

Clark-Knowles, K. V., K. Garson, J. Jonkers and B. C. Vanderhyden. Conditional inactivation of Brca1 in the mouse ovarian surface epithelium results in an increase in preneoplastic changes. *Experimental Cell Research* 2007. 313; 1: 133-145.

Cohen, C. J. and T. S. Jennings. Screening for ovarian cancer: the role of noninvasive imaging techniques. *American Journal of Obstetrics and Gynecology* 1994. 170; 4: 1088-1094.

Colina, R., M. Costa-Mattioli, R. J. Dowling, M. Jaramillo, L. H. Tai, C. J. Breitbach, Y. Martineau, O. Larsson, L. Rong, Y. V. Svitkin, A. P. Makrigiannis, J. C. Bell and N. Sonenberg. Translational control of the innate immune response through IRF-7. *Nature* 2008. 452; 7185: 323-328.

Connolly, D. C., R. Bao, A. Y. Nikitin, K. C. Stephens, T. W. Poole, X. Hua, S. S. Harris, B. C. Vanderhyden and T. C. Hamilton. Female mice chimeric for expression of the simian virus 40 TAg under control of the MISIIR promoter develop epithelial ovarian cancer. *Cancer Research* 2003. 63; 6: 1389-1397.

Crompton, A. M. and D. H. Kirn. From ONYX-015 to armed vaccinia viruses: the education and evolution of oncolytic virus development. *Current Cancer Drug Targets* 2007. 7; 2: 133-139.

Daoud, E. and G. Bodor. CA-125 concentrations in malignant and nonmalignant disease. *Clinical Chemistry* 1991. 37; 11: 1968-1974.

Depace, N. Sulla scomparsa di un enormo cancro vegetante del collo dell'utero senza cura chirurgica. *Ginecologia* 1912. 9; 82.

Desforges, M., J. Charron, S. Berard, S. Beausoleil, D. F. Stojdl, G. Despars, B. Laverdiere, J. C. Bell, P. J. Talbot, C. P. Stanners and L. Poliquin. Different host-cell shutoff strategies related to the matrix protein lead to persistence of vesicular stomatitis virus mutants on fibroblast cells. *Virus Research* 2001. 76; 1: 87-102.

Di Gennaro, E., F. Bruzzese, M. Caraglia, A. Abruzzese and A. Budillon. Acetylation of proteins as novel target for antitumor therapy: review article. *Amino Acids* 2004. 26; 4: 435-441.

Dinulescu, D. M., T. A. Ince, B. J. Quade, S. A. Shafer, D. Crowley and T. Jacks. Role of K-ras and Pten in the development of mouse models of endometriosis and endometrioid ovarian cancer. *Nature Medicine* 2005. 11; 1: 63-70.

Dock, G. The influence of complicating disease upon leukemia. *The American Journal of the Medical Sciences*, 1904. 127; 4: 563-592.

Durbin, R. K., S. E. Mertz, A. E. Koromilas and J. E. Durbin. PKR protection against intranasal vesicular stomatitis virus infection is mouse strain dependent. *Viral Immunology* 2002. 15; 1: 41-51.

Dutertre, M., L. Gouedard, F. Xavier, W. Q. Long, N. di Clemente, J. Y. Picard and R. Rey. Ovarian granulosa cell tumors express a functional membrane receptor for anti-Mullerian hormone in transgenic mice. *Endocrinology* 2001. 142; 9: 4040-4046.

Ebert, O., S. Harbaran, K. Shinozaki and S. L. Woo. Systemic therapy of experimental breast cancer metastases by mutant vesicular stomatitis virus in immune-competent mice. *Cancer Gene Therapy* 2005. 12; 4: 350-358.

Ebert, O., K. Shinozaki, T. G. Huang, M. J. Savontaus, A. Garcia-Sastre and S. L. Woo. Oncolytic vesicular stomatitis virus for treatment of orthotopic hepatocellular carcinoma in immune-competent rats. *Cancer Research* 2003. 63; 13: 3605-3611.

Enninga, J., D. E. Levy, G. Blobel and B. M. Fontoura. Role of nucleoporin induction in releasing an mRNA nuclear export block. *Science (New York, N.Y.)* 2002. 295; 5559: 1523-1525.

Fernandez, M., M. Porosnicu, D. Markovic and G. N. Barber. Genetically engineered vesicular stomatitis virus in gene therapy: application for treatment of malignant disease. *Journal of Virology* 2002. 76; 2: 895-904.

Fitzgerald, K. A., S. M. McWhirter, K. L. Faia, D. C. Rowe, E. Latz, D. T. Golenbock, A. J. Coyle, S. M. Liao and T. Maniatis. IKKepsilon and TBK1 are essential components of the IRF3 signaling pathway. *Nature Immunology* 2003. 4; 5: 491-496.

Flesken-Nikitin, A., K. C. Choi, J. P. Eng, E. N. Shmidt and A. Y. Nikitin. Induction of carcinogenesis by concurrent inactivation of p53 and Rb1 in the mouse ovarian surface epithelium. *Cancer Research* 2003. 63; 13: 3459-3463.

Flint, S.J., Enquist, L.W., Racaniello, V.R., Shalka, A.M (2004). Principles of Virology: Molecular Biology Pathogenesis and Control (Second Edition). Washington, DC, USA: *American Society for Microbiology*.

Gagnon, A. and B. Ye. Discovery and application of protein biomarkers for ovarian cancer. *Current Opinion in Obstetrics & Gynecology* 2008. 20; 1: 9-13.

Gallinari, P., S. Di Marco, P. Jones, M. Pallaoro and C. Steinkuhler. HDACs, histone deacetylation and gene transcription: from molecular biology to cancer therapeutics. *Cell Research* 2007. 17; 3: 195-211.

Ganly, I., D. Kirn, G. Eckhardt, G. I. Rodriguez, D. S. Soutar, R. Otto, A. G. Robertson, O. Park, M. L. Gulley, C. Heise, D. D. Von Hoff and S. B. Kaye. A phase I study of Onyx-015, an E1B attenuated adenovirus, administered intratumorally to patients with recurrent head and neck cancer. *Clinical Cancer Research : An OfficialJjournal of the American Association for Cancer Research* 2000. 6; 3: 798-806.

Garson, K., T. J. Shaw, K. V. Clark, D. S. Yao and B. C. Vanderhyden. Models of ovarian cancer--are we there yet? *Molecular and Cellular Endocrinology* 2005. 239; 1-2: 15-26.

Gojo,I., Jiemjit,A., Trepel,J., Sparreboom,A., Figg, W.D., Rollins,S. Phase I and pharmacological study of MS-275, a histone deacetylase inhibitor, in adults with refractory and relapsed acture leukemias. *Blood* 2006.

Gore,L., Holden,S., Basche,M., Raj,S., arnold,I., O'Bryant,C. Updated results from a phase I trial of the histone deacetylase inhibitor MS-275 in patients with refractory solid tumours. *Journal of Clinical Oncology* 2004. 22; 14s: 3026.

Greenaway, J., R. Moorehead, P. Shaw and J. Petrik. Epithelial-stromal interaction increases cell proliferation, survival and tumorigenicity in a mouse model of human epithelial ovarian cancer. *Gynecologic Oncology* 2008. 108; 2: 385-394.

Greenlee, R. T., M. B. Hill-Harmon, T. Murray and M. Thun. Cancer statistics, 2001. *CA: A Cancer Journal for Clinicians* 2001. 51; 1: 15-36.

Hadaschik, B. A., K. Zhang, A. I. So, L. Fazli, W. Jia, J. C. Bell, M. E. Gleave and P. S. Rennie. Oncolytic vesicular stomatitis viruses are potent agents for intravesical treatment of high-risk bladder cancer. *Cancer Research* 2008. 68; 12: 4506-4510.

Hashiguchi, Y., H. Tsuda, K. Yamamoto, T. Inoue, O. Ishiko and S. Ogita. Combined analysis of p53 and RB pathways in epithelial ovarian cancer. *Human Pathology* 2001. 32; 9: 988-996.

Hauschild,A., Trefzer,U., Garbe,C., Kaehler,K.C., Ugurel,S., Kiecker,F. A phase II multicenter study on the histone deacetylase (HDAC) inhibitor MS-275, comparing two dosage schedules in metastic melanoma. *Journal of Clinical Oncology* 2006. 24; 18s: 8044.

Hess-Stumpp, H., Hoffman. MS-275, a potent orally active inhibitor of histone deacetylases is highly active in experimental tumor models of melanoma and prostate cancer. *European Journal of Cancer Supplement* 2004. 2; 8: 28.

Hess-Stumpp, H., T. U. Bracker, D. Henderson and O. Politz. MS-275, a potent orally available inhibitor of histone deacetylases--the development of an anticancer agent. *The International Journal of Biochemistry & Cell Biology* 2007. 39; 7-8: 1388-1405.

Honda, K., H. Yanai, H. Negishi, M. Asagiri, M. Sato, T. Mizutani, N. Shimada, Y. Ohba, A. Takaoka, N. Yoshida and T. Taniguchi. IRF-7 is the master regulator of type-I interferon-dependent immune responses. *Nature* 2005. 434; 7034: 772-777.

Howe, J. A., G. W. Demers, D. E. Johnson, S. E. Neugebauer, S. T. Perry, M. T. Vaillancourt and B. Faha. Evaluation of E1-mutant adenoviruses as conditionally replicating agents for cancer therapy. *Molecular Therapy :TheJjournal of the American Society of Gene Therapy* 2000. 2; 5: 485-495.

Hu, E., E. Dul, C. M. Sung, Z. Chen, R. Kirkpatrick, G. F. Zhang, K. Johanson, R. Liu, A. Lago, G. Hofmann, R. Macarron, M. de los Frailes, P. Perez, J. Krawiec, J. Winkler and M. Jaye. Identification of novel isoform-selective inhibitors within class I histone deacetylases. *The Journal of Pharmacology and Experimental Therapeutics* 2003. 307; 2: 720-728.

Huang, T. G., O. Ebert, K. Shinozaki, A. Garcia-Sastre and S. L. Woo. Oncolysis of hepatic metastasis of colorectal cancer by recombinant vesicular stomatitis virus in immune-competent mice. *Molecular Therapy : The Journal of the American Society of Gene Therapy* 2003. 8; 3: 434-440.

Hung, C. F., Y. C. Tsai, L. He, G. Coukos, I. Fodor, L. Qin, H. Levitsky and T. C. Wu. Vaccinia virus preferentially infects and controls human and murine ovarian tumors in mice. *Gene Therapy* 2007. 14; 1: 20-29.

Hunter-Craig, I., K. A. Newton, G. Westbury and B. W. Lacey. Use of vaccinia virus in the treatment of metastatic malignant melanoma. *British Medical Journal* 1970. 2; 5708: 512-515.

Inoue, S., A. Mai, M. J. Dyer and G. M. Cohen. Inhibition of histone deacetylase class I but not class II is critical for the sensitization of leukemic cells to tumor necrosis factor-related apoptosis-inducing ligand-induced apoptosis. *Cancer Research* 2006. 66; 13: 6785-6792.

Johnstone, R. W. Histone-deacetylase inhibitors: novel drugs for the treatment of cancer. *Nature Reviews.Drug Discovery* 2002. 1; 4: 287-299.

Kananen, K., M. Markkula, E. Rainio, J. G. Su, A. J. Hsueh and I. T. Huhtaniemi. Gonadal tumorigenesis in transgenic mice bearing the mouse inhibin alpha-subunit promoter/simian virus T-antigen fusion gene: characterization of ovarian tumors and establishment of gonadotropin-responsive granulosa cell lines. *Molecular Endocrinology (Baltimore, Md.)* 1995. 9; 5: 616-627.

Keri, R. A., K. L. Lozada, F. W. Abdul-Karim, J. H. Nadeau and J. H. Nilson. Luteinizing hormone induction of ovarian tumors: oligogenic differences between mouse strains dictates tumor disposition. *Proceedings of the National Academy of Sciences of the United States of America* 2000. 97; 1: 383-387.

Khuri, F. R., J. Nemunaitis, I. Ganly, J. Arseneau, I. F. Tannock, L. Romel, M. Gore, J. Ironside, R. H. MacDougall, C. Heise, B. Randlev, A. M. Gillenwater, P. Bruso, S. B. Kaye, W. K. Hong and D. H. Kirn. a controlled trial of intratumoral ONYX-015, a selectively-replicating adenovirus, in combination with cisplatin and 5-fluorouracil in patients with recurrent head and neck cancer. *Nature Medicine* 2000. 6; 8: 879-885.

Kim, T. Y., Y. J. Bang and K. D. Robertson. Histone deacetylase inhibitors for cancer therapy. *Epigenetics : Official Journal of the DNA Methylation Society* 2006. 1; 1: 14-23.

Kopecky, S. A., M. C. Willingham and D. S. Lyles. Matrix protein and another viral component contribute to induction of apoptosis in cells infected with vesicular stomatitis virus. *Journal of Virology* 2001. 75; 24: 12169-12181.

Koyama, A. H. Induction of apoptotic DNA fragmentation by the infection of vesicular stomatitis virus. *Virus Research* 1995. 37; 3: 285-290.

Kumar, T. R., G. Palapattu, P. Wang, T. K. Woodruff, I. Boime, M. C. Byrne and M. M. Matzuk. Transgenic models to study gonadotropin function: the role of follicle-stimulating hormone in gonadal growth and tumorigenesis. *Molecular Endocrinology (Baltimore, Md.)* 1999. 13; 6: 851-865.

Laurie, S. A., J. C. Bell, H. L. Atkins, J. Roach, M. K. Bamat, J. D. O'Neil, M. S. Roberts, W. S. Groene and R. M. Lorence. A phase 1 clinical study of intravenous administration of PV701, an oncolytic virus, using two-step desensitization. *Clinical Cancer Research : An Official Journal of the American Association for Cancer Research* 2006. 12; 8: 2555-2562.

Lee, B. I., S. H. Park, J. W. Kim, E. A. Sausville, H. T. Kim, O. Nakanishi, J. B. Trepel and S. J. Kim. MS-275, a histone deacetylase inhibitor, selectively induces transforming growth factor beta type II receptor expression in human breast cancer cells. *Cancer Research* 2001. 61; 3: 931-934.

Letchworth, G. J., L. L. Rodriguez and J. Del cbarrera. Vesicular stomatitis. *Veterinary Journal* 1999. 157; 3: 239-260.

Lichty, B. D., A. T. Power, D. F. Stojdl and J. C. Bell. Vesicular stomatitis virus: re-inventing the bullet. *Trends in Molecular Medicine* 2004. 10; 5: 210-216.

Liu, T. C., T. Hwang, B. H. Park, J. Bell and D. H. Kirn. The targeted oncolytic poxvirus JX-594 demonstrates antitumoral, antivascular, and anti-HBV activities in patients with hepatocellular carcinoma. *Molecular Therapy : The Journal of the American Society of Gene Therapy* 2008. 16; 9: 1637-1642.

Mai, A., S. Massa, D. Rotili, I. Cerbara, S. Valente, R. Pezzi, S. Simeoni and R. Ragno. Histone deacetylation in epigenetics: an attractive target for anticancer therapy. *Medicinal Research Reviews* 2005. 25; 3: 261-309.

Markman, M. The genetics, screening, and treatment of epithelial ovarian cancer: an update. *Cleveland Clinic Journal of Medicine* 2000. 67; 4: 294-298.

Markman, M., B. N. Bundy, D. S. Alberts, J. M. Fowler, D. L. Clark-Pearson, L. F. Carson, S. Wadler and J. Sickel. Phase III trial of standard-dose intravenous cisplatin plus paclitaxel versus moderately high-dose carboplatin followed by intravenous paclitaxel and intraperitoneal cisplatin in small-volume stage III ovarian carcinoma: an intergroup study of the Gynecologic Oncology Group, Southwestern Oncology Group, and Eastern Cooperative Oncology Group. *Journal of Clinical Oncology : Official Journal of the American Society of Clinical Oncology* 2001. 19; 4: 1001-1007.

Marks, P., R. A. Rifkind, V. M. Richon, R. Breslow, T. Miller and W. K. Kelly. Histone deacetylases and cancer: causes and therapies. *Nature Reviews.Cancer* 2001. 1; 3: 194-202.

Mastrangelo, M. J., L. C. Eisenlohr, L. Gomella and E. C. Lattime. Poxvirus vectors: orphaned and underappreciated. *The Journal of Clinical Investigation* 2000. 105; 8: 1031-1034.

Mastrangelo, M. J., H. C. Maguire Jr, L. C. Eisenlohr, C. E. Laughlin, C. E. Monken, P. A. McCue, A. J. Kovatich and E. C. Lattime. Intratumoral recombinant GM-CSF-encoding virus as gene therapy in patients with cutaneous melanoma. *Cancer Gene Therapy* 1999. 6; 5: 409-422.

McCart, J. A., J. M. Ward, J. Lee, Y. Hu, H. R. Alexander, S. K. Libutti, B. Moss and D. L. Bartlett. Systemic cancer therapy with a tumor-selective vaccinia virus mutant lacking thymidine kinase and vaccinia growth factor genes. *Cancer Research* 2001. 61; 24: 8751-8757.

McCormick, F. Interactions between adenovirus proteins and the p53 pathway: the development of ONYX-015. *Seminars in Cancer Biology* 2000. 10; 6: 453-459.

Minucci, S. and P. G. Pelicci. Histone deacetylase inhibitors and the promise of epigenetic (and more) treatments for cancer. *Nature Reviews.Cancer* 2006. 6; 1: 38-51.

Moens, U., O. M. Seternes, B. Johansen and O. P. Rekvig. Mechanisms of transcriptional regulation of cellular genes by SV40 large T- and small T-antigens. *Virus Genes* 1997. 15; 2: 135-154.

Moloughney, B., J. Snider and L. Villeneuve. Ovarian cancer in Canada. *CMAJ : Canadian Medical Association Journal* 2000. 162; 5: 690.

Mor, G., I. Visintin, Y. Lai, H. Zhao, P. Schwartz, T. Rutherford, L. Yue, P. Bray-Ward and D. C. Ward. Serum protein markers for early detection of ovarian cancer. *Proceedings of the National Academy of Sciences of the United States of America* 2005. 102; 21: 7677-7682.

Morley, S., G. MacDonald, D. Kirn, S. Kaye, R. Brown and D. Soutar. The dl1520 virus is found preferentially in tumor tissue after direct intratumoral injection in oral carcinoma. *Clinical Cancer Research : An Official Journal of the American Association for Cancer Research* 2004. 10; 13: 4357-4362.

Munshi, N., M. Merika, J. Yie, K. Senger, G. Chen and D. Thanos. Acetylation of HMG I(Y) by CBP turns off IFN beta expression by disrupting the enhanceosome. *Molecular Cell* 1998. 2; 4: 457-467.

Munshi, N., Y. Yie, M. Merika, K. Senger, S. Lomvardas, T. Agalioti and D. Thanos. The IFN-beta enhancer: a paradigm for understanding activation and repression of inducible gene expression. *Cold Spring Harbor Symposia on Quantitative Biology* 1999. 64; 149-159.

Munster, P. N., T. Troso-Sandoval, N. Rosen, R. Rifkind, P. A. Marks and V. M. Richon. The histone deacetylase inhibitor suberoylanilide hydroxamic acid induces differentiation of human breast cancer cells. *Cancer Research* 2001. 61; 23: 8492-8497.

Nemunaitis, J., I. Ganly, F. Khuri, J. Arseneau, J. Kuhn, T. McCarty, S. Landers, P. Maples, L. Romel, B. Randlev, T. Reid, S. Kaye and D. Kirn. Selective replication and oncolysis in p53 mutant tumors with ONYX-015, an E1B-55kD gene-deleted adenovirus, in patients with advanced head and neck cancer: a phase II trial. *Cancer Research* 2000. 60; 22: 6359-6366.

Nguyen, T. L., H. Abdelbary, M. Arguello, C. Breitbach, S. Leveille, J. S. Diallo, A. Yasmeen, T. A. Bismar, D. Kirn, T. Falls, V. E. Snoulten, B. C. Vanderhyden, J. Werier, H. Atkins, M. J. Vaha-Koskela, D. F. Stojdl, J. C. Bell and J. Hiscott. Chemical targeting of the innate antiviral response by histone deacetylase inhibitors renders refractory cancers sensitive to viral oncolysis. *Proceedings of the National Academy of Sciences of the United States of America* 2008. 105; 39: 14981-14986.

Nishida, T., T. Sugiyama, A. Kataoka, K. Ushijima and M. Yakushiji. Histologic characterization of rat ovarian carcinoma induced by intraovarian insertion of a 7,12-dimethylbenz[a]anthracene-coated suture: common epithelial tumors of the ovary in rats? *Cancer* 1998. 83; 5: 965-970.

Nusinzon, I. and C. M. Horvath. Positive and negative regulation of the innate antiviral response and beta interferon gene expression by deacetylation. *Molecular and Cellular Biology* 2006. 26; 8: 3106-3113.

Nusinzon, I. and C. M. Horvath. Interferon-stimulated transcription and innate antiviral immunity require deacetylase activity and histone deacetylase 1. *Proceedings of the National Academy of Sciences of the United States of America* 2003. 100; 25: 14742-14747.

Obuchi, M., M. Fernandez and G. N. Barber. Development of recombinant vesicular stomatitis viruses that exploit defects in host defense to augment specific oncolytic activity. *Journal of Virology* 2003. 77; 16: 8843-8856.

Otsuki, A., A. Patel, K. Kasai, M. Suzuki, K. Kurozumi, E. A. Chiocca and Y. Saeki. Histone deacetylase inhibitors augment antitumor efficacy of herpes-based oncolytic viruses. *Molecular Therapy :The Journal of the American Society of Gene Therapy* 2008. 16; 9: 1546-1555.

Ovarian Cancer Canada. www.ovariancancer.org

Park, B. H., T. Hwang, T. C. Liu, D. Y. Sze, J. S. Kim, H. C. Kwon, S. Y. Oh, S. Y. Han, J. H. Yoon, S. H. Hong, A. Moon, K. Speth, C. Park, Y. J. Ahn, M. Daneshmand, B. G. Rhee, H. M. Pinedo, J. C. Bell and D. H. Kirn. Use of a targeted oncolytic poxvirus, JX-594, in patients with refractory primary or metastatic liver cancer: a phase I trial. *The Lancet Oncology* 2008. 9; 6: 533-542.

Park, S. H., S. R. Lee, B. C. Kim, E. A. Cho, S. P. Patel, H. B. Kang, E. A. Sausville, O. Nakanishi, J. B. Trepel, B. I. Lee and S. J. Kim. Transcriptional regulation of the transforming growth factor beta type II receptor gene by histone acetyltransferase and deacetylase is mediated by NF-Y in human breast cancer cells. *The Journal of Biological Chemistry* 2002. 277; 7: 5168-5174.

Pecora, A. L., N. Rizvi, G. I. Cohen, N. J. Meropol, D. Sterman, J. L. Marshall, S. Goldberg, P. Gross, J. D. O'Neil, W. S. Groene, M. S. Roberts, H. Rabin, M. K. Bamat and R. M. Lorence. Phase I trial of intravenous administration of PV701, an oncolytic virus, in patients with advanced solid cancers. *Journal of Clinical Oncology : Official Journal of the American Society of Clinical Oncology* 2002. 20; 9: 2251-2266.

Petersen, J. M., L. S. Her, V. Varvel, E. Lund and J. E. Dahlberg. The matrix protein of vesicular stomatitis virus inhibits nucleocytoplasmic transport when it is in the nucleus and associated with nuclear pore complexes. *Molecular and Cellular Biology* 2000. 20; 22: 8590-8601.

Phuangsab, A., R. M. Lorence, K. W. Reichard, M. E. Peeples and R. J. Walter. Newcastle disease virus therapy of human tumor xenografts: antitumor effects of local or systemic administration. *Cancer Letters* 2001. 172; 1: 27-36.

Puhlmann, M., C. K. Brown, M. Gnant, J. Huang, S. K. Libutti, H. R. Alexander and D. L. Bartlett. Vaccinia as a vector for tumor-directed gene therapy: biodistribution of a thymidine kinase-deleted mutant. *Cancer Gene Therapy* 2000. 7; 1: 66-73.

Rahman, N. A. and I. T. Huhtaniemi. Ovarian tumorigenesis in mice transgenic for murine inhibin alpha subunit promoter-driven Simian Virus 40 T-antigen: ontogeny, functional characteristics, and endocrine effects. *Biology of Reproduction* 2001. 64; 4: 1122-1130.

Risma, K. A., C. M. Clay, T. M. Nett, T. Wagner, J. Yun and J. H. Nilson. Targeted overexpression of luteinizing hormone in transgenic mice leads to infertility, polycystic ovaries, and ovarian tumors. *Proceedings of the National Academy of Sciences of the United States of America* 1995. 92; 5: 1322-1326.

Roby, K. F., C. C. Taylor, J. P. Sweetwood, Y. Cheng, J. L. Pace, O. Tawfik, D. L. Persons, P. G. Smith and P. F. Terranova. Development of a syngeneic mouse model for events related to ovarian cancer. *Carcinogenesis* 2000. 21; 4: 585-591.

Roenigk, H. H.,Jr, S. Deodhar, R. St Jacques and K. Burdick. Immunotherapy of malignant melanoma with vaccinia virus. *Archives of Dermatology* 1974. 109; 5: 668-673.

Ryan, Q. C., D. Headlee, M. Acharya, A. Sparreboom, J. B. Trepel, J. Ye, W. D. Figg, K. Hwang, E. J. Chung, A. Murgo, G. Melillo, Y. Elsayed, M. Monga, M. Kalnitskiy, J. Zwiebel and E. A. Sausville. Phase I and pharmacokinetic study of MS-275, a histone deacetylase inhibitor, in patients with advanced and refractory solid tumors or lymphoma. *Journal of Clinical Oncology : Official Journal of the American Society of Clinical Oncology* 2005. 23; 17: 3912-3922.

Saito, A., T. Yamashita, Y. Mariko, Y. Nosaka, K. Tsuchiya, T. Ando, T. Suzuki, T. Tsuruo and O. Nakanishi. A synthetic inhibitor of histone deacetylase, MS-27-275, with marked in vivo antitumor activity against human tumors. *Proceedings of the National Academy of Sciences of the United States of America* 1999. 96; 8: 4592-4597.

Sakamoto, S., R. Potla and A. C. Larner. Histone deacetylase activity is required to recruit RNA polymerase II to the promoters of selected interferon-stimulated early response genes. *The Journal of Biological Chemistry* 2004. 279; 39: 40362-40367.

Samuelsson, C. V., S. Lienenklaus, P. P. Muller, R. Zawatzky, H. Hauser and S. Weiss. Transformation of mouse fibroblasts alters the induction pattern of type I IFNs after virus infection. *Biochemical and Biophysical Research Communications* 2005. 335; 2: 584-589.

Sharma, S., B. R. tenOever, N. Grandvaux, G. P. Zhou, R. Lin and J. Hiscott. Triggering the interferon antiviral response through an IKK-related pathway. *Science (New York, N.Y.)* 2003. 300; 5622: 1148-1151.

Shaw, T. J., M. K. Senterman, K. Dawson, C. A. Crane and B. C. Vanderhyden. Characterization of intraperitoneal, orthotopic, and metastatic xenograft models of human ovarian cancer. *Molecular Therapy : The Journal of the American Society of Gene Therapy* 2004. 10; 6: 1032-1042.

Shimizu, Y., E. Akagaki, K. Hirota, M. Kono, S. Miura and Y. Okudaira. Analysis of CA 125 assay system and its diagnostic significance in gynecologic tumors. *Nippon Sanka Fujinka Gakkai zasshi* 1985. 37; 12: 2813-2820.

Shimizu, Y., H. Fujiwara, E. Akagaki, K. Hirota, M. Kono, T. Irie, S. Miura and Y. Okudaira. Significance of CA 125 antigen levels in patients with ovarian cancer. .*Cancer & Chemotherapy* 1986. 13; 1: 46-52.

Shinozaki, K., O. Ebert and S. L. Woo. Treatment of multi-focal colorectal carcinoma metastatic to the liver of immune-competent and syngeneic rats by hepatic artery infusion of oncolytic vesicular stomatitis virus. *International Journal of Cancer* 2005. 114; 4: 659-664.

Silva, E. G., C. Tornos, M. Deavers, K. Kaisman, K. Gray and D. Gershenson. Induction of epithelial neoplasms in the ovaries of guinea pigs by estrogenic stimulation. *Gynecologic Oncology* 1998. 71; 2: 240-246.

Silva, E. G., C. Tornos, H. A. Fritsche Jr, A. el-Naggar, K. Gray, N. G. Ordonez, M. Luna and D. Gershenson. The induction of benign epithelial neoplasms of the ovaries of guinea pigs by testosterone stimulation: a potential animal model. *Modern Pathology : An Official Journal of the United States and Canadian Academy of Pathology, Inc* 1997. 10; 9: 879-883.

Stakleff, K. D. and V. E. Von Gruenigen. Rodent models for ovarian cancer research. *International Journal of Gynecological Cancer : Official Journal of the International Gynecological Cancer Society* 2003. 13; 4: 405-412.

Stark, G. R., I. M. Kerr, B. R. Williams, R. H. Silverman and R. D. Schreiber. How cells respond to interferons. *Annual Review of Biochemistry* 1998. 67; 227-264.

Stojdl, D. F., B. Lichty, S. Knowles, R. Marius, H. Atkins, N. Sonenberg and J. C. Bell. Exploiting tumor-specific defects in the interferon pathway with a previously unknown oncolytic virus. *Nature Medicine* 2000. 6; 7: 821-825.

Stojdl, D. F., B. D. Lichty, B. R. tenOever, J. M. Paterson, A. T. Power, S. Knowles, R. Marius, J. Reynard, L. Poliquin, H. Atkins, E. G. Brown, R. K. Durbin, J. E. Durbin, J. Hiscott and J. C. Bell. VSV strains with defects in their ability to shutdown innate immunity are potent systemic anti-cancer agents. *Cancer Cell* 2003. 4; 4: 263-275.

Strait, K. A., B. Dabbas, E. H. Hammond, C. T. Warnick, S. J. Iistrup and C. D. Ford. Cell cycle blockade and differentiation of ovarian cancer cells by the histone deacetylase inhibitor trichostatin A are associated with changes in p21, Rb, and Id proteins. *Molecular Cancer Therapeutics* 2002. 1; 13: 1181-1190.

Strait, K. A., C. T. Warnick, C. D. Ford, B. Dabbas, E. H. Hammond and S. J. Ilstrup. Histone deacetylase inhibitors induce G2-checkpoint arrest and apoptosis in cisplatinum-resistant ovarian cancer cells associated with overexpression of the Bcl-2-related protein Bad. *Molecular Cancer Therapeutics* 2005. 4; 4: 603-611.

Tunca, J. C., E. Erturk, E. Erturk and G. T. Bryan. Chemical induction of ovarian tumors in rats. *Gynecologic Oncology* 1985. 21; 1: 54-64.

Vaha-Koskela, M. J., J. E. Heikkila and A. E. Hinkkanen. Oncolytic viruses in cancer therapy. *Cancer Letters* 2007. 254; 2: 178-216.

Vannini, A., C. Volpari, G. Filocamo, E. C. Casavola, M. Brunetti, D. Renzoni, P. Chakravarty, C. Paolini, R. De Francesco, P. Gallinari, C. Steinkuhler and S. Di Marco. Crystal structure of a eukaryotic zinc-dependent histone deacetylase, human HDAC8, complexed with a hydroxamic acid inhibitor. *Proceedings of the National Academy of Sciences of the United States of America* 2004. 101; 42: 15064-15069.

Vasey, P. A., G. C. Jayson, A. Gordon, H. Gabra, R. Coleman, R. Atkinson, D. Parkin, J. Paul, A. Hay, S. B. Kaye and Scottish Gynaecological Cancer Trials Group. Phase III randomized trial of docetaxel-carboplatin versus paclitaxel-carboplatin as first-line chemotherapy for ovarian carcinoma. *Journal of the National Cancer Institute* 2004. 96; 22: 1682-1691.

Visintin, I., Z. Feng, G. Longton, D. C. Ward, A. B. Alvero, Y. Lai, J. Tenthorey, A. Leiser, R. Flores-Saaib, H. Yu, M. Azori, T. Rutherford, P. E. Schwartz and G. Mor. Diagnostic markers for early detection of ovarian cancer. *Clinical Cancer Research : An OfficialJjournal of the American Association for Cancer Research* 2008. 14; 4: 1065-1072.

von Kobbe, C., J. M. van Deursen, J. P. Rodrigues, D. Sitterlin, A. Bachi, X. Wu, M. Wilm, M. Carmo-Fonseca and E. Izaurralde. Vesicular stomatitis virus matrix protein inhibits host cell gene expression by targeting the nucleoporin Nup98. *Molecular Cell* 2000. 6; 5: 1243-1252.

Weichert, W., C. Denkert, A. Noske, S. Darb-Esfahani, M. Dietel, S. E. Kalloger, D. G. Huntsman and M. Kobel. Expression of class I histone deacetylases indicates poor prognosis in endometrioid subtypes of ovarian and endometrial carcinomas. *Neoplasia (New York, N.Y.)* 2008a. 10; 9: 1021-1027.

Weichert, W., A. Roske, V. Gekeler, T. Beckers, M. P. Ebert, M. Pross, M. Dietel, C. Denkert and C. Rocken. Association of patterns of class I histone deacetylase expression with patient prognosis in gastric cancer: a retrospective analysis. *The Lancet Oncology* 2008b. 9; 2: 139-148.

Weichert, W., A. Roske, V. Gekeler, T. Beckers, C. Stephan, K. Jung, F. R. Fritzsche, S. Niesporek, C. Denkert, M. Dietel and G. Kristiansen. Histone deacetylases 1, 2 and 3 are highly expressed in prostate cancer and HDAC2 expression is associated with shorter PSA relapse time after radical prostatectomy. *British Journal of Cancer* 2008c. 98; 3: 604-610.

Weichert, W., A. Roske, S. Niesporek, A. Noske, A. C. Buckendahl, M. Dietel, V. Gekeler, M. Boehm, T. Beckers and C. Denkert. Class I histone deacetylase expression has independent prognostic impact in human colorectal cancer: specific role of class I histone deacetylases in vitro and in vivo. *Clinical Cancer Research : An Official Journal of the American Association for Cancer Research* 2008d. 14; 6: 1669-1677.

Wu, R., N. Hendrix-Lucas, R. Kuick, Y. Zhai, D. R. Schwartz, A. Akyol, S. Hanash, D. E. Misek, H. Katabuchi, B. O. Williams, E. R. Fearon and K. R. Cho. Mouse model of human ovarian endometrioid adenocarcinoma based on somatic defects in the Wnt/beta-catenin and PI3K/Pten signaling pathways. *Cancer Cell* 2007. 11; 4: 321-333.

Wu, Y., X. Lun, H. Zhou, L. Wang, B. Sun, J. C. Bell, J. W. Barrett, G. McFadden, J. A. Biegel, D. L. Senger and P. A. Forsyth. Oncolytic efficacy of recombinant vesicular stomatitis virus and myxoma virus in experimental models of rhabdoid tumors. *Clinical Cancer Research : An Official Journal of the American Association for Cancer Research* 2008. 14; 4: 1218-1227.

Xu, W. S., R. B. Parmigiani and P. A. Marks. Histone deacetylase inhibitors: molecular mechanisms of action. *Oncogene* 2007. 26; 37: 5541-5552.